DISSERTATION

REGULATION OF LOCAL L-TYPE CALCIUM CHANNEL SIGNALING IN ANTERIOR PITUITARY GONADOTROPES

Submitted by

An Khanh Dang

Department of Biomedical Sciences

In partial fulfillment of the requirements

For the Degree of Doctor of Philosophy

Colorado State University

Fort Collins, Colorado

Fall 2017

Doctoral Committee:

Advisor: Greg Amberg
Co-Advisor: Colin Clay

Michael Tamkun
Amy Navratil
Dawn Duval

ABSTRACT

REGULATION OF LOCAL L-TYPE CALCIUM CHANNEL SIGNALING IN ANTERIOR PITUITARY GONADOTROPES

The binding of gonadotropin-releasing hormone (GnRH) to its receptor initiates signaling cascades in gonadotropes which result in enhanced luteinizing hormone (LH) and follicle stimulating hormone (FSH) biosynthesis and secretion. Most dramatic is the sharp rise in LH secretion ("LH surge") that precedes and is necessary for follicular maturation and ovulation. Ca^{2+} influx activates mitogen-activated protein kinases (MAPKs) which lead to increased transcription of LH and FSH genes. Interestingly, previous research suggests that two MAPK signaling pathways, ERK and JNK, are activated by either Ca^{2+} influx through L-type Ca^{2+} channels or by global Ca^{2+} signals originating from intracellular stores, respectively. These discrete Ca^{2+} sources for divergent signaling cascades provides a mechanism in which gonadotropes can decode different pathways for appropriate gonadotropin release during various stages of the ovulatory cycle.

However, direct evidence supporting an underlying subplasmalemmal local Ca^{2+} signaling through L-type Ca^{2+} channels distinct from intracellular Ca^{2+} was lacking. Here we used a combination of electrophysiology and total internal reflection fluorescence (TIRF) microscopy to visualize discrete sites of Ca^{2+} influx (Ca^{2+} sparklets) in gonadotrope-derived αT3-1 cells in real time. These localized GnRH-induced Ca^{2+} influxes are mediated by L-type Ca^{2+} channels and important for downstream ERK activation. In addition, precise structural and molecular elements to create a microenvironment suitable for localized subplasmalemmal L-type Ca^{2+} channel signaling was necessary for gonadotrope function, in which GnRH-dependent stimulation of L-type Ca^{2+} channel influx was found to require PKC and a dynamic actin cytoskeleton.

More recently, we have further elucidated molecular mechanisms modulating localized L-type Ca^{2+} channel influx. Reactive oxygen species (ROS) are cognate signaling molecules that mediate cell function, but their role in regulating Ca^{2+} in gonadotropes is unknown. We have explored GnRH regulation of both NADPH oxidase complexes and mitochondrial sources of ROS and assessed ROS modulation of L-type Ca^{2+} channel activity in gonadotropes. We identified GnRH-induced spatially localized ROS "puncta" in αT3-1 cells, and ROS increased local Ca^{2+} channel activity in both αT3-1 cells and primary mouse gonadotropes. In addition, GnRH increased mitochondrial oxidation activity at the subplasmalemmal surface and mitochondrial ROS increased localized L-type Ca^{2+} channel influx. Also, active L-type Ca^{2+} channels were associated with subplasmalemmal mitochondria.

Taken together, this dissertation explored the first direct evidence for localized L-type Ca^{2+} channel signaling in αT3-1 cells and elucidated signaling mechanisms in gonadotropes. Specifically, cellular organization via an intact cytoskeletal platform and ROS regulated L-type Ca^{2+} channel sparklet activity that are important for the downstream ERK activation and gonadotropin gene expression that regulates reproduction.

ACKNOWLEDGEMENTS

This graduate career has been one of the most difficult, yet rewarding endeavors in my life. Never would I have imagined I would have the opportunity to make my small mark in research and find something yet to be discovered. Being surrounded by brilliant minded professors and students has kept me driven over the years and made this challenging experience worthwhile.

My advisors Greg Amberg and Colin Clay have been my foundation, given me much strength, faith and room to grow intellectually and personally. My committee members Mike Tamkun, Amy Navratil, and Dawn Duval have always provided exceptional encouragement, pushing me to my limits and motivating me to think bigger. Co-workers in both labs, including Nathan Chaplin, Heather Szerlong, Jimmy Singh, Dilka Murtazina, Kelly Kirkley, and Jeremy Cantlon have been there for me every day when I needed guidance and reassurance. All the BMS faculty have been my inspiration and support as well, having opened doors to help me with scientific and life questions, including Susan Tsunoda, Josef Vigh, Stu Tobet, Leslie Stone-Roy, Shane Hengtes, Tiana Magee, Anna Fails and Tod Clapp.

Graduate school colleagues and friends have also made this journey much more enjoyable, so thank you to Mallory Shields, Ben Johnson, Matt Bowers, Nathan Byers, Allison Cleymaet, Naser Eadaim, Girma Waro, Jasmin Hicks, Ashley Leek, Ashley Turnidge, Eric Marr, Emily Maverick, Laura Sole, Yaping Moshier, Marissa Metz, Alex Miller, Vanessa Selwyn, Kristen Brown, Sarah Kane, Rachel West, Max Vallejos, Tyler Wallace, Phil Fox, Mario Oyola, Liz Akin, Krystle Frahm, Kenny Ivie, Shazette Pierce, Karen Solomon, Erin Bisenius, Heather Hall, and Krysta Chapin. Jonathan Lee and Kyle Blake have been there through all the good and bad times and I could not have done this without them.

Last but not least, I must thank my parents, Tien Dang and Natalie Luong, and brother Huy Dang for their love and support through this journey and making sure I never gave up.

TABLE OF CONTENTS

LIST OF FIGURES

Chapter 1. Background

1.1 Introduction

For normal reproduction and fertility, precise signaling occurs within the hypothalamic-pituitary-gonadal (HPG) axis. This signaling from the brain to regulate reproductive organs converges in the pituitary on specific cells known as gonadotropes. Gonadotropes therefore are fundamental intermediates both anatomically and mechanistically for reproductive physiology. Gonadotropes uniquely have receptors to bind gonadotropin-releasing hormone (GnRH) to initiate a complex array of intracellular signaling mechanisms to produce and secrete gonadotropin hormones, luteinizing hormone (LH) and follicle stimulating hormone (FSH) for downstream reproductive behaviors.

Signaling pathways are the chief driving force and fundamental basis for cellular communication. These intricate signaling cascades occur within a single cell, but also are the foundation of how entire organs are able to interconnect for broader physiological purposes. Signal transduction allows for balance in a dynamic environment with a multitude of external stimuli, and therefore must be precisely regulated for normal function. Identifying all facets that allow gonadotropes to respond to GnRH, and understanding the molecular basis for gonadotropin transcription and release, will provide great insight into reproductive signaling and physiology. Therefore, this dissertation aims to understand GnRH-induced intracellular signal transduction pathways, specifically the critical role of localized calcium (Ca^{2+}) influx through L-type Ca^{2+} channels in gonadotropes. In addition, mechanisms that regulate the L-type Ca^{2+} channel activity, including cytoskeletal organization and reactive oxygen species (ROS) are also addressed. These aims will provide greater understanding of GnRH signaling mechanisms under physiological conditions to better discern how dysregulation and imbalance can lead to infertility.

The first chapter of this dissertation provides a comprehensive review of the signaling within the gonadotrope that leads to gonadotropin gene expression and hormone release. An overview of the HPG axis and the role of gonadotropin hormones for reproduction is provided. Details about the GnRH peptide, including its importance for pulsatile signaling and various regulatory mechanisms that modulate GnRH secretion are also included. Next, this dissertation provides details about the GnRH receptor, since receptor activation is the fundamental initiator of all signaling cascades within the gonadotrope, having unique properties and organization on the plasma membrane. Studies detailing GnRH signaling mechanisms and second messenger cascades are discussed in detail. Ca^{2+} plays a crucial role in gonadotrope signaling and background information about mitogen-activated protein kinase (MAPK) activation, specifically extracellular signal-regulated kinase (ERK) for LH synthesis are reviewed. This dissertation addresses multiple mechanisms of ERK modulation, but with an emphasis on L-type Ca^{2+} channel regulation of ERK. Further understanding of L-type Ca^{2+} channel properties and function in gonadotropes are included. Ca^{2+} influx through L-type Ca^{2+} channels are capable of a localized signal known as Ca^{2+} sparklets, which are characterized in detail in other cell types and included for background.

In addition, this chapter overviews ROS and their ability to modulate Ca^{2+} channels. Understanding the role of ROS in normal physiological signaling can help identify homeostatic signaling compared to disease states within the cell. Highlighted in this section are general properties of ROS, specifically hydrogen peroxide, and understanding sources of ROS generation in the cell, including NADPH oxidase and mitochondria. Furthermore, this section includes details about ROS and Ca^{2+} functional coupling studied in other cell types, and recognizing ROS signaling in localized areas in a similar fashion to Ca^{2+} sparklets. Lastly, this background concludes with specific hypotheses that are addressed in the following chapters.

1.2 HPG Axis

The HPG axis regulates reproductive function and requires precise signaling events mediated by both hypothalamic and gonadal factors that converge at the pituitary. Most proximately, this HPG axis cascade is dependent on a subset of hypothalamic neurons secreting the neuropeptide GnRH. GnRH circulates through the hypophyseal portal system and binds to GnRH receptors on the cell surface of specific anterior pituitary cells called gonadotropes. Gonadotropes synthesize and secrete two gonadotropins: luteinizing hormone (LH) and follicle stimulating hormone (FSH). Gonadotropins are heterodimeric glycoproteins that share a common α-subunit (αGSU), paired with distinctly different β subunits (FSHβ) and (LHβ).

These gonadotropins bind to their receptors on target cells in the testes and ovaries vital for gonadal function and behavior, participating in spermatogenesis and follicle maturation, in addition to the secretion of steroid hormones. In the male, FSH binds to receptors on Sertoli cells for androgen binding protein synthesis important for sperm production and maturation. In females, FSH stimulates ovarian granulosa cells to ultimately produce estradiol. LH in males stimulates testicular Leydig cells to produce testosterone and Sertoli cells to produce androgen binding protein. In the female, LH supports thecal cells that surround the developing ovarian follicle to produce androgens and hormonal precursors for estradiol production. During the terminal stages of follicular growth and beginning of the luteal phase, LH also drives the production of progesterone from the granulosa cells (2).

In females, maintaining appropriate levels of GnRH and gonadotropins is necessary to dictate the different stages of follicular development and ovulation, which occurs when the mature egg is released from the ovarian follicles into the oviduct every month. Precise signaling occurs to produce an acute rise in LH, known as the “LH surge,” to induce ovulation, and as such is a mandatory event for normal reproduction and fertility. Understanding the molecular mechanisms of the HPG axis is critical, especially since many clinical processes modulate this signaling cascade for fertility treatments. Assisted reproductive technology commonly uses

fertility drug treatments to enhance ovulation. For example, inducing ovulation and superovulation are methods that increase chances in fertility by eliciting more LH production. Alternatively, hormone contraceptives (e.g. estradiol derivatives) are prescribed to suppress the release of LH and ovulation.

1.3 Gonadotropin-releasing Hormone (GnRH)

GnRH is the master regulator for reproduction in vertebrates and plays a central role for signaling events in the HPG axis. Like many other neuropeptides, GnRH is synthesized as a precursor and enzymatically processed, splicing prepro-GnRH into the intermediate pro-GnRH, and ultimately into GnRH. Although different isoforms of GnRH exist, the decapeptide has many conserved amino acids across species despite millions of years of evolution. In vertebrates, there are at least 2 forms of GnRH that occur in anatomically and distinct neuronal populations, GnRH-I and GnRH-II. GnRH-I predominately is located in the hypothalamus, but is found in other tissues such as the ovary, placenta, endometrium, and trophoblast. GnRH-II is found both in the central nervous system and peripheral tissues (3).

GnRH neurons from the hypothalamus are known to be “pulse generators” and specific patterns of GnRH secretion are crucial for appropriate gonadotropin production (4-6). The pulsatile manner of GnRH release (which occurs every 30-120 minutes depending on species) involves complex processes and strict regulation (7). Given the distinct roles for LH and FSH for different biological tasks, and the dynamic gonadotropin levels during various phases of the monthly ovulatory cycle, GnRH release at the appropriate amplitude and frequency would seem logical to dictate those differences. Indeed, the requirement of pulsatile GnRH stimulation has been demonstrated in both clinical and experimental settings for normal gonadotrope function and fertility (8-10).

In rats, lower frequency GnRH stimulation was observed during the follicular phase favoring FSH production and secretion, while higher frequency GnRH pulses stimulated the LH surge (11). Furthermore, specific GnRH pulse frequencies are necessary for normal estrous

cycles as well, in which extremely low GnRH pulses were associated with amenorrhea and fertility complications, and continuously high GnRH frequencies led to reproductive difficulties correlated with polycystic ovarian syndrome (2,12,13). In clinical uses, continuous GnRH administration paradoxically decreased gonadotropin production, possibly due to receptor desensitization and uncoupling the gonads from pituitary regulation without appropriate GnRH pulsatility (2). Consistent with defects from continuous GnRH, the lack of GnRH production associated with Kallman syndrome can also disturb reproductive development. Kallman syndrome, a prime example of hypogonadotropic hypogonadism, occurs when GnRH neurons fail to migrate appropriately from the olfactory epithelium to the hypothalamus during development, and often leads to conditions of delayed or absent puberty (14).

The HPG axis has regulatory mechanisms that involve both positive and negative feedback loops at multiple levels to control appropriate amounts of GnRH and gonadotropins. Sex steroid hormones from the gonads, which include estrogen and testosterone, provide feedback both at the level of the hypothalamus and pituitary. In the male, testosterone provides negative feedback on the hypothalamus and therefore inhibits GnRH release (15). In females, sex steroid regulation is species-specific, with dynamic changes depending on the stage of the ovulatory cycle. Estrogen initially provides negative feedback during the early follicular phase, but switches to provide positive feedback to the hypothalamus and pituitary during the preovulatory period (16-18). This rapid rise in estrogen during the follicular phase primes the gonadotrope for the mandatory LH surge to elicit ovulation.

1.4 Gonadotropes and Experimental Models

The anterior pituitary is comprised of five endocrine cell types (gonadotropes, somatotropes, lactotropes, corticotropes, and thyrotropes) that are defined by the hormones they secrete. Despite the heterogenous population within the pituitary, distinct networks and organization occur to interpret inputs and outputs for appropriate hormone release (19). Although gonadotropes play a crucial role in connecting hypothalamic GnRH neurons and

downstream gonadal regulation, gonadotropes only make up ~10% of the cell population in the anterior pituitary. Therefore, identification and segregation of these gonadotrope cells to understand their signaling mechanisms are difficult. Early experiments dissociated primary pituitaries, but isolation and purification of gonadotropes using methods such as centrifugal elutriation were technically challenging (20). In addition, lack of a homogenous in vitro model of gonadotropes and cross talk among gonadotropes and other pituitary cell types in dissociated pituitaries made results difficult to interpret. For example, investigating baseline transcript levels within gonadotropes can be influenced by other pituitary cell types that also expressed the same gene of interest and skew interpretation.

The creation of experimental cell lines to study gonadotrope function provided great advances in understanding signal transduction. The Mellon laboratory created immortalized αT3-1 and LβT-2 murine gonadotrope cell lines by directed expression of the SV40 large T antigen oncogene in developing pituitary cells (21,22). αT3-1 cells were developed from mice in earlier stages of development, which have the characteristic GnRH receptor and αGSU subunit. LβT2 cells were generated from mice in subsequent stages of development, therefore have both LHβ and FSHβ subunits in addition to GnRHR and αGSU subunits found in αT3-1 cells. Both cell types are still widely used today to study gonadotrope function for different purposes. αT3-1 cells are commonly used in understanding proximal events relating to the GnRHR and transcription of αGSU, whereas LβT-2 cells are most often used in investigating LH and FSH secretion mechanisms. More recently, transgenic mouse lines to easily identify gonadotropes have allowed greater insight in understanding GnRH signaling in a physiological setting. GRIC (GnRH receptor IRES Cre) mice were generated using gene targeting in which Cre recombinase was coexpressed with the *GnRHR* gene (23). The GRIC mice bred to fluorescent reporter mouse lines allowed for direct Cre-mediated recombination of a fluorescent protein reporter allele specifically in gonadotropes. These various experimental models provided a

major breakthrough in understanding the signaling cascade and interactive network within gonadotropes.

1.5 GnRH Receptor (GnRHR)

The GnRH receptor (GnRHR) on the cell surface of gonadotropes plays the initial role to decode pulsatile nature of GnRH secretion and activating downstream signaling cascades ultimately leading to differential gonadotropin synthesis and release. Like the GnRH peptide, there are multiple forms of GnRHR, but GnRHR-I is the predominant and mammalian form that can bind both GnRH-I and GnRH-II ligands. GnRHRs are expressed in many tissues beyond the gonadotrope, including breast, gonadal, prostate, and uterine tissues. Because the GnRHR is found in peripheral tissues, understanding GnRHR signaling beyond fertility regulation is important due to its role in hormonally sensitive cancers (e.g. breast cancer, prostate cancer, etc.). GnRH analogs are often used as cancer treatment drugs since continued stimulation with GnRH desensitizes and downregulates the GnRH receptor leading to decreased gonadotropin levels and sex steroid hormones in these tissues (24-26).

The GnRHR is a typical member of the rhodopsin-like G-protein coupled receptor (GPCR) superfamily, consisting of the conventional seven hydrophobic transmembrane domains, connected through three extracellular and three intracellular loops. Although the receptor contains the extracellular amino terminal domain, the GnRHR lacks the classical carboxyl-terminal cytoplasmic domain (27). Only having a short 1-2 amino acid C-terminal tail makes the GnRHR structurally and functionally unique. Classically, GPCR C-terminal tails are phosphorylated to recruit the multifunctional β-arrestin family of adaptor proteins, which mediate rapid desensitization and internalization of a receptor (28). Because the GnRHR lacks these phosphorylation sites, GnRHR undergoes unconventional signaling and has been shown to be biologically resistant to agonist-dependent phosphorylation, desensitization and internalization (29-31). Chimeric receptors in which the C-terminal tail of various GPCRs (e.g. C-terminal tail of catfish (nonmammalian) GnRHR or rat TRH receptor) was fused to the C-terminus of the

mammalian type I GnRHR exhibited rapid desensitization and internalization (32-38). The wildtype GnRHR is not completely exempt from internalization following GnRH treatment, however this process appears to undergo slow, constitutive, agonist-independent manner (38,39). Both the rat and human GnRHR internalize in a clathrin-dependent manner, colocalizing with transferrin which is internalized via clathrin-coated structures (33,39,40). Dynamin-mediated internalization, however, is species specific, in which rat GnRHR internalizes in a dynamin dependent manner (36), whereas the human internalizes independently of dynamin (41,42).

These unique characteristics of the GnRHR enable the receptor to be readily available for the varying GnRH pulse frequencies and provide necessary signaling for the rapid preovulatory LH surge response. Therefore, appropriate trafficking and surface level expression of GnRHRs are important. Like abnormalities in GnRH, mutations in the GnRHR have also been linked to hypogonadotropic hypogonadism (43). Studies have shown that although certain mutations allow the GnRHR to bind GnRH normally, defective intracellular transport by misfolding, abnormal trafficking, and increased degradation can occur (44). Therefore, understanding mechanisms of proper GnRHR expression and membrane targeting can be useful as a therapeutic approach for disorders linked to inappropriate GnRH signaling and gonadotropin release.

Previous researchers have investigated the lateral mobilization of the GnRHR on the plasma membrane. Fluorescence recovery after photobleaching (FRAP) studies demonstrated that GnRH receptors in the absence of agonist are dynamic monomeric proteins with substantial lateral mobility (45-47). However, upon agonist binding the lateral mobility of GnRH receptors decreases and the probability of homologous receptor interaction increases (45-48). In addition, fluorescence resonance energy transfer (FRET) studies established that GnRH receptor interactions increased following agonist exposure (45,46).

Delayed kinetics in internalization and lateral mobilization dynamics of the GnRHR emphasizes the versatility of the plasma membrane as a critical foundation for many signaling cascades in gonadotropes. Contrary to previous models characterizing the plasma membrane as a uniform fluid mosaic with freely diffusing lipids and proteins, more recent evidence displays plasma membrane organization to be a heterogeneous network of spatially and functionally distinct domains (49-51). In gonadotropes, researchers investigated the biophysical properties of the plasma membrane and identified specialized compartments called “lipid rafts”, in which the GnRHR and other important proteins were often associated, characterized by low-bouyant density membrane fractions highly enriched with sphingolipids and cholesterol (52-54).

Another emerging model in defining membrane domains emphasizes the importance of the cytoskeletal architecture to create signaling platforms. Actin is one of the most important cytoskeletal proteins involved in cell movement and organization, in which the highly dynamic processes of continual polymerization and depolymerization occur during different cellular responses (55,56). In gonadotropes, GnRH application stimulated morphology changes and rearrangement mediated by the actin cytoskeleton and actin binding proteins such as cortactin have been shown to be necessary for GnRH-induced cell movement at leading edges of gonadotropes and was important for gonadotropin hormone secretion (57,58). In addition, this dynamic plasticity seen in individual cells has been confirmed at population levels as well, in which *ex vivo* slices demonstrated cell movement in response to GnRH and *in vivo* analyses showed gonadotropes to be located near vasculature that would be important for hormone secretion (59).

1.6 GnRH Signaling

Upon GnRH binding to its receptors, a wide range of intracellular signaling pathways are activated in gonadotropes which ultimately regulate the synthesis and secretion of gonadotropins for reproductive functions. GnRH receptor binding follows the canonical GPCR initiation pathway in which ligand binding leads to receptor conformational changes that activate

the heterotrimeric G-proteins, comprised of Gα, β, and γ subunits. Specifically, GnRHR activation results in the exchange of GDP for GTP on the Gα subunit, and the GTP-loaded Gα dissociates from Gβ/γ to stimulate downstream effectors. Gonadotropes preferentially bind $G\alpha_{q/11}$ subunits, although $G\alpha_s$ and $G\alpha_i$ have been found to be important in cell context dependent regulation for other signaling cascades (60-64). GTP loading of $G\alpha_{q/11}$ leads to the activation of phospholipase Cβ (PLCβ). PLCβ contains an N-terminal pleckstrin homology (PH) domain, four EF hands, a catalytic domain, and a C2 domain. Specifically, the PH domain and long 200 amino-acid C-terminal extension allow for the enzymes to undergo constitutive and reversible membrane targeting necessary for signaling (65). PLCβ activation leads to rapid cleavage of phosphatidylinositol 4,5-bisphosphate (PIP_2) to generate second messengers phophatidylinositol-trisphosphate (IP_3) and diacylglycerol (DAG). In addition to the role of PLCβ as effector molecules, these enzymes also play a secondary role as GTPase activating proteins (GAP) to provide negative feedback and terminate additional signaling input by stimulating hydrolysis of $G\alpha_{q/11}$ bound GTP (66,67).

DAG facilitates subsequent translocation and activation of protein kinase C (PKC). PKC, a serine/threonine kinase, is involved in a multitude of cellular mechanisms, such as cellular growth and differentiation, metabolism, contraction, exocytosis, ion channel regulation, and gene expression (68,69). The structure of PKC includes an amino-terminal regulatory domain with conserved C1 and C2 regions tethered to a carboxy-terminal catalytic domain that makes up the kinase core of the protein. The regulatory domain binds PKC activators, including Ca^{2+} and DAG, and also contains motifs to mediate protein–protein interactions that are crucial for substrate recognition and localizing PKC to particular cellular compartments (70). The PKC family is composed of at least 10 related isoforms and are often classified into the three major groups: conventional (cPKC: α, β, and γ), novel (nPKC: δ, ε, θ, and η/λ) and atypical (aPKC: ξ and -ι/λ). Conventional PKCs, also known as "Ca^{2+}-dependent PKCs," require Ca^{2+} and can be activated by DAG and phosphatidylserine (PS). Novel PKCs are activated only by DAG and PS,

and therefore known as "Ca^{2+}-independent PKCs". Atypical isoforms are Ca^{2+} and DAG-independent and activated by PS and other lipid mediators (71). Gonadotropes contain many of these PKC isoforms, in which fractionation experiments identified PKCα, ε, and ξ isoforms to be activated by GnRH (72), while other groups found GnRH treatment to stimulate PKCβ, ε, and δ gene expression in αT3-1 cells (73-75).

Data suggests PKC activation leads to downstream cross talk with Ca^{2+} for gonadotropin mRNA expression and secretion (76-78). Therefore, understanding the role of Ca^{2+} is essential for GnRH signaling. Ca^{2+} ions are ubiquitous intracellular second messengers with wide-ranging physiological roles, such as fertilization, cell differentiation and proliferation, transcription factor activation, and apoptosis (79). Ca^{2+} has great versatility due to its varying kinetics, amplitude, and spatio-temporal distribution, and therefore capable to participate in different signaling cascades and function within the same cell (71). Similar to decoding GnRH frequencies and amplitude for different gonadotropin subunit expression, gonadotropes also have unique Ca^{2+} responses that have been implicated in pulse frequency interpretation (80,81). For example, gonadotropes have been shown to have distinct Ca^{2+} signatures, including both sub-threshold Ca^{2+} responses and baseline Ca^{2+} oscillations important for signaling (82-84). Interestingly, GnRH stimulation has also been shown to induce a biphasic elevation of intracellular Ca^{2+} (85). The initial phase is comprised of a sharp rise in cytosolic Ca^{2+}, predominantly from IP_3-mediated Ca^{2+} release from the endoplasmic reticulum (ER). The subsequent phase of a more sustained Ca^{2+} occurs through PKC-dependent extracellular Ca^{2+} influx through L-type Ca^{2+} channels (82,86). As with other classical secretory vesicle release, Ca^{2+} mobilization is necessary for gonadotropin release and exocytosis. "Hot spots" of Ca^{2+} near exocytotic sites were found to have the biphasic Ca^{2+} response, in which Ca^{2+} release from internal stores raised Ca^{2+} levels by five-fold near vesicle release sites, followed by a delayed, more sustained Ca^{2+} phase (87).

If specific Ca^{2+} oscillation frequencies are important for decoding GnRH pulsatility for downstream events, experiments to recreate different Ca^{2+} pulses should lead to differential

gonadotropin subunit gene expression. Indeed, rat pituitary cells perifused with different pulses of the Ca^{2+} channel agonist BayK8644 or KCL resulted in distinct patterns of gonadotropin subunit transcription, in which faster Ca^{2+} pulse frequencies (~15-60 min pulses) led to maximal expression of αGSU and LHβ, while slower pulse frequencies (~180 minute pulses) produced preferential mRNA expression of FSHβ (88).

1.7 GnRH-induced ERK signaling

GnRH-mediated Ca^{2+} signals are ultimately necessary for gonadotropin subunit expression and secretion. The intermediate signaling mechanism between these signals involves mitogen-activated protein kinase (MAPK) cascades. MAPKs are highly conserved pathways that allow for signal transduction from the plasma membrane to the nucleus and regulate many cellular responses, such as cellular fate determination, proliferation, motility, and growth (89). Therefore, MAPKs are relevant mediators between GnRH-induced signaling on the cell surface and downstream gene expression. The MAPK cascades are comprised of tiered protein kinases that sequentially activate each other through phosphorylation steps. The pathway begins with phosphorylation of an upstream MAP kinase kinase kinase (MAPKKK), which phosphorylates and activates an intermediate MAP kinase kinase (MAPKK), which ultimately activates the terminal MAP kinase (MAPK) via dual phosphorylation of threonine and tyrosine residues (2). Activated MAPKs can then phosphorylate various substrates, including cytoskeletal structures and other enzymes, although the majority of activated MAPKs translocate into the nucleus to activate transcription factors (90,91).

MAPK activation is mediated by a wide variety of pathways, including growth factors (e.g. epidermal growth factors), cytokines, and importantly GPCRs (24,92). Although many MAPKs have been identified, mammals most commonly have the conventional MAPK pathways: extracellular signal-regulated kinase (ERK), jun-N-terminal kinase (JNK), p38, and ERK5/BigMAP kinase (ERK/BMK). Indeed, in αT3-1 and LβT-2 gonadotrope cells, GnRH receptor stimulation led to activation of all four major cascades of MAPKs (93-97). The

mechanisms of differential MAPK activation by GnRH occurs in a cell-context dependent manner in which particular interactions with different intracellular protein complexes can lead to activation of specific signal transduction pathways (98).

Since LH synthesis and secretion are critical to establish the LH surge necessary for ovulation, the mechanisms underlying LH transcription have been heavily investigated. ERK phosphorylation has been shown to play a key role for LH gene expression (99). ERK activation occurs rapidly and transiently following GnRH stimulation and involves PKC (92,100). However, subsequent mechanisms and specific protein interactions for this GnRH-induced ERK phosphorylation have been unclear, with varying results using different model systems and treatment parameters (101-104). ERK in other cell types can be activated in a β-arrestin dependent manner, but since the GnRHR lacks the C-terminal tail for β-arrestin interaction, this mechanism seems less likely to apply (105).

GnRH stimulation leads to rapid translocation of activated ERK into the nucleus to initiate many transcriptional responses (106,107). In LβT-2 cells, many immediate early genes were upregulated within 60 min of GnRH treatment using microarray techniques (108). ERK phosphorylation has been shown to be important for the induction of many of those genes, including c-Fos, c-Jun, STAT, and Egr1 (99,109). Consequently, ERK-dependent activation of transcription factor Egr-1 binds to LHβ-subunit promoter regions to enhance LH gene expression (110-112).

1.8 Regulation of ERK Activation

ERK signaling for gonadotrope function and fertility is crucial, in which genetic loss of both ERK isoforms resulted in anovulatory infertility in female mice (113). Because of the important role for ERK in reproduction, understanding the cell machinery that regulate ERK activation is critical. Mechanisms that directly modulate ERK activity include: 1) the phosphorylation status of ERK, 2) GnRH pulsatility, 3) ERK compartmentalization, and 4) Ca^{2+} signaling. First, in order to have rapid ERK responses following GnRH treatment, direct action to

modify the phosphorylation status of ERK through phosphatases and intracellular negative feedback loops would be expected. The MAP kinase phosphatases (MKPs) represent a distinct subfamily within a larger group of dual-specificity protein phosphatases (DUSPs) that bind and dephosphorylate MAPKs to regulate MAPK signaling (114). In gonadotropes, MKP-1 and MKP-2 (DUSP 1 and 4) were upregulated by GnRH and associated with inactivating both ERK and JNK activity (108,115-117). In addition, ERK activation and Egr-1 may play a role in mediating GnRH-dependent transcriptional activation of the MKP-2 gene, suggesting to a potential feedback loop for terminating ERK signaling (118). However, the role of MKPs for GnRH-induced ERK regulation are unclear since others have reported that although GnRH increased expression of MKP-1 and MKP-2, knockdown of MKPs in heterologous expression systems did not alter GnRH-mediated ERK signaling (119).

Next, GnRH pulse frequency has been implicated in modulating Ca^{2+} signals and gonadotropin gene expression. Not surprisingly, GnRH pulsatility patterns can also regulate MAPK signaling as well, including ERK activation (80,120,121). Faster GnRH pulse frequencies in LβT2 cells and primary gonadotropes led to rapid maximal phosphorylation of ERK (within 10 min) that was not sustained (returned to baseline within 20 min) relative to slower GnRH pulse frequencies. Therefore, GnRH pulsatility resulting in different patterns of ERK activation is a mechanism gonadotropes utilize for differential stimulation of LHβ and FSHβ transcription (121).

Third, to maintain specificity in signaling, highly arranged organization of membrane-associated cascades following GnRH activation is necessary for ERK regulation. Due to the canonical role of ERK for gene expression, many studies have investigated the mechanisms of ERK translocation to the nucleus (99,104,122). However, ERK has also been shown to reside in extranuclear compartments and associate with membrane bound signaling complexes as well (123,124). ERK along with the GnRHR were found in plasma membrane regions in gonadotropes, particularly lipid raft fractions, in which cholesterol depletion uncoupled GnRHR signaling and decreased ERK activation (52). In addition, engagement of the actin cytoskeleton

has also been implicated in MAPK activation following GnRH stimulation (58,125). In gonadotropes, disruption of cytoskeletal components, whether directly disrupting actin or disturbing protein complexes that regulate actin, such as mTORC2/Rictor, c-Src, FAK and Rac have all been shown to reduce ERK phosphorylation (58,126,127).

Lastly, given the importance for various Ca^{2+} patterns mentioned previously following GnRH pulsatility and its role for gonadotropin gene expression, direct regulation of MAPK pathways utilizing discrete Ca^{2+} signals in gonadotropes would be expected. Interestingly, Roberson et al. found different Ca^{2+} signals to be important for specific MAPK activation (86,128). In αT3-1 and primary rat pituitary cells, intracellular Ca^{2+} from IP_3-mediated internal stores was necessary for JNK activation, and Ca^{2+} influx through plasmalemmal L-type Ca^{2+} channels was required for ERK activation. These findings demonstrate a divergence in Ca^{2+} signaling to uniquely regulate different MAPK pathways and mechanistically connects GnRH-induced plasmalemmal events for downstream ERK phosphorylation. How the gonadotrope can decode these different Ca^{2+} signals from their different sources (e.g. Ca^{2+} influx from L-type Ca^{2+} channels vs. intracellular Ca^{2+} from internal stores) in the gonadotrope is unknown. Therefore, further understanding the properties and regulation of L-type Ca^{2+} channel signaling for ERK phosphorylation and LH synthesis requires additional investigation and understanding.

1.9 L-type Ca^{2+} Channels and Sparklets

There are many different types of voltage-dependent Ca^{2+} channels based on their gating properties, location, and function. L-type (long-lasting) Ca^{2+} channels were initially discovered in cardiac cells, but are found in many other systems, including endocrine cells, skeletal muscle, and neurons. L-type Ca^{2+} channels are comprised of several different subunits: α_1, α_2, δ, β_{1-4}, and γ. The α_1 subunit forms the ion conducting pore, and the other subunits are associated with modulating the gating properties of the Ca^{2+} channel. The α_1 subunit is a single polypeptide of about 2000 amino acid residues with four homologous domains (I-IV). Within each domain, there are six transmembrane spanning segments, S1-S6 and a pore

loop. Segments S5, S6 and the pore loop are responsible for ion conduction, and the S4 segment contributes to the voltage-sensing capabilities of the channel. The S4 segment contains many positively charged amino acid residues and serves as a sensor that detects changes in the electrical potential across the cell membrane. Therefore, membrane depolarization influences the charged amino acids such that the helix undergoes a conformational change, which in turn allows the channel pore to open (129). The associated subunits, such as the β subunit are important for shifting the kinetics and voltage dependence for gating Ca^{2+}, and will alter the physiological function of the α_1 subunit (130).

Early work in cultured pituitary cells identified the requirement of extracellular Ca^{2+} following GnRH stimulation for gonadotropin release (131,132). However, nifedipine-sensitive L-type Ca^{2+} channels were identified in gonadotropes when the biphasic Ca^{2+} response to GnRH was characterized, in which removal of external Ca^{2+} and Ca^{2+} channel antagonists abolished the slower, secondary Ca^{2+} response (133). Further characterization of the L-type Ca^{2+} channels occurred following the development of immortalized cell culture lines of gonadotropes. Hille et al. used classical electrophysiology to initially classify various ion channel function in αT3-1 cells, which also included the identification of Na^+ channels and K^+ channels (134). These ion channels have been confirmed and studied in other animal models, including rat, ovine, and genetically labeled mouse gonadotropes (23,135-138). The electrical activity from these channels, however, are not coupled directly to GnRH-mediated secretion, but rather maintain the gonadotrope cell in a responsive state with $[Ca^{2+}]_i$ near the threshold level for hormone release (135,137,139).

Ca^{2+} localized into specific parts of the cell has been a prevalent and recurrent theme for understanding how this versatile intracellular messenger can provide specific cell signaling mechanisms. These Ca^{2+} microdomains have been explored in other cell types, and "elementary events," defined as opening of single or small groups of Ca^{2+} channels, have been characterized (140). For example, Ca^{2+} sparks are areas of Ca^{2+} release from a group of

ryanodine receptors in cardiac cells important for excitation-contraction coupling (141). Ca^{2+} puffs are unitary events from the release of Ca^{2+} following IP_3 binding to their receptors on the ER (142,143).

Contrary to Ca^{2+} microdomains from channels located intracellularly, localized Ca^{2+} influx on the plasma membrane through L-type Ca^{2+} channels are termed Ca^{2+} sparklets. These Ca^{2+} channel events stimulated by membrane depolarization and L-type Ca^{2+} channel agonists were first identified in cardiac myocytes (144). Using a cell permeable ratiometric Ca^{2+} indicator to visualize localized Ca^{2+} influx events that were temporally comparable to single channel Ca^{2+} recordings, these Ca^{2+} sparklets were important for activating adjacent ryanodine receptors. Ca^{2+} sparklets have since been identified in other cell types for various functions, including a role for exocytosis at synaptic endings necessary for neurotransmitter release and increased firing rates in neurons, as well as being important for cell migration in endothelial cells (140,145,146). Further characterization and spatial resolution of these Ca^{2+} sparklets were determined using total internal reflection fluorescence (TIRF) microscopy (147). TIRF microscopy focuses the laser beam at an oblique angle in which the light is reflected away from the sample. However, this setup generates an evanescent wave that is capable of exciting fluorophores above the cover slip up to ~200 nm. Therefore, events and proteins at the cell surface and plasma membrane can be visualized with less excess fluorescence and intracellular interference.

Ca^{2+} sparklets in vascular smooth muscle have been highly characterized for their roles in regulating tone and arterial contraction. Native L-type Ca^{2+} sparklets were identified in smooth muscle cells using pharmacological manipulations with dihydropyridine (specific to L-type Ca^{2+} channels) agonists and antagonists and compared the Ca^{2+} influxes from Ca^{2+} indicators to the simultaneously recorded current traces. Further analysis of the ratiometric Ca^{2+} fluorescence led to quantification of single channel Ca^{2+} concentrations. In addition, multiple Ca^{2+} channels may be opened at a single Ca^{2+} sparklet site, seen by quantal steps in Ca^{2+} influx profiles, identical to

electrophysiology recordings, but with the added advantage of spatial visualization of Ca^{2+} influx in real time on the plasma membrane. Therefore, utilizing Ca^{2+} sparklet analyses are powerful tools in understanding localized L-type Ca^{2+} channel activity to understand cell signaling and biological function.

Sparklet activity has often been characterized in two ways: sparklet activity and sparklet density. Sparklet activity quantifies how active one specific Ca^{2+} microdomain is on a cell, determined by calculating the nP_s of each site (analogous to nP_o values obtained from electrophysiological recordings), where n is the number of quantal levels detected, and P_s is the probability that the site is active. To quantify the number of Ca^{2+} sparklet sites on the cell surface, L-type Ca^{2+} channel sparklet site densities (Ca^{2+} sparklet sites per μm^2) are defined as the number of active sites divided by the area of the cell membrane. When smooth muscle cells are voltage clamped at -70mV, detection of both low activity and high activity sites can be identified. Low activity sites are defined as having lower nP_s values ($nP_s < 0.2$) with occasional gating, and high activity sites ($nP_s \geq 0.2$) have persistent gating and higher levels of Ca^{2+} influx (148-151). Characterization of these different types of Ca^{2+} sparklet activity have been shown to be physiologically relevant, in which high activity sparklets are associated with disease models by changing smooth muscle contraction and transcription (152,153).

1.10 Reactive Oxygen Species (ROS)

ROS consist of several reactive molecules and free radicals derived from molecular oxygen. The oxygen molecule has two unpaired electrons in separate orbits in its outer shell, and these electron structures make oxygen susceptible to radical formation. The sequential reduction of oxygen through the addition of electrons leads to the formation of various ROS, such as superoxide (O_2^-), hydrogen peroxide (H_2O_2), hydroxide (OH^-), and nitric oxide (NO). ROS have widely been studied for their role in disease states due to cellular apoptosis and oxidative stress. However, it is important to recognize that under physiological conditions, ROS are necessary signaling molecules for normal metabolism, and are involved in a multitude of

processes, including mitochondrial electron transport, signal transduction, activation of nuclear transcription factors, and gene expression (154). Therefore, it is important to distinguish the homeostatic balance between ROS production and removal, and to continue to understand ROS function and regulation mechanisms for biological functions.

One common form of ROS is H_2O_2, a product of incomplete reduction of O_2, and a byproduct of many biological processes (155). Although H_2O_2 itself is a poorly reactive oxidizing agent, its ability to cross the plasma membrane and rapid conversion to alternative ROS makes H_2O_2 a useful signaling molecule. One-electron reduction of O_2 initially generates the superoxide anion ($O2^{-}\bullet$), which is then spontaneously or enzymatically (via the action of superoxide dismutase) converted to H_2O_2. H_2O_2 can be reduced further to the hydroxyl radical ($OH\bullet$) via the Fenton reaction in the presence of Cu^{2+} or Fe^{2+} ions. The ability of H_2O_2 to generate highly reactive $OH\bullet$ is important since it reacts with almost every macromolecule found in living cells, including nucleic acids, amino acids, membrane lipids, and carbohydrates. All ROS, including H_2O_2, modulate protein function most commonly by oxidizing thiol groups on key amino acids that operate as redox-dependent allosteric switches to form protein carbonyls. Specifically, sulfur containing amino acids, such as cysteine and methionine, are most susceptible to oxidative modification, and these changes to proteins can lead to alterations in enzymatic activity and binding (156).

NADPH oxidase is one of the most common sources of generating ROS. NADPH oxidase is a multiple-subunit complex that functions to redox-couple NADPH and molecular oxygen to generate $O2^{-}\bullet$, a highly reactive radical that can spontaneously or enzymatically be degraded to H_2O_2 for protein oxidation. The NADPH complexes are composed of two membrane-bound subunits, a large glycosylated protein $gp91^{phox}$ and a smaller adapter protein $p22^{phox}$, in addition to at least three cytoplasmic subunits (e.g. $p47^{phox}$, $p67^{phox}$, Rac2) (157). Mitochondria are also important in producing ROS. More than 90% of total cellular oxygen is reduced to water via electron carriers of the mitochondrial electron transport chain located on

the inner mitochondrial membrane (158). Isolated mitochondria have been shown to still inherently generate $O2^{-}$• in the presence of inhibitors of electron transfer in the heart and brain samples of many mammalian species (159,160). Therefore, understanding mitochondrial ROS for physiological roles are equally as important as other ROS generators to understand oxidative metabolism and normal cell function. Furthermore, there has been evidence in which H_2O_2 led to greater mitochondrial H_2O_2 efflux (161). These events, known as ROS-induced ROS release (RIRR) are feed forward mechanisms in which signaling can be amplified beyond the initial activity in a self-accelerating cycle and demonstrate an interconnection among NADPH oxidase and mitochondria (162,163).

One important role for ROS are their functional coupling and reciprocal relationship to Ca^{2+}. One suggested mechanism by which Ca^{2+} increases oxidant production includes Nox proteins responding directly to Ca^{2+} through N-terminal EF-hand motifs (164). Other studies have shown that Nox isoforms that lack EF-hand domains still are able to respond to Ca^{2+} through EF-hand Ca^{2+}-binding proteins, MRP8 and MRP14, that sequentially associate with $p47^{phox}$ and $p67^{phox}$ to enhance oxidation (165). Conversely, ROS oxidation has been shown to also directly regulate Ca^{2+} signals. For example, in endothelial cells, H_2O_2 decreases the threshold of IP_3 required to release intracellular Ca^{2+} from internal stores (166). The reciprocity of Ca^{2+} and ROS signaling provides a mechanism in which these second messenger molecules can modulate each other, allowing for rapid and localized feedback loops.

Mitochondria are coupled to Ca^{2+} due to their innate ability to sequester large amounts of Ca^{2+} in the cell. In many cell types, mitochondria are often arranged in intimate association with the ER (167,168). Opening of ER Ca^{2+} channels have been shown to result in Ca^{2+} levels greater than 20-fold higher than other areas within the cytosol, and nearby mitochondria are necessary to sequester these Ca^{2+} signals. In gonadotropes, mitochondria were organized near sites of exocytosis to lower local Ca^{2+} and spatially limit the Ca^{2+} signal. In addition, mitochondria

take up Ca^{2+} rapidly during GnRH-induced Ca^{2+} elevation and accounted for 40% of the Ca^{2+} clearance from the cytosol during each burst of intracellular Ca^{2+} (169).

Notably, ER Ca^{2+} channels associated with IP_3 and ryanodine receptors are sensitive to oxidation. Consequently, adjacent mitochondrial oxidant production is necessary for physiological Ca^{2+} events (170). Ca^{2+} sparks, for example, are regulated by mitochondrial ROS in a wide variety of systems, including cerebral arteries, skeletal muscle, and cardiac myocytes (171-173). Oxidant regulation of L-type Ca^{2+} channels on the plasma membrane has also been widely investigated (174-176). For example, in cardiac myocytes H_2O_2 stimulation increased L-type Ca^{2+} channel influx that resulted in increased intracellular Ca^{2+} concentrations. In smooth muscle cells, L-type Ca^{2+} channels have been shown to be oxidatively regulated increasing sparklet activity (149,177).

Despite ROS being ubiquitous molecules, they share similar properties to Ca^{2+} due to their capability to act locally. Localized ROS similar to Ca^{2+} microdomains would allow for the cell to distinguish between a global scale of ROS with nonspecific oxidative modifications that may occur during oxidative stress, compared to localized ROS in discrete regions for divergent and homeostatic signaling (164). Indeed, Nox subunits are directed to specific platforms and are regulated by actin cytoskeletal components for subcellular restriction. In endothelial cells, cytoskeletal disruption interrupted oxidant-mediated MAPK signaling, demonstrating an interplay among cytoskeletal rearrangement, ROS, and downstream signaling events (178).

Previous studies have found that oxidative stress is implicated in endometriosis, polycystic ovarian syndrome (PCOS), and other fertility complications (179). Despite these studies, understanding ROS and their mechanistic role within the HPG axis has been limited. However, researchers have recently identified various Nox isoforms in gonadotropes and identified GnRH-induced ROS signaling important for ERK activation and gonadotropin gene expression (180). Although these findings are important in demonstrating ROS signaling in

gonadotropes, mechanisms of the signaling were not identified and should be further investigated to determine parallels of ROS signaling with Ca^{2+} in different biological systems.

1.11 Conclusion

In conclusion, this chapter highlights the importance of GnRH signaling in gonadotropes leading to Ca^{2+} signals that are essential for many reproductive functions, including activating various MAPK cascades for fertility. Prior work suggested that two different Ca^{2+} signals, Ca^{2+} influx through L-type Ca^{2+} channels at the plasma membrane and Ca^{2+} release from internal stores, activate two distinct MAPK signaling cascades: IP_3-mediated Ca^{2+} release from the ER promotes JNK activation while Ca^{2+} influx through L-type channels activates ERK (86,128). Importantly, the activation of ERK is the key signal required for enhanced LH synthesis and the LH surge (181,182).

In demonstrating these divergent Ca^{2+} signals in gonadotropes, Roberson and colleagues suggested a highly localized Ca^{2+} signal generated by the L-type Ca^{2+} channel is specifically necessary for ERK but not JNK activation. However, technical limitations precluded a direct experimental test of this intriguing proposition. The striking divergence in Ca^{2+} signaling to ERK and JNK is an exquisite demonstration of the importance of spatially restricted Ca^{2+} signaling in gonadotropes. Herein, this dissertation aims to examine this concept using an innovative imaging approach to confirm previous assumptions in order to explore novel mechanisms by which GnRH receptor activation leads to ERK phosphorylation.

In conclusion, this dissertation addresses my overall hypothesis that stimulation of the GnRH receptor leads to ERK activation through discrete Ca^{2+} microdomains produced by L-type Ca^{2+} channels. Furthermore, my proposal focuses on novel mechanistic molecular components and structures necessary for transducing GnRH receptor activation to these localized Ca^{2+} microdomains and ultimately phosphorylation of ERK. Specifically, this includes two specific mechanistic hypotheses regarding the regulation of localized Ca^{2+} influx in gonadotropes: 1) Test the hypothesis that actin cytoskeletal reorganization is necessary for transducing GnRH

receptor activation to localized Ca^{2+} influx and 2) Test the hypothesis that ROS are regulated by GnRH and coupled to local L-type Ca^{2+} channel function. Therefore, this dissertation adds to the field of GnRH signaling and supports the concept that precise structural and molecular elements create a microenvironment suitable for localized subplasmalemmal Ca^{2+} signaling necessary for gonadotrope function.

Chapter 2. GnRH Evokes Localized Subplasmalemmal Calcium Signaling in Gonadotropes[1]

2.1 Overview

Identifying how gonadotropes decode GnRH pulsatility for LH and FSH release is important since gonadotropin levels are dynamic during various stages of the ovulatory cycle. Therefore, the cellular machinery needs to distinguish different signals simultaneously. One method through which this may occur is unique utilization and compartmentalization of second messengers within the cell. For example, Ca^{2+} would not be global and nonspecific, but rather intracellular Ca^{2+} produced from internal stores would be distinct from Ca^{2+} influx through voltage-gated Ca^{2+} channels at the plasma membrane. Roberson et al. identified distinct Ca^{2+} populations necessary for ERK and JNK activation, and alluded to localized Ca^{2+}, however, "experiments that provide definitive results in regard to the presence and function of a microdomain of Ca^{2+} would be technically difficult…[and] further biophysical studies are required to analyze Ca^{2+} flux through voltage-gated Ca^{2+} channels following activation" (86,128). Now, using techniques that provide this opportunity to separate Ca^{2+} signals, we can explore how GnRH impacts L-type Ca^{2+} channel activity in gonadotropes. In addition, manipulation of the signaling cascade to identify important intermediate players between the GnRH receptor and L-type Ca^{2+} channel and identifying necessary components for organized signaling platforms at the plasma membrane can provide insight at a molecular scale necessary for reproduction.

2.2 Summary

The binding of gonadotropin-releasing hormone (GnRH) to its receptor initiates signaling cascades in gonadotropes which result in enhanced luteinizing hormone (LH) and follicle

[1] Dang AK, Murtazina DA, Magee C, Navratil AM, Clay CM, Amberg GC. GnRH evokes localized subplasmalemmal calcium signaling in gonadotropes. Molecular endocrinology (Baltimore, MD) 2014; 28:2049-2059

stimulating hormone (FSH) biosynthesis and secretion. This process is necessary for follicular maturation and ovulation. Ca^{2+} influx activates mitogen-activated protein kinases (MAPKs) which lead to increased transcription of LH and FSH genes. Previous research suggests that two MAPK signaling pathways, ERK and JNK, are activated by either Ca^{2+} influx through L-type Ca^{2+} channels or by global Ca^{2+} signals originating from intracellular stores, respectively. Here we continued this investigation to further elucidate molecular mechanisms transducing GnRH receptor stimulation to ERK activation. Although it is known that GnRH-activation of ERK requires Ca^{2+} influx through L-type Ca^{2+} channels, direct evidence supporting an underlying local Ca^{2+} signaling mechanism was lacking. Here we used a combination of electrophysiology and total internal reflection fluorescence (TIRF) microscopy to visualize discrete sites of Ca^{2+} influx (Ca^{2+} sparklets) in gonadotrope-derived αT3-1 cells in real time. GnRH increased localized Ca^{2+} influx and promoted ERK activation. The L-type Ca^{2+} channel agonist FPL 64176 enhanced Ca^{2+} sparklets and ERK activation in a manner indistinguishable from GnRH. Conversely, the L-type Ca^{2+} channel antagonist nicardipine inhibited not only localized Ca^{2+} sparklets but also ERK activation in response to GnRH. GnRH-dependent stimulation of L-type Ca^{2+} channels was found to require PKC and a dynamic actin cytoskeleton. Taken together, we provide the first direct evidence for localized L-type Ca^{2+} channel signaling in αT3-1 cells and demonstrate the utility of our approach for investigating signaling mechanisms and cellular organization in gonadotropes.

2.3 Introduction

The hypothalamic neuropeptide gonadotropin-releasing hormone (GnRH) is secreted into the hypophyseal portal circulation and binds to receptors on a subpopulation of anterior pituitary cells termed gonadotropes. The binding of GnRH to its cognate receptor elicits multiple transcriptional and biosynthetic events leading to increased synthesis and secretion of luteinizing hormone (LH) and follicle stimulating hormone (FSH). Most dramatic is the sharp rise

in LH secretion (the “LH surge”) that precedes and is necessary for final follicular maturation and ovulation (183).

Following GnRH activation of the G-protein-coupled GnRH receptor, the $G\alpha_{q/11}$ subunit stimulates phospholipase C (PLC) leading to cleavage of plasma membrane-bound phosphatidylinositol-4-5-bisphosphate (PIP_2) and generation of the classical second messengers inositol-1,4,5-trisphosphate (IP_3) and diacylglycerol (DAG) (63). While IP_3 promotes Ca^{2+} release from the endoplasmic reticulum via activation of IP_3 receptors, DAG stimulates various protein kinase C (PKC) isoforms including conventional isoforms (PKC α, β, and γ) which are activated by DAG and Ca^{2+} and novel isoforms (PKC δ, ε, θ, and η/λ) which are activated by DAG but are Ca^{2+} independent. Increased PKC activity ultimately stimulates Ca^{2+} influx through voltage-dependent L-type Ca^{2+} channels (71).

Increased intracellular Ca^{2+} contributes to activation of mitogen-activated protein kinase (MAPK) signaling in gonadotropes. In general, Ca^{2+}-dependent MAPK initiates transcriptional changes ultimately leading to increased production of LH and FSH (181). Prior work suggests that these two distinct Ca^{2+} signals (i.e., Ca^{2+} influx and Ca^{2+} release from the endoplasmic reticulum) activate two distinct MAPK signaling cascades: IP_3-mediated Ca^{2+} release from the endoplasmic reticulum promotes jun-N-terminal kinase (JNK) activation while Ca^{2+} influx through L-type Ca^{2+} channels activates extracellular signal-regulated kinase (ERK) (86,128). Importantly, ERK is the key signal required for enhanced LH synthesis and the preovulatory LH surge (181,182).

Previously, Roberson and colleagues (86,128) used a pharmacological approach to frame the hypothesis that a local L-type Ca^{2+} channel signal insensitive to intracellular chelation was necessary for ERK activation; however, technical limitations precluded direct experimental confirmation of this intriguing hypothesis. Herein, we employed a powerful Ca^{2+} imaging approach to directly test in real time the hypothesis that GnRH receptor activation leads to a local L-type Ca^{2+} channel-mediated signal coupled to ERK activation.

Our approach, based on a combination of voltage-clamp electrophysiology and total internal reflection fluorescence (TIRF) microscopy has allowed, for the first time, to unambiguously visualize localized Ca^{2+} influx through L-type Ca^{2+} channels (i.e., Ca^{2+} sparklets (1,148,184)) in single αT3-1 gonadotropes. Using this approach we found that GnRH increases local L-type Ca^{2+} channel sparklet activity. Furthermore, pharmacological manipulations demonstrate that L-type Ca^{2+} channel sparklets are coupled to ERK activation and that GnRH-dependent activation of local L-type Ca^{2+} channel function requires PKC and a functional actin cytoskeleton. Our findings are not only consistent with the hypothesis that GnRH induces the local L-type Ca^{2+} channel signal that is critical for ERK activation, but demonstrate directly the existence of a biologically-relevant GnRH-induced Ca^{2+} microdomain in αT3-1 gonadotropes. Importantly, these findings open new and heretofore unavailable opportunities to further uncover the spatial and temporal events underlying the distinct subcellular biochemical and biophysical processes underlying GnRH stimulated gonadotropin synthesis. Finally, as Ca^{2+} sparklets have been identified predominantly in cardiovascular tissue, these data suggest a broader regulatory role for this unique Ca^{2+} signal in mediating a diverse array of cellular events and biological processes.

2.4 Materials and Methods

Materials

DMEM was from HyClone (Logan, UT), Fetal Bovine Serum (FBS) was from Atlas Biologicals (Fort Collins, CO), and L-glutamine and the antibiotic-antimycotic solution were from Mediatech (Herndon, VA). Rabbit polyclonal antibodies to ERK (pERK (E-4) catalog # cs7388; ERK-1 (K-23) catalog #sc-94) were from Santa Cruz Biotechnology (Santa Cruz, CA), Matrigel was from BD Biosciences (San Jose, CA), and fluo-5F (pentapotassium salt) was from Invitrogen (Carlsbad, CA). All other chemicals were from Sigma (St. Louis, MO).

Cell culture

αT3-1 cells (22), a generous gift from Pam Mellon (UCSD), were incubated in high-glucose DMEM supplemented with FBS and horse serum (5% each), L-glutamine (2 mM), and Antibiotic-Antimycotic solution (1%). Cells were maintained at 37°C in 5% CO_2 humidified air.

Electrophysiology and total internal reflection fluorescence microscopy

αT3-1 cells were plated onto Matrigel coated glass-bottomed Mattek dishes 24 hours prior to experimentation. Simultaneous electrophysiology and Ca^{2+} imaging experiments were carried out using the conventional dialyzed whole-cell patch clamp technique as described previously (1,148-150). Briefly, Ca^{2+} influx through L-type Ca^{2+} channels was visualized with a TILL Photonics (Victor, NY) through-the-lens TIRF system built around an inverted Olympus IX-71 microscope (Center Valley, PA) with a 100X TIRF oil-immersion objective (numerical aperture = 1.45) and an Andor iXON EMCCD camera (Andor Technology, South Windsor, CT). To monitor Ca^{2+} influx, gonadotropes were loaded with the Ca^{2+} indicator fluo-5F (200 μM) and an excess of EGTA (10 mM; to lower background noise while minimally interfering with fluo-5F (1,148,149,184)) via the patch pipette. Membrane potential was controlled with an Axopatch 200B amplifier (Molecular Devices, Sunnyvale, CA); fluo-5F excitation was achieved with a 491-nm laser with excitation and emission light being separated with appropriate filters. Ca^{2+} influx was recorded with 2 mM external Ca^{2+} at a frame rate of 50 Hz and holding potential of -70 mV to increase the driving force for Ca^{2+} entry. To preclude potential contaminating Ca^{2+} release events from the endoplasmic reticulum, the Ca^{2+}-ATPase inhibitor thapsigargin (1 μM) was present during all experiments. Cells were imaged for 2 min before acute treatment with GnRH (3 nM), the L-type Ca^{2+} channel agonist FPL 64176 (500 nM), the L-type Ca^{2+} channel antagonist nicardipine (10 μM), the PKC agonist phorbol 12, 13-dibutyrate (PDBu; 50 nM), the broad-spectrum PKC inhibitor GF109203X (GFX; 1 μM), the PKCα and β inhibitor Gö6976 (100 nM), or the actin stabilizer jasplakinolide (100 nM) and imaged for an additional 10 min. Vehicle

controls were performed as appropriate. All experiments were performed at room temperature (22 - 25°C).

L-type Ca^{2+} channel sparklet analysis

Background subtracted fluo-5F fluorescence signals were converted to intracellular Ca^{2+} concentrations ($[Ca^{2+}]_i$) as described previously (148-150,185). Briefly, fluo-5F fluorescence images were analyzed with custom software kindly supplied by L. Fernando Santana (University of California, Davis) and L-type Ca^{2+} channel sparklet activity was determined by calculating the nP_s of each site, where n is the number of quantal levels detected, and P_s is the probability that the site is active. nP_s values were obtained using pCLAMP 10.0 (Molecular Devices, Sunnyvale, CA) on imported $[Ca^{2+}]_i$ time course records using an initial unitary $[Ca^{2+}]_i$ elevation of ≈ 20 nM as determined empirically. Active L-type Ca^{2+} channel sparklet site densities (Ca^{2+} sparklet sites per μm^2) were calculated by dividing the number of active sites by the area of cell membrane visible in the TIRF images. Image stacks selected for analysis were obtained between 5 and 10 min of pharmacological manipulation.

Normally distributed data are presented as means ± SEM. Two-sample comparisons of these data were performed using either a paired or unpaired (as appropriate) two-tailed Student's t test and comparisons between more than two groups were performed using a one way ANOVA with Tukey's multiple comparison post-test. L-type Ca^{2+} channel sparklet activity (i.e. nP_s) datasets were bimodally distributed (1,148,149), thus two-sample comparisons of nP_s data were examined with the non-parametric Wilcoxon matched pairs test (two-tailed) and comparisons between more than two groups were performed using the non-parametric Friedman test with Dunn's multiple comparison post-test. Arithmetic means of nP_s datasets are indicated in the figures (solid grey horizontal lines) for nonstatistical visual purposes, and dashed grey lines mark the threshold for high-activity Ca^{2+} sparklet sites (n$P_s \geq 0.2$) (148-151). P values < 0.05 were considered significant and asterisks (*) used in the figures indicate a significant difference between groups.

Western blot analysis/ERK activation assay

A monolayer of αT3-1 cells (≈ 8 x 10^5 cells) in 60 mm tissue culture dishes were washed twice with PBS and incubated in serum-free DMEM for 2 hours. After serum starvation, cells were exposed to either vehicle (0.1% DMSO) or GnRH (3 nM) with or without additional treatments for 5 or 10 min (at 37°C) on the same gel. Cells were washed in ice-cold PBS and lysed in RIPA buffer containing a protease inhibitor cocktail. Total cell lysates (10 - 15 μg) were separated on 10 % SDS-PAGE gels and transferred onto nitrocellulose membranes. Phosphorylated ERK, which we used as a surrogate measure of ERK activation, was detected with p-ERK antibody (1: 2000) using the ECL prime reagent. Following stripping, total ERK was probed with anti-ERK1 antibody (1: 2000) that recognizes ERK-1 and ERK-2 independent of phosphorylation state on the same blot. Data are presented as mean ± SEM phosphorylated ERK normalized to total ERK; comparisons were performed using ANOVA with Newman-Keuls multiple comparison post-test.

2.5 Results

To test the hypothesis that acute application of GnRH induces local Ca^{2+} influx through L-type Ca^{2+} channels and ERK activation in pituitary gonadotropes we proposed five experimental criteria: 1) L-type Ca^{2+} channels must produce observable sites of localized Ca^{2+} influx (i.e., Ca^{2+} sparklets) in response to GnRH; 2) L-type Ca^{2+} channel activators must increase Ca^{2+} sparklets and ERK signaling; 3) conversely, inhibition of L-type Ca^{2+} channels must prevent Ca^{2+} sparklets and decrease ERK signaling; 4) signaling modalities known to regulate localized L-type Ca^{2+} channel function (e.g., PKC) should regulate ERK signaling in a concurrent manner, and 5) changes in actin cytoskeletal organization should disrupt GnRH-induced Ca^{2+} influx and ERK activation.

Total internal reflection fluorescence (TIRF) microscopy reveals localized Ca^{2+} influx in αT3-1 cells following GnRH exposure

Conventional experimental approaches used to investigate intracellular Ca^{2+} dynamics (e.g., wide-field fluorescence microscopy) generally provide poor signal discrimination and limited temporal and spatial resolution. To overcome these technical inadequacies, we used a combination of electrophysiology and TIRF microscopy to visualize local Ca^{2+} influx in αT3-1 cells. This approach provides high temporal and spatial resolution which is ideal for visualizing small Ca^{2+} influx events in the plasma membrane (1,184,186) due to the high signal-to-noise ratio achieved with the inherently limited depth of penetration of the TIRF evanescent wave (≈ 100 nm; Figure 2.1A).

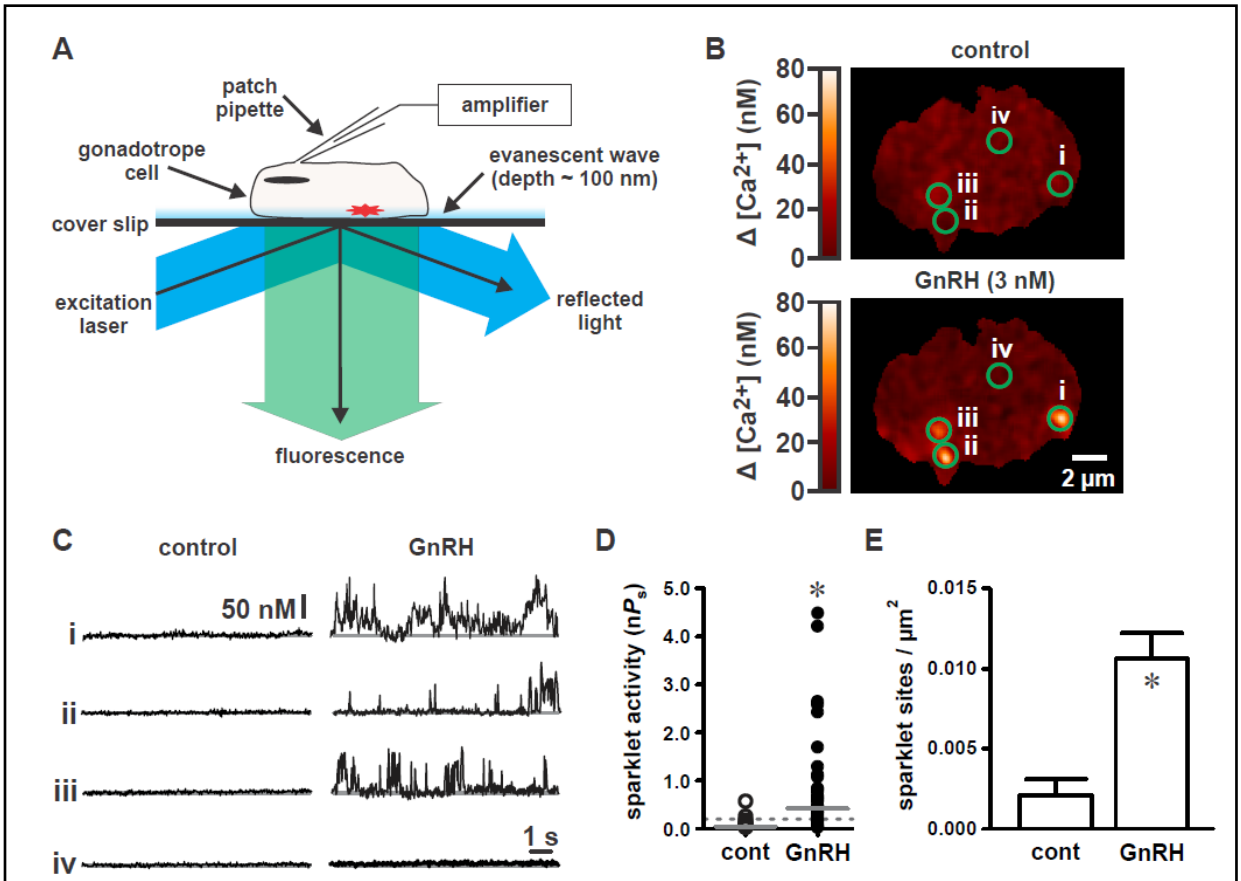

Figure 2.1. GnRH induces localized Ca^{2+} influx in αT3-1 cells. A, Schematic illustrating the electrophysiological and TIRF imaging method used to visualize Ca^{2+} influx in αT3-1 cells. B, Representative TIRF images showing localized Ca^{2+} influx in αT3-1 cells before and after GnRH (3 nM). C, Traces showing the time course of localized Ca^{2+} influx at the four circled sites before and after GnRH. The scale bar provides reference for changes in $[Ca^{2+}]_i$ during the traces (see Materials and Methods). D, Plot of Ca^{2+} sparklet site activities (nP_s; see Materials and Methods) before and after GnRH (n = 32 cells); solid grey lines are the arithmetic means of each group and dashed lines mark the threshold for high-activity Ca^{2+} sparklet sites ($nP_s \geq 0.2$; (1)). E, Plot of mean ± SEM Ca^{2+} sparklet site densities (Ca^{2+} sparklet sites/µm^2) before and after GnRH (n = 32 cells). *$P < 0.05$

To begin, we applied GnRH (3 nM) to αT3-1 cells and monitored for changes in Ca^{2+} influx across the plasma membrane. To preclude potential contaminating Ca^{2+} release events from the endoplasmic reticulum the Ca^{2+}-ATPase inhibitor thapsigargin (1 μM) was present during all experiments. In addition, cells were dialyzed with an excess of the Ca^{2+} chelator EGTA (10 mM) via the patch pipette to buffer global changes in intracellular Ca^{2+}. Consistent with our hypothesis that GnRH induces a local Ca^{2+} signal, GnRH exposure promoted discrete sites of repetitive Ca^{2+} influx (i.e., Ca^{2+} sparklets; Figure 2.1, B & C and Supplemental Movie 1; n = 32 cells). The average area of these Ca^{2+} sparklets was 2.65 ± 0.10 μm^2. Note that many areas of the plasma membrane visible in the TIRF image were optically silent (i.e., showed no evidence of Ca^{2+} influx) as illustrated by region *iv* in Figure 2.1, B & C.

To quantify Ca^{2+} sparklet activity we determined the nP_s value for each site where n is the number of quantal levels observed and P_s is the probability that the Ca^{2+} sparklet site is active (1,148,150,184). Similar to arterial smooth muscle cells (1,150), Ca^{2+} sparklet site activity (nP_s) in αT3-1 cells was bimodal with low activity sites (nP_s < 0.2) and high activity sites (nP_s ≥ 0.2). Qualitatively, low nP_s sites are characterized as having short Ca^{2+} sparklet events resulting in minimal Ca^{2+} influx while high nP_s sites have longer, more continuous Ca^{2+} sparklet events resulting in substantial Ca^{2+} influx (184). In αT3-1 cells, GnRH increased Ca^{2+} sparklet site activity (nP_s) compared to vehicle control (Figure 2.1D; $P < 0.05$, n = 32 cells). The density of detected Ca^{2+} sparklet sites (number of Ca^{2+} sparklet sites per μm^2) also increased following GnRH exposure (Figure 2.1E; $P < 0.05$, n = 32 cells). These data demonstrate that GnRH induces localized Ca^{2+} influx in αT3-1 cells by increasing the number of active Ca^{2+} sparklet sites and by increasing the activity at each of those sites.

GnRH stimulates L-type Ca^{2+} channel sparklets in αT3-1 cells which contribute to ERK activation

Next we used a pharmacological approach to test the hypothesis that Ca^{2+} sparklets observed in αT3-1 cells are produced by L-type Ca^{2+} channels. Consistent with this hypothesis,

the non-dihydropyridine (187) L-type Ca^{2+} channel agonist FPL 64176 (500 nM) increased Ca^{2+} sparklet activity and density (Figure 2.2, A & B; $P < 0.05$, n = 12 cells). Interestingly, the Ca^{2+} sparklet site activity and density following FPL 64176 exposure was not different from that induced by GnRH ($P > 0.05$). To more directly establish that Ca^{2+} sparklets induced by GnRH are produced through L-type Ca^{2+} channels we applied GnRH in the presence of the dihydropyridine L-type Ca^{2+} channel antagonist nicardipine (10 µM).

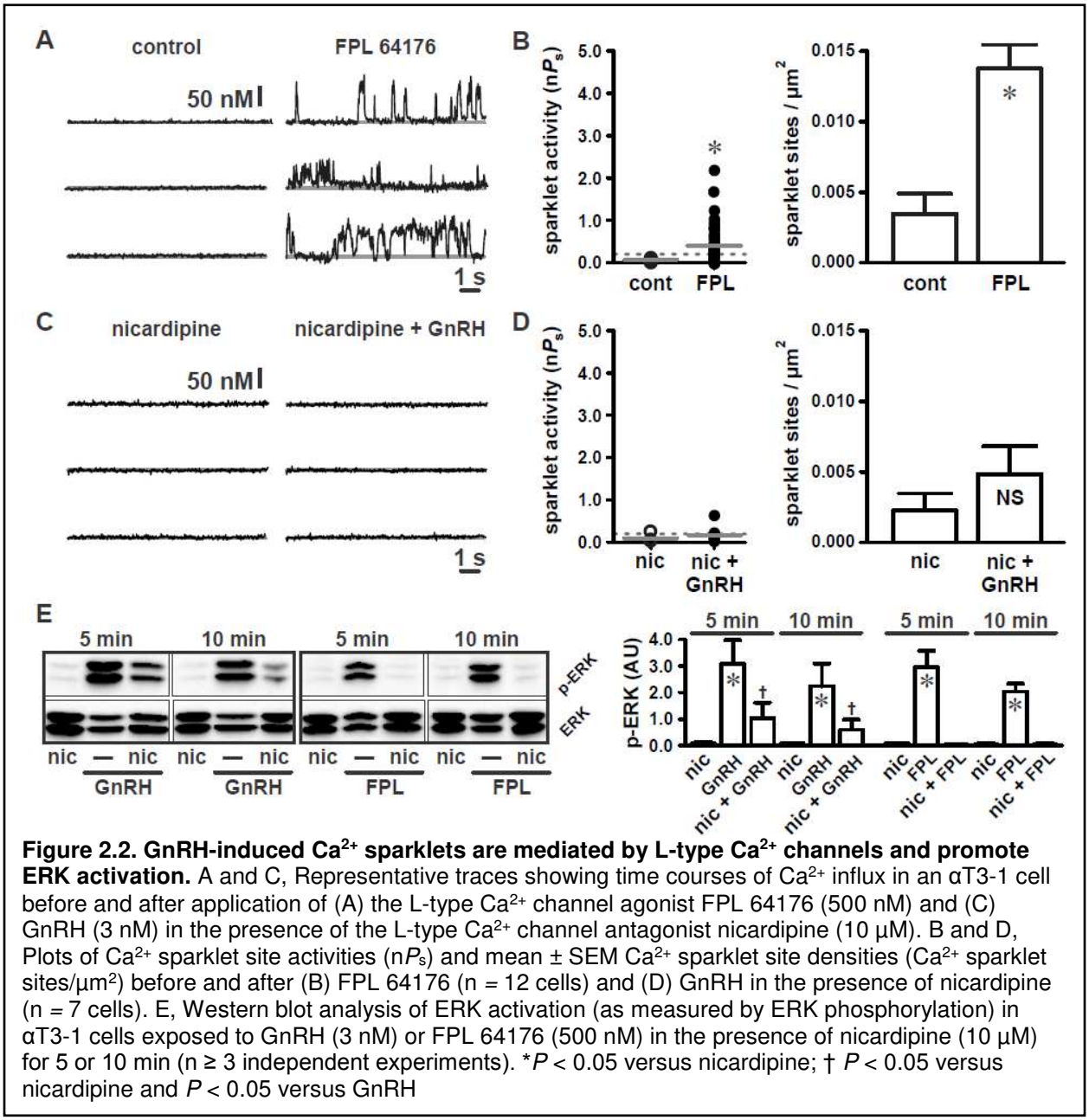

Figure 2.2. GnRH-induced Ca^{2+} sparklets are mediated by L-type Ca^{2+} channels and promote ERK activation. A and C, Representative traces showing time courses of Ca^{2+} influx in an αT3-1 cell before and after application of (A) the L-type Ca^{2+} channel agonist FPL 64176 (500 nM) and (C) GnRH (3 nM) in the presence of the L-type Ca^{2+} channel antagonist nicardipine (10 µM). B and D, Plots of Ca^{2+} sparklet site activities (nP_s) and mean ± SEM Ca^{2+} sparklet site densities (Ca^{2+} sparklet sites/µm^2) before and after (B) FPL 64176 (n = 12 cells) and (D) GnRH in the presence of nicardipine (n = 7 cells). E, Western blot analysis of ERK activation (as measured by ERK phosphorylation) in αT3-1 cells exposed to GnRH (3 nM) or FPL 64176 (500 nM) in the presence of nicardipine (10 µM) for 5 or 10 min (n ≥ 3 independent experiments). *$P < 0.05$ versus nicardipine; † $P < 0.05$ versus nicardipine and $P < 0.05$ versus GnRH

In contrast to GnRH alone (see Figure 2.1), GnRH did not significantly increase Ca^{2+} sparklet activity or density in the presence of nicardipine (Figure 2.2, C & D; $P > 0.05$, n = 7 cells). These data provide strong evidence that the subplasmalemmal Ca^{2+} influx in αT3-1 cells as a result of GnRH is due to L-type Ca^{2+} channel sparklets.

To further establish the importance of L-type Ca^{2+} channels we examined the effects of FPL 64176 (500 nM) on ERK activation in αT3-1 cells. For these and related experiments we used ERK phosphorylation as a surrogate measure of ERK activation. Similar to GnRH, FPL 64176 (which promoted localized Ca^{2+} influx; Figure 2.2A) also promoted ERK activation (Figure 2.2E; $P < 0.05$, n ≥ 3 independent experiments). Conversely, inhibition of L-type Ca^{2+} channels with nicardipine (10 μM) abolished FPL 64176-induced ERK activation (Figure 2.2E; $P > 0.05$, n ≥ 3 independent experiments). Inhibition of local L-type Ca^{2+} channel signaling with nicardipine (e.g., Figure 2.2C) attenuated but did not eliminate GnRH-dependent ERK activation (Figure 2.2E; $P > 0.05$, n ≥ 3 independent experiments). The observed loss or attenuation of ERK activation following inhibition of localized L-type Ca^{2+} channel activity in these experiments supports the hypothesis that localized L-type Ca^{2+} channel function regulates ERK activation in αT3-1 cells.

PKC promotes localized L-type Ca^{2+} channel signaling and subsequent ERK activation in response to GnRH

In arterial smooth muscle cells PKC promotes localized L-type Ca^{2+} channel sparklet activity similar to what we describe after GnRH exposure in αT3-1 cells (1,184). In gonadotropes PKC is known to induce global Ca^{2+} signals via dihydropyridine-sensitive Ca^{2+} channels in response to GnRH (86). Accordingly, we hypothesized that exposing αT3-1 cells to GnRH induces GnRH receptor-dependent PKC activation which in turn stimulates local L-type Ca^{2+} channel sparklets. Consistent with this hypothesis, the PKC agonist phorbol 12, 13-dibutyrate (PDBu; 50 nM) increased L-type Ca^{2+} channel sparklet site activity and density (Figure 2.3, A & B; $P < 0.05$, n = 11 cells). The increase in L-type Ca^{2+} channel sparklet activity and density

induced by PDBu was not different from that observed with GnRH or FPL 64176 (see Figures 2.1 and 2.2; $P > 0.05$). Suggesting that the population of L-type Ca^{2+} channels stimulated by GnRH and PDBu are one in the same, the effects of GnRH and PDBu were not additive with respect to Ca^{2+} sparklet activity (median GnRH nP_s = 0.19, interquartile range = 0.41; median GnRH + PDBu nP_s = 0.24, interquartile range = 0.71; $P > 0.05$, n = 16 cells) or density (GnRH density = 0.010 ± 0.002 sparklet sites/μm^2; GnRH + PDBu density = 0.007 ± 0.001 Ca^{2+} sparklet sites/μm^2; $P > 0.05$, n = 16 cells).

We then used the broad-spectrum PKC inhibitor GF109203X (188,189) to link GnRH-dependent activation of PKC to stimulation of L-type Ca^{2+} channel sparklets. Indicative of the necessity of PKC, inhibition with GF109203X (GFX; 1 μM) abolished GnRH-dependent stimulation of L-type Ca^{2+} channel sparklets (Figure 2.3, C & D; $P > 0.05$, n = 9 cells). At a concentration of 1 μM GFX inhibits the following PKC isoforms known to be expressed in αT3-1 cells: α, β, δ, and ε (190). To narrow our investigation of the isoforms involved with L-type Ca^{2+} channel sparklets in αT3-1 cells we used the PKC inhibitor Gö6976 which is selective for PKCα and β (191). Application of Gö6976 (100 nM) had no significant effect on GnRH-dependent stimulation of L-type Ca^{2+} channel sparklet activity (median GnRH nP_s = 0.19, interquartile range = 0.41; median GnRH + Gö6976 nP_s = 0.06, interquartile range = 0.43; $P > 0.05$, n = 7 cells) or density (GnRH density = 0.010 ± 0.002 sparklet sites/μm^2; GnRH + Gö6976 density = 0.011 ± 0.002 Ca^{2+} sparklet sites/μm^2; $P > 0.05$, n = 7 cells). These data indicate that PKCα and β are not essential for GnRH-dependent activation of L-type Ca^{2+} channels in αT3-1 cells. This observation is consistent with previous work suggesting that PKCδ and ε play a greater role in GnRH-dependent ERK activation than PKCα and β (190).

In agreement with our Ca^{2+} sparklet data, PKC stimulation with PDBu (50 nM) increased ERK activation (Figure 2.3E; $P < 0.05$, n ≥ 3 independent experiments). Demonstrating the necessity of Ca^{2+} influx through L-type Ca^{2+} channels, αT3-1 cells pre-incubated with nicardipine (10 μM) showed no significant increase in ERK signaling following PDBu exposure (Figure 2.3E;

$P > 0.05$, n ≥ 3 independent experiments). Once again in agreement with the effect on Ca^{2+} sparklets, PKC inhibition with GFX (1 μM) reduced GnRH-dependent ERK activation (Figure 2.3E; $P < 0.05$, n ≥ 3 independent experiments) while Gö6976 (1 μM) was without effect ($P > 0.05$, n ≥ 3 independent experiments; data not shown). Note that PKC inhibition with GFX had no effect on ERK phosphorylation induced by direct stimulation of L-type Ca^{2+} channels with FPL 64176 (Figure 2.3E; $P > 0.05$, n ≥ 3 independent experiments).

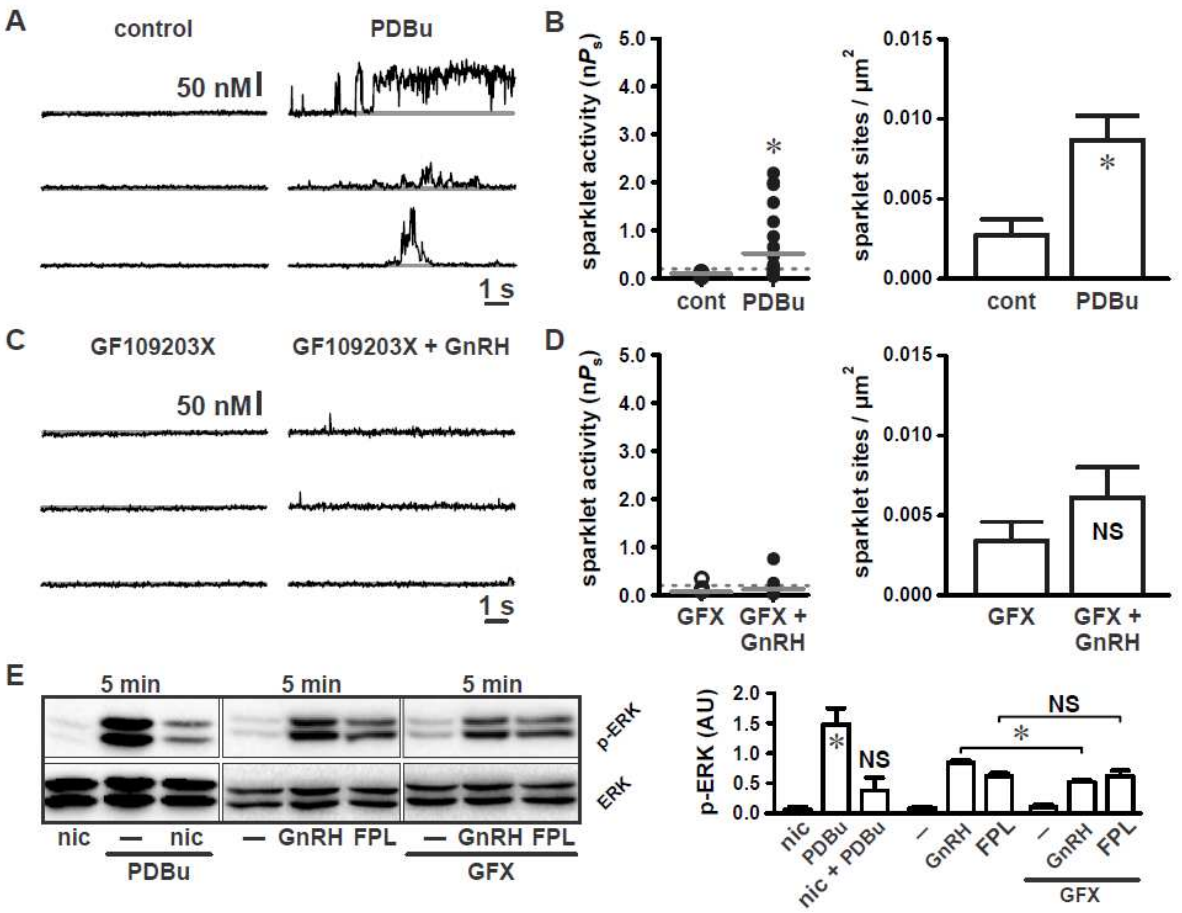

Figure 2.3. GnRH-induced L-type Ca^{2+} channel sparklets and ERK activation require PKC. A and C, Representative traces showing time courses of Ca^{2+} influx in an αT3-1 cell before and after application of (A) the PKC activator PDBu (50 nM) and (C) GnRH (3 nM) in the presence of the broad-spectrum PKC inhibitor GF109203X (GFX; 1 μM). B and D, Plots of Ca^{2+} sparklet site activities (nP_s) and mean ± SEM Ca^{2+} sparklet site densities (Ca^{2+} sparklet sites/μm^2) before and after (B) PDBu (n = 11 cells) and (D) GnRH in the presence of GF109203X (n = 9 cells). E, Western blot analysis of ERK activation (as measured by ERK phosphorylation) in αT3-1 cells exposed to PDBu (50 nM) or PDBu with nicardipine (1 μM) for 5 min and αT3-1 cells exposed to GnRH (3 nM) or FPL 64176 (500 nM) for 5 min in the presence or absence of GF109203X (1 μM; n ≥ 3 independent experiments). *$P < 0.05$

This suggests that PKC activity occurs upstream of L-type Ca^{2+} channels in the signaling cascade linking GnRH receptor stimulation to ERK activation. Taken together, our data indicate that GnRH induces localized PKC-dependent L-type Ca^{2+} channel sparklets and that this mechanism plays a fundamental role in GnRH-dependent activation of ERK signaling in αT3-1 cells.

A dynamic actin cytoskeleton is necessary for transducing GnRH receptor activation to localized Ca^{2+} influx and ERK activation

Our data support the concept that precise structural and molecular elements create a microenvironment suitable for localized subplasmalemmal L-type Ca^{2+} channel signaling necessary for gonadotrope function. Thus, it is logical to suggest that cellular structural features such as the cortical actin cytoskeleton could be involved in the organization of molecular components responsible for transducing GnRH receptor activation to the L-type Ca^{2+} channel. In accordance with this hypothesis, previous work has demonstrated that rapid remodeling of the actin cytoskeleton occurs following GnRH treatment and that an intact actin cytoskeleton is necessary for GnRH signaling to ERK (57,58,125). However, the point(s) in this pathway where actin dynamics participate in ERK activation is (are) unclear.

Therefore, we investigated if actin dynamics are involved with GnRH induction of localized Ca^{2+} sparklets upstream of ERK activation to narrow down where actin reorganization may be necessary in this signaling pathway. To begin we examined the effect of jasplakinolide (100 nM for 5 min), which stabilizes filamentous actin, on localized L-type Ca^{2+} channel function. By itself, jasplakinolide had no effect on basal L-type Ca^{2+} channel activity (Figure 2.4, B & C; $P > 0.05$, n = 9 cells). However, jasplakinolide reduced the stimulatory effect of GnRH (3 nM) on L-type Ca^{2+} channel sparklet activity (Figure 2.4, A & B; $P < 0.05$, n = 9 cells).

Consistent with previous work (58), ERK activation in response to GnRH was also reduced by jasplakinolide (Figure 2.4D; $P < 0.05$; n ≥ 3 independent experiments).

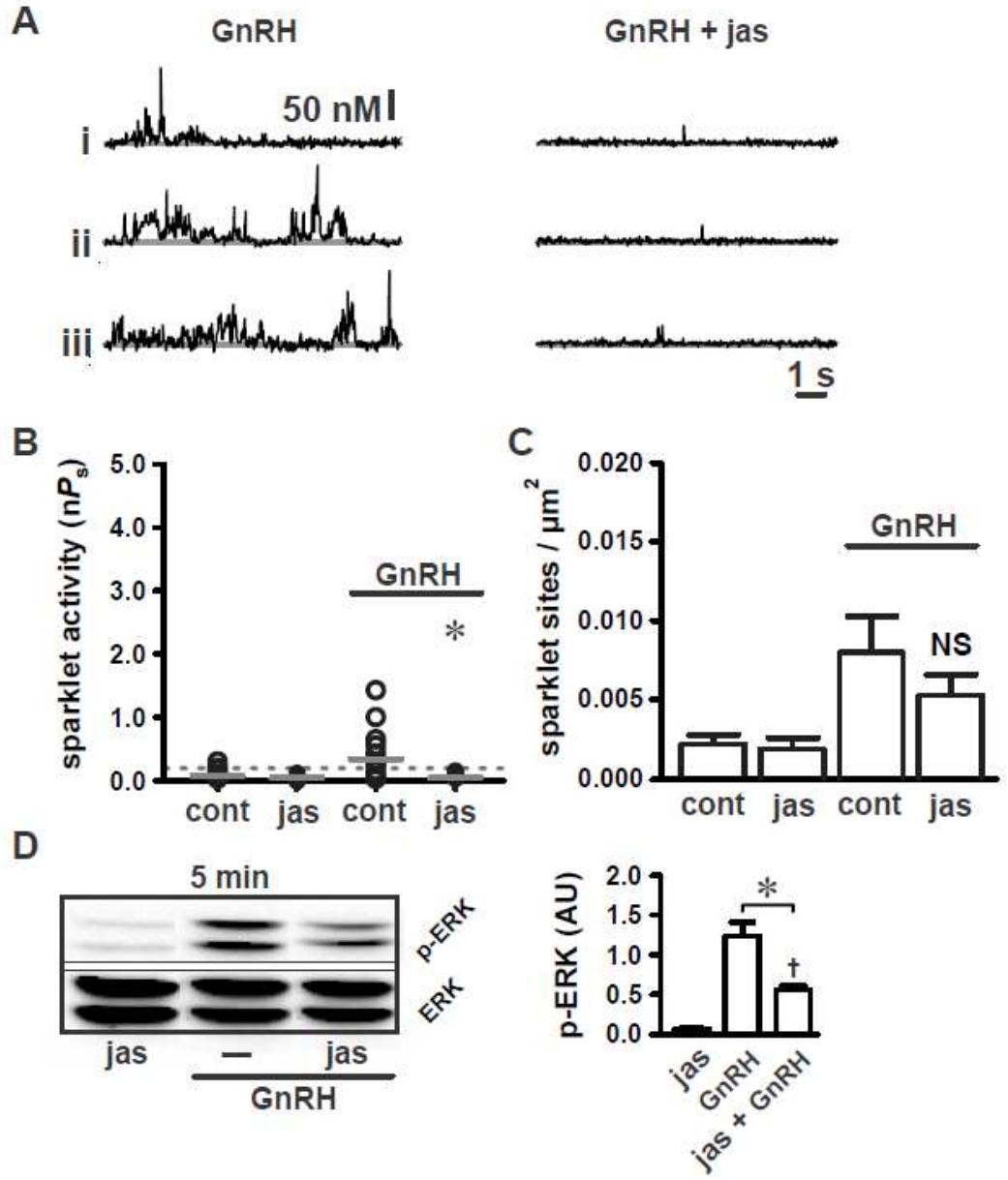

Figure 2.4. Actin stabilization disrupts GnRH-dependent Ca^{2+} sparklet stimulation. A, Representative traces showing time courses of Ca^{2+} influx in αT3-1 cells exposed to GnRH (3 nM) in the presence or absence of jasplakinolide (100 nM for 5 min). B and C, Plots of Ca^{2+} sparklet site activities (nP_s) and mean ± SEM Ca^{2+} sparklet site densities (Ca^{2+} sparklet sites/μm^2) for GnRH (3 nM; n = 9 cells in each group) with or without jasplakinolide (100 nM for 5 min). D, Western blot analysis of ERK activation (as measured by ERK phosphorylation) in αT3-1 cells exposed to GnRH (3 nM) with or without jasplakinolide (100 nM for 5 min; n ≥ 3 independent experiments). *$P < 0.05$; † $P < 0.05$ versus jasplakinolide and $P < 0.05$ versus GnRH

Unlike Ca^{2+} sparklet site activity (i.e., nP_s), Ca^{2+} sparklet site density (i.e., the number of Ca^{2+} sparklet sites/μm^2) in response to GnRH was not reduced by jasplakinolide (Figure 2.4C; $P >$ 0.05; n = 9 cells). These observations suggest that actin stabilization does not perturb the

number of functional L-type Ca^{2+} channels available for stimulation following GnRH application. Rather, actin stabilization with jasplakinolide disrupts the ability of GnRH signaling to evoke high-activity Ca^{2+} sparklet sites.

To test this hypothesis we examined the effect of the direct L-type Ca^{2+} channel activator FPL 64176 (500 nM) on Ca^{2+} sparklets in the presence and absence of jasplakinolide. In contrast to GnRH, jasplakinolide had no inhibitory effect on Ca^{2+} sparklet activation by FPL 64176 (Figure 2.5, A & C; $P > 0.05$; n = 8). Jasplakinolide also had no effect on Ca^{2+} sparklet density (i.e., the number of Ca^{2+} sparklet sites/μm^2; Figure 2.5D; $P > 0.05$; n = 8) induced by FPL 64176 and had no effect on subsequent ERK activation (Figure 2.5E; $P > 0.05$; n ≥ 3 independent experiments). These observations are consistent with the hypothesis that stabilization of filamentous actin disrupts communication between the GnRH receptor and the L-type Ca^{2+} channel rather than interfering with the L-type Ca^{2+} channel itself or subsequent ERK activation.

The observed effects of jasplakinolide indicate that actin dynamics are important for the transduction of GnRH receptor activation to stimulation of the L-type Ca^{2+} channel. Given the importance of PKC in this transduction pathway (128) and the data presented above (Figure 2.3) we examined the effect of the PKC activator phorbol 12, 13-dibutyrate (PDBu; 50 nM) on cells pretreated with jasplakinolide. In contrast to GnRH, but similar to FPL64176, jasplakinolide had no effect on PDBu-dependent stimulation of Ca^{2+} sparklets (Figure 2.5, B, C & D; $P > 0.05$, n = 11 cells) and ERK activation (Figure 2.5E; $P > 0.05$; n ≥ 3 independent experiments). These data suggest that stabilization of filamentous actin does not preclude PKC-dependent activation of local L-type Ca^{2+} channel function and ERK activation. Taken together, our data support the concept that precise structural and molecular elements create a microenvironment suitable for localized subplasmalemmal Ca^{2+} signaling necessary for gonadotrope function.

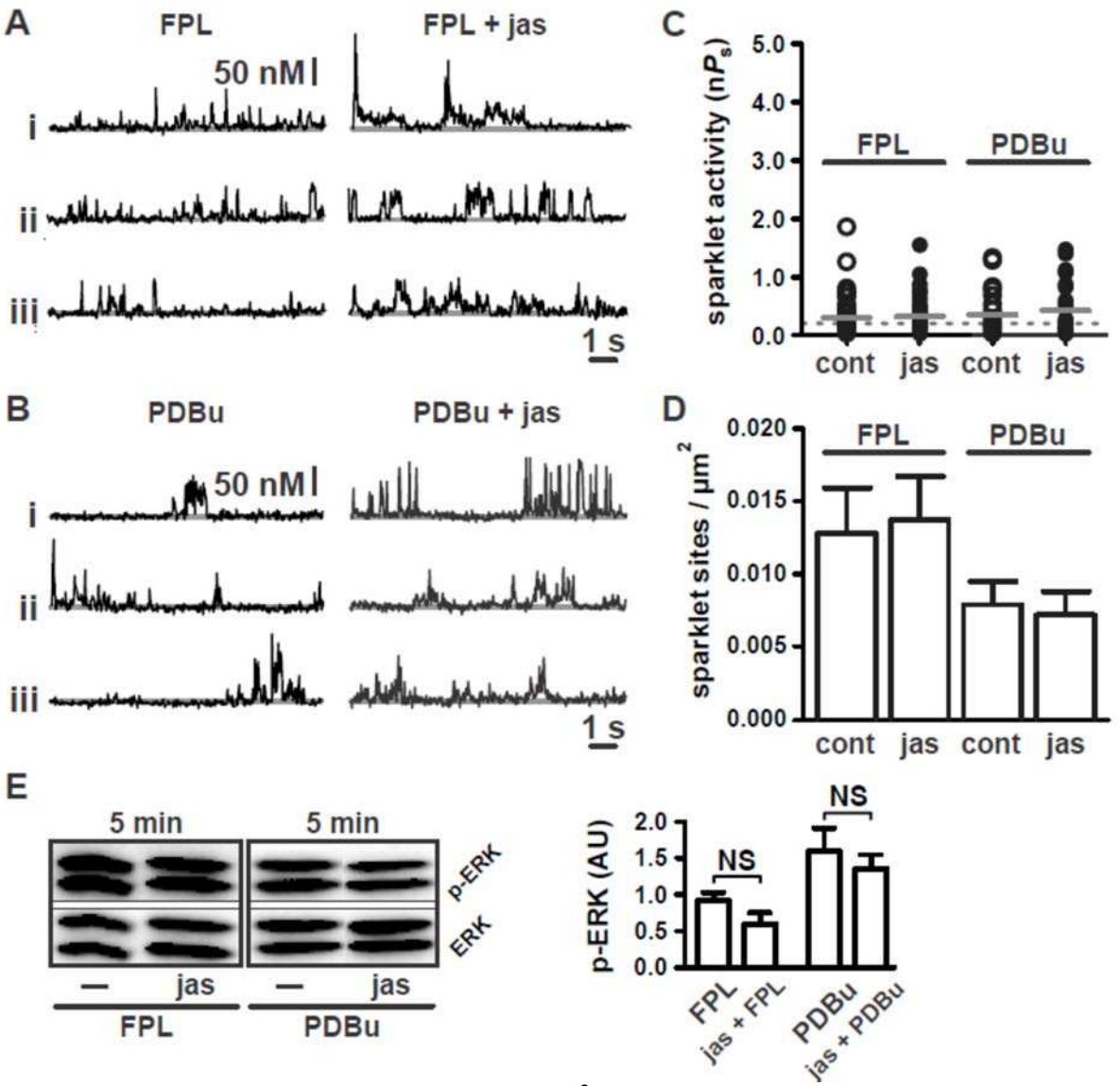

Figure 2.5. Actin stabilization does not disrupt Ca^{2+} sparklet stimulation by direct activation of L-type Ca^{2+} channels or PKC. A and B, Representative traces showing time courses of Ca^{2+} influx in αT3-1 cells exposed to (A) the L-type Ca^{2+} channel agonist FPL 64176 (500 nM) or (B) the PKC activator PDBu (50 nM) with or without jasplakinolide (100 nM for 5 min). C and D, Plots of Ca^{2+} sparklet site activities (nP_s) and mean ± SEM Ca^{2+} sparklet site densities (Ca^{2+} sparklet sites/μm^2) for FPL 64176 (500 nM; n = 8 cells in each group) and PDBu (50 nM; n = 11 cells in each group) with or without jasplakinolide (100 nM for 5 min). E, Western blot analysis of ERK activation (as measured by ERK phosphorylation) in αT3-1 cells exposed to FPL 64176 (500 nM) and PDBu (50 nM) with or without jasplakinolide (100 nM for 5 min; n ≥ 3 independent experiments). *$P < 0.05$

2.6 Discussion

Consistent with the hypothesis that GnRH binding to the GnRH receptor evokes a rapid increase in localized subplasmalemmal Ca^{2+} signals that lead to ERK activation in αT3-1

gonadotropes we find that: 1) GnRH application promoted experimentally evident localized sites of Ca^{2+} influx across the plasma membrane (i.e., Ca^{2+} sparklets); 2) direct pharmacological activation of L-type Ca^{2+} channels induced localized Ca^{2+} influx and increased ERK signaling; 3) pharmacological inhibition of L-type Ca^{2+} channels decreased observable Ca^{2+} influx events and decreased ERK signaling; 4) PKC activation, which is associated with increased ERK signaling in gonadotropes and stimulation of L-type Ca^{2+} channel sparklets in arterial myocytes (1,149,150), increased localized L-type Ca^{2+} channel function in αT3-1 cells; 5) PKC inhibition decreased GnRH-dependent stimulation of L-type Ca^{2+} channel sparklets and ERK activation; and 6) actin cytoskeletal rearrangement, which is involved with GnRH receptor signaling (57,58,125), is necessary for GnRH-induced stimulation of localized Ca^{2+} influx through L-type Ca^{2+} channels and ERK activation. From these observations we conclude that GnRH-dependent activation of ERK signaling in αT3-1 gonadotropes requires localized PKC-dependent L-type Ca^{2+} channel activity.

Our data provide strong evidence that Ca^{2+} influx in αT3-1 gonadotropes is highly localized across the plasma membrane (see Supplemental Movie 1). To quantify the spatial confinement of the observed Ca^{2+} influx we compared the average Ca^{2+} sparklet surface area ($2.65 \pm 0.10\ \mu m^2$) to the estimated total surface area of the αT3-1 cells studied ($2096 \pm 56.04\ \mu m^2$) as determined by cell capacitance measurements obtained with voltage clamp (192). Individual Ca^{2+} sparklet sites therefore corresponded to ≈ 0.13% (2.65/2096) of the αT3-1 cell surface area; each cell had ≈ 20.96 ± 0.56 active sites ($2096\ \mu m^2$ x 0.01 Ca^{2+} sparklet sites/μm^2). Thus, in αT3-1 cells stimulated with GnRH, Ca^{2+} influx was highly localized and limited to ≈ 2.72% (0.13% x 20.96) of the total surface area. In addition, high activity ($nP_s \geq 0.2$) Ca^{2+} sparklet sites with values > 1 were occasionally observed. This is of interest as it indicates clustering and functional coupling of L-type Ca^{2+} channels (186,193). Future experiments to

characterize the biochemical nature of these clusters in gonadotropes in greater detail are needed.

Previous efforts using conventional experimental approaches have established the importance of PKC-mediated Ca^{2+} influx through L-type Ca^{2+} channels with respect to ERK activation in gonadotropes (86,128). On the basis of substantial indirect evidence a local Ca^{2+} signaling mechanism was hypothesized. Using our experimental approach we are able to visualize Ca^{2+} influx through L-type Ca^{2+} channels. This allows us not only to test directly and confirm a local Ca^{2+} signaling hypothesis but also permits investigation of participating signaling components (e.g., PKC and actin cytoskeletal dynamics) with unprecedented spatial and temporal resolution. Our data demonstrate that GnRH and PDBu stimulate Ca^{2+} sparklet activity within 5 min (at 22-25°C). This time course is similar to that observed by direct channel activation with the L-type Ca^{2+} channel activator FPL 64176. Consistent with a highly localized signaling process, GnRH receptor stimulation and (subsequent) PKC stimulation therefore appears to involve a relatively rapid mechanism of L-type Ca^{2+} channel activation.

Consistent with previous work (190) and our Ca^{2+} sparklet data, we found that inhibition of PKC with the broad-spectrum PKC inhibitor GF109203X (but not the PKCα/β selective inhibitor Gö6976) reduced GnRH-dependent activation of ERK signaling. These observations suggest that other PKC isoforms such as PKCδ and/or PKCε are involved in ERK activation in αT3-1 cells. Future experiments with isoform-specific PKC inhibitors and isoform-selective knockdown approaches are necessary to further clarify the PKC isoform(s) involved with GnRH-dependent activation of L-type Ca^{2+} channels. Note that PKC inhibition with GF109203X produced a modest reduction in ERK activation when compared to L-type Ca^{2+} channel inhibition with nicardipine. One scenario likely contributing to this observation involves differences in the effect of nicardipine and PKC inhibition on L-type channel Ca^{2+} sparklets: Nicardipine inhibits low ($nP_s < 0.2$) and high activity ($nP_s \geq 0.2$) L-type channel Ca^{2+} sparklets whereas the effects of PKC inhibition are limited primarily to high activity Ca^{2+} sparklets

(1,150,184,194). In addition, when using 2 mM external Ca^{2+}, as in our experiments, many low activity Ca^{2+} sparklets are likely below our detection threshold (1). Thus, substantial low activity Ca^{2+} sparklets (not necessarily evident in our recordings) present following PKC inhibition could result in more Ca^{2+} influx and ERK activation as compared to L-type Ca^{2+} channel inhibition with nicardipine.

The findings presented here are consistent with previous research in arterial smooth muscle cells where localized L-type Ca^{2+} channel sparklets were previously described (1,148,150,184,186,195). Similar to the vasoconstrictor angiotensin II (148,196), which stimulates G_q-coupled AT1 receptors (197), GnRH receptor activation promoted Ca^{2+} influx in αT3-1 cells by increasing Ca^{2+} sparklet site activity (nP_s) and density (sites per μm^2). As with Ca^{2+} sparklet activity in arterial smooth muscle cells, Ca^{2+} sparklets in αT3-1 cells were stimulated by L-type Ca^{2+} channel agonists and inhibited by L-type Ca^{2+} channel antagonists (1,150). Also similar to arterial smooth muscle (1,148,150,194,198), L-type channel Ca^{2+} sparklets in αT3-1 cells are subject to PKC regulation (see Figure 2.3). However, in contrast to arterial smooth muscle where PKCα is the isoform responsible for stimulation of L-type channel Ca^{2+} sparklets (150), GnRH-dependent activation of Ca^{2+} sparklets in αT3-1 cells does not appear to be dependent on PKCα but rather seems to require other isoforms such as PKCδ and/or ε. Future studies should focus on clarifying this important issue.

While PKC is known to activate ERK, the underling mechanism remains unclear (100,181,199). Direct activation of Raf-1 kinase by PKC has been proposed with little supporting evidence and Raf-1 involvement in GnRH-dependent activation of ERK activation is not apparent (2). Here, we demonstrate that GnRH-dependent activation of PKC stimulates Ca^{2+} influx through L-type Ca^{2+} channels. Further emphasizing the temporal relationship between GnRH receptor and L-type Ca^{2+} channel activation is our observation of enhanced ERK phosphorylation (via Western blot analysis) within 5 min of GnRH application (at 37°C). Thus, the time course of L-type Ca^{2+} channel sparklet activation (recordings made between 5 and 10

min after applying GnRH) roughly parallels that of ERK activation. Furthermore, our Western blot data (at 5 and 10 min) supports previous work where ERK was shown to be maximally phosphorylated within 5-15 min. (190). Future efforts are necessary to clarify the intermediate molecular mechanisms by which PKC stimulation of L-type Ca^{2+} channels leads to ERK activation in gonadotropes.

Our data demonstrate the importance of spatially restricted subplasmalemmal Ca^{2+} microdomain signaling in mediating ERK activation in response to GnRH receptor stimulation. These findings suggest that a local Ca^{2+} signal (i.e., L-type Ca^{2+} channel sparklets) could promote discrete sites of ERK activation at or near the sites of Ca^{2+} influx. Consistent with this hypothesis, work in pancreatic beta cells has shown that localized Ca^{2+}influx through L-type Ca^{2+} channels was sufficient for activating ERK in response to glucagon-like peptide-1 (200). In gonadotropes, evidence supporting the concept of localized ERK activation includes the observation that phosphorylated ERK not only associates with membrane fractions containing the GnRH receptor but the two proteins also coimmunoprecipitate with one another (54). Given these observations we hypothesize that the localized L-type Ca^{2+} channel sparklet signaling described in this study could lead to localized ERK activation at the sites of Ca^{2+} influx. Future studies are required to examine this important concept.

Dynamic remodeling of the actin cytoskeleton is necessary for GnRH receptor-dependent ERK activation (57,58,125). Here, we have identified that the necessity of actin cytoskeletal organization occurs downstream of GnRH receptor activation but upstream of PKC-dependent activation of L-type Ca^{2+} channels as direct stimulation of the channels (with FPL 64176) or PKC (with PDBu) leads to Ca^{2+} influx in the presence of jasplakinolide. These data suggest that stabilization of filamentous actin does not preclude PKC-dependent activation of local L-type Ca^{2+} channel function and ERK activation *per se*. However, as global phorbol ester-induced activation of PKC is non-physiological it is unreasonable to conclude that actin dynamics are not involved with physiologically relevant instances of PKC activation (e.g., by

GnRH receptor stimulation). Future studies are required to address this important issue and to further dissect the role of actin cytoskeletal dynamics with respect to the subcellular structural organization required for the generation of biologically-relevant L-type channel Ca^{2+} microdomains in gonadotropes.

Although we provide compelling evidence demonstrating the importance of localized Ca^{2+} influx in mediating ERK activation, our observations do not preclude the involvement of other mechanisms. Close inspection of our data suggests that other mechanisms could be involved. PKC inhibition and actin cytoskeletal disruption with jasplakinolide abolished the stimulatory effect of GnRH on L-type Ca^{2+} channels but the inhibitory effects on ERK activation were incomplete. Similarly, nicardipine eliminated L-type Ca^{2+} channel sparklet activity in response to GnRH but did not fully eliminate changes in ERK phosphorylation. These findings are in contrast to experiments where we bypassed GnRH receptor signaling altogether and stimulated the L-type Ca^{2+} channels directly with FPL 64176. With this approach we found that nicardipine not only eliminated Ca^{2+} sparklet activity but also abolished FPL 64176-mediated ERK activation. Taken together, we conclude that while local L-type Ca^{2+} channel signaling is a major mechanism underlying ERK activation in response to GnRH other contributing mechanisms are likely involved.

In summary, we provide the first direct evidence for localized, subplasmalemmal Ca^{2+} signaling in gonadotropes. Since our approach allows us to detect and quantify GnRH-induced Ca^{2+} sparklets in real time, the field is now positioned to address an entirely new set of questions as to the identity of proximate cellular and molecular events that convey the extracellular GnRH signal to its most distal and biologically critical intracellular targets. From the therapeutic perspective this is key as the ability of the gonadotrope to integrate multiple molecular events in response to a GnRH signal resides at the core of the hypothalamic-pituitary-gonadal axis and, thus, reproductive function in mammals. In light of this, it is not surprising that the gonadotrope is the primary target of the vast majority of pro- and anti-fertility drugs (201-

204). Thus, increasingly refined pharmacological modulation of reproductive and sexual function unequivocally depends on a complete understanding of GnRH signaling in the pituitary. Finally, understanding localized Ca^{2+} signaling in αT3-1 cells may well have relevance beyond GnRH action. Indeed, the similarities between L-type Ca^{2+} channel sparklets in arterial smooth muscle (186) and pituitary endocrine cells suggests a conserved signaling mechanism fundamental to a diverse group of physiological and cellular processes.

Chapter 3. Reactive Oxygen Species Modulate GnRH-induced Local L-type Ca^{2+} Channel Signaling in Gonadotropes

3.1 Overview

The previous chapter outlined novel characteristics of L-type Ca^{2+} channel activity in gonadotropes. Now that we have discovered GnRH activation of localized Ca^{2+} influx on the cell surface, our next goal was to examine intermediate players within this physiological cascade. Given the endless possibilities, we narrowed our focus to signaling molecules that would most likely regulate these L-type Ca^{2+} channel sparklets based on stringent criteria. These parameters include identifying molecular candidates capable of localized signaling with rapid and sensitive cellular responses. Molecules with slower activation kinetics would be inconsistent in modulating this receptive and dynamic GnRH signaling cascade that leads to L-type Ca^{2+} channel activation. In addition, likely candidates would have inherent properties to signal in organized compartments, and in this case, specifically at the plasma membrane. Finally, the intermediate would also need to have evidence of modulating Ca^{2+} and be regulated by GnRH in gonadotropes for physiological relevance. Given this paradigm, a prospective candidate that encompasses all these characteristics led us to focus on reactive oxygen species (ROS). ROS are ubiquitous signaling molecules that regulate multiple aspects of cell function, and identifying whether they play a role in gonadotropes and L-type Ca^{2+} channel signaling would provide great insight for reproduction and further understanding of conditions in which oxidative imbalance would create aberrant signaling and complications.

3.2 Summary

The binding of GnRH to its receptor on gonadotrope cells initiates signaling cascades that result in the activation of extracellular signal-regulated kinase (ERK) and subsequently enhanced LH biosynthesis. Most dramatic is the sharp rise in LH secretion (“LH surge”) that precedes and is necessary for follicular maturation and ovulation. Previous work has

established that Ca^{2+} influx through L-type Ca^{2+} channels is necessary for ERK phosphorylation. More recently, we have identified discrete microdomains of GnRH-induced Ca^{2+} influx mediated by L-type Ca^{2+} channels ("Ca^{2+} sparklets"). ROS are cognate signaling molecules that mediate cell function, but their role in regulating Ca^{2+} in gonadotropes is unknown. We hypothesize that ROS are modulated by GnRH and are important in modulating local L-type Ca^{2+} channel activity. We found that GnRH induced spatially localized ROS "puncta" in αT3-1 cells. Using a combination of electrophysiology and TIRF microscopy to visualize discrete sites of Ca^{2+} influx, we found that hydrogen peroxide (H_2O_2) increased local Ca^{2+} channel activity in both αT3-1 cells and mouse gonadotropes. Conversely, inhibition of endogenous ROS decreased GnRH-mediated ROS formation and Ca^{2+} influx on the plasma membrane. Mitochondria are another important source of ROS, in which GnRH stimulation increased mitochondrial oxidation activity at the subplasmalemmal surface of gonadotropes and mitochondrial ROS increased L-type Ca^{2+} channel activity. In addition, active L-type Ca^{2+} channels are associated with subplasmalemmal mitochondria. Collectively, these data provide strong evidence that ROS signaling plays an important role in GnRH-dependent Ca^{2+} channel activity in gonadotropes.

3.3 Introduction

The hypothalamic-pituitary-gonadal (HPG) axis regulates reproductive function and requires precise signaling events. The HPG axis signaling cascade is initiated by gonadotropin-releasing hormone (GnRH), a hypothalamic neuropeptide that is secreted into the hypophyseal portal system and binds to GnRH receptors on anterior pituitary cells called gonadotropes. Gonadotropes synthesize and secrete the gonadotropins luteinizing hormone (LH) and follicle stimulating hormone (FSH). In females, an acute rise in LH is obligatory for inducing ovulation and as such is a mandatory event for reproduction and fertility.

Following activation of the GnRH receptor, $G\alpha_q$ proteins stimulate phospholipase C (PLC) leading to cleavage of phosphatidylinositol-4-5-bisphosphate (PIP_2) and generation of the second messengers inositol-1,4,5-trisphosphate (IP_3) and diacylglycerol (DAG) (205). While IP_3

promotes Ca^{2+} release from the endoplasmic reticulum (ER), DAG stimulates protein kinase C (PKC) which ultimately increases Ca^{2+} influx through voltage-dependent L-type Ca^{2+} channels. These two Ca^{2+} signals activate key components necessary for ovulation, including mitogen-activated protein kinases (MAPKs). MAPKs transduce signals from the cell surface to the nucleus where phosphorylation initiates transcriptional activation of gonadotropin genes.

A large body of evidence indicates that jun-N-terminal kinase (JNK) activation relies on Ca^{2+} from the ER while Ca^{2+} influx via L-type Ca^{2+} channels is necessary for activating extracellular signal-regulated kinase (ERK) (86,128). The divergence of Ca^{2+}-dependent regulation of ERK and JNK is an exquisite demonstration of the importance of spatially restricted Ca^{2+} signaling. Furthermore, we have demonstrated that Ca^{2+} channel influx occurs at very discrete, localized sites on the plasma membrane termed "Ca^{2+} sparklets" in gonadotropes (206). These microdomains of Ca^{2+} influx are regulated by GnRH and PKC, occur through the L-type Ca^{2+} channel, and are fundamental for downstream ERK activation necessary for LH production.

Our primary goal now is to understand specific molecular signaling mechanisms that modulate L-type Ca^{2+} channel activity following GnRH receptor activation in gonadotropes. Reactive oxygen species (ROS) are recognized as cognate signaling molecules that regulate cell function. Interestingly, evidence suggests that GnRH-dependent ERK signaling also involves ROS (180). However, the mechanistic role of ROS upstream of these MAPK events has not been investigated in gonadotropes. We hypothesize that ROS are important in regulating localized L-type Ca^{2+} channels in gonadotropes. The functional relationships between Ca^{2+} and ROS signaling pathways, as well as underlying mechanisms, are unknown in gonadotropes. Ca^{2+} and ROS are ubiquitous signaling molecules that, as second messengers, share four key attributes relevant to this hypothesis: **1)** Ca^{2+} and ROS signaling cascades can reside spatially in subcellular compartments (79,164); **2)** Ca^{2+} and ROS signaling events have been shown to be functionally coupled (207,208); **3)** the vast majority of cells employ Ca^{2+} and

ROS signaling cascades for specific cellular functions; and **4)** disruption of Ca^{2+} and ROS homeostasis is strongly associated with the development of major chronic diseases including but not limited to metabolic, endocrine, neoplastic, cardiovascular, and neurodegenerative pathologies (209-212). Understanding how ROS can mediate downstream Ca^{2+} channel activity following GnRH receptor activation can provide further insight into signaling mechanisms used in gonadotropes necessary for reproduction. However, given the range of Ca^{2+} and ROS signaling and the various mechanisms they regulate, conclusions and concepts from these findings can be applicable to many biological systems.

The sources of ROS in many cell types include the plasmalemmal NADPH oxidase enzyme complexes and the mitochondrial electron transport chain. Therefore, we explored GnRH regulation of both NADPH oxidase and mitochondrial sources of ROS and how these ROS generators modulate L-type Ca^{2+} channel activity in gonadotropes. In addition, we also explored GnRH-mediated mitochondrial oxidation changes, and the localization of ROS at the subplasmalemmal surface and its relative distribution compared to active Ca^{2+} sparklet sites.

We found that GnRH induced localized, punctate ROS formation on the subplasmalemmal surface in gonadotropes. In addition, hydrogen peroxide (H_2O_2) stimulated localized Ca^{2+} influx through L-type Ca^{2+} channels in both αT3-1 cells and primary mouse gonadotropes. Conversely, endogenous ROS played a role in GnRH-mediated ROS formation and Ca^{2+} influx on the plasma membrane since inhibition of ROS with catalase and NADPH oxidase inhibitors prevented increases in subplasmalemmal ROS generation and Ca^{2+} channel activity. In addition, GnRH modulated mitochondrial oxidation and ROS from mitochondrial sources affected L-type Ca^{2+} channel sparklets. We also found active L-type Ca^{2+} channels associated with subplasmalemmal mitochondria in gonadotropes. Taken together, we have identified functionally coupled Ca^{2+} and ROS microdomain signaling in gonadotropes following GnRH receptor activation. This is clearly important relative to the regulation of fertility, in which

the wide-spread clinical use of GnRH receptor agonists and antagonists underscores the need for a better understanding of GnRH receptor function (213-215).

3.4 Materials and Methods

Materials

DMEM was from HyClone (Logan, UT), Fetal Bovine Serum (FBS) was purchased from Atlas Biologicals (Fort Collins, CO), Matrigel was from BD Biosciences (San Jose, CA) and MitoTEMPO was purchased through Enzo (Farmingdale, NY). Fluo-5F (pentapotassium salt), WGA-Alexa Fluor 633 conjugate, sodium pyruvate, MitoSOX-Red, DCF, and mitoTracker Green FM were purchased from Invitrogen (Carlsbad, CA). Catalase and papain were from Worthington Biochemical (Lakewood, NJ). All other chemicals were from Sigma (St. Louis, MO).

Cell culture

αT3-1 gonadotrope cells (22), a generous gift from Pam Mellon (UCSD), were incubated in high-glucose DMEM supplemented with FBS (10%) and sodium pyruvate (1 mM). Cells were maintained at 37°C in 5% CO_2 humidified air.

Mouse pituitary cell dissociation and gonadotrope isolation

Transgenic mice with genetically-labeled fluorescent gonadotropes as a result of animals with a GnRHR promoter driven Cre recombinase (GRIC) crossed to ROSA26-YFP and ROSA-tdTomato animals were used to identify gonadotropes (23). Sexually mature (6-12 weeks of age) male and female mice were euthanized with sodium pentobarbital (200 mg/kg intraperitoneally) in accordance with institutional guidelines and approved by the Institutional Animal Care and Use Committee of Colorado State University. Whole pituitaries were removed and enzymatically digested in Ca^{2+}-free buffer containing papain (10 U/mL) and dithiothreitol (1 mg/mL) for 15 min at 37°C followed by a second incubation (15 min at 37°C) in Ca^{2+}-free buffer supplemented with collagenase (300 U/mL, Type II). Pituitary tissue was then washed with and placed in high-glucose DMEM for 30 min after which trituration with a fire-polished Pasteur pipette was used to create a cell suspension and plated on poly-L-lysine coated Mattek dishes

overnight at 37˚C and 5% CO_2. Cells were used for experiments the following day within 24-36 h of dispersion. Both YFP and tdTomato-labeled gonadotrope transgenic mice were used to ensure consistency among different mouse lines. There were no significant differences between the groups for each treatment and therefore all the data were combined for analysis.

Detection of ROS generation

αT3-1 cells were plated onto Matrigel coated glass-bottomed Mattek dishes 24 hours prior to experimentation. TIRF microscopy was used to visualize subplasmalemmal ROS generation as described previously (2). Cells were loaded in Ca^{2+}-free buffer supplemented with the cell-permeant ROS indicator 5-(and- 6)-chloromethyl-2'7'-dichlorodihydrofluorescein diacetate acetyl ester (DCF; 1μM;) for 30 min at room temperature (22 - 25°C). Following removal of excess DCF, cells were placed in Ca^{2+}-free or Ca^{2+} (2 mM) buffer, excitation of subplasmalemmal DCF was achieved with a 491-nm laser and excitation and emission light was separated with appropriate filters. Similar to Ca^{2+} sparklets (1) and ROS puncta in smooth muscle (148,149), for an area of elevated DCF fluorescence to be considered a localized site of increased ROS generation (a ROS "puncta"), a grid of 3 x 3 contiguous pixels must have a fluorescence amplitude equal to or larger than the mean basal DCF fluorescence plus three times its standard deviation (2, 26). ROS puncta densities (ROS puncta per μm^2) were calculated by dividing the number of sites detected by the area of cell membrane visible in the TIRF images. Cells chosen had 1-2 baseline nascent ROS puncta to ensure that the cell was properly loaded with DCF. Changes in DCF fluorescence (Δ DCF) were calculated from the mean pixel intensities of the background DCF fluorescence of the cell surface area visible in the TIRF images (average Δ DCF) and the areas confined to nascent ROS puncta (puncta Δ DCF).

Electrophysiology and total internal reflection fluorescence microscopy

αT3-1 cells were plated onto Matrigel coated glass-bottomed Mattek dishes 24 hours prior to experimentation. Simultaneous electrophysiology and Ca^{2+} imaging experiments were carried out using the conventional dialyzed whole-cell patch clamp technique as described

previously (1,148-150,206). Briefly, subplasmalemmal Ca^{2+} influx through L-type Ca^{2+} channels was visualized with a TILL Photonics (Victor, NY) through-the-lens TIRF system built around an inverted Olympus IX-71 microscope (Center Valley, PA) with a 100X TIRF oil-immersion objective (numerical aperture = 1.45) and an Andor iXON EMCCD camera (Andor Technology, South Windsor, CT). To monitor Ca^{2+} influx, gonadotropes were loaded with the Ca^{2+} indicator fluo-5F (200 µM) and an excess of EGTA (10 mM; to lower background noise while minimally interfering with fluo-5F (1,148,149,216)) via the patch pipette. Membrane potential was controlled with an Axopatch 200B amplifier (Molecular Devices, Sunnyvale, CA); fluo-5F excitation was achieved with a 491-nm laser with excitation and emission light being separated with appropriate filters. Ca^{2+} influx was recorded with 2 mM external Ca^{2+} at a frame rate of 50 Hz and holding potential of -70 mV to increase the driving force for Ca^{2+} entry. To preclude potential contaminating Ca^{2+} release events from the endoplasmic reticulum, the Ca^{2+}-ATPase inhibitor thapsigargin (1 µM) was present during all experiments. Cells were imaged for 2 min before acute treatment with GnRH (10 nM), H_2O_2 (100 µM), L-type Ca^{2+} channel antagonist nicardipine (10 µM), NADPH oxidase inhibitor apocynin (25 µM), catalase (500 U/mL), mitochondrial Complex III inhibitor antimycin A (500 nM), or mitochondrial ROS inhibitor mitoTEMPO (25 nM) and imaged for an additional 10 min. Vehicle controls were performed as appropriate. All experiments were performed at room temperature (22 - 25°C).

L-type Ca^{2+} channel sparklet analysis

Background subtracted fluo-5F fluorescence signals were converted to intracellular Ca^{2+} concentrations ($[Ca^{2+}]_i$) as described previously (148-150,185,206). Briefly, fluo-5F fluorescence images were analyzed with custom software kindly supplied by L. Fernando Santana (University of California, Davis) and L-type Ca^{2+} channel sparklet activity was determined by calculating the nP_s of each site, where n is the number of quantal levels detected, and P_s is the probability that the site is active. nP_s values were obtained using pCLAMP 10.0 (Molecular Devices, Sunnyvale, CA) on imported $[Ca^{2+}]_i$ time course records using an initial unitary $[Ca^{2+}]_i$ elevation of ≈ 20 nM

as determined empirically. L-type Ca^{2+} channel sparklet activity (i.e. nP_s) datasets were bimodally distributed (1,148,149), thus two-sample comparisons of nP_s data were examined with the non-parametric Wilcoxon matched pairs test (two-tailed) and comparisons between more than two groups were performed using the non-parametric Friedman test with Dunn's multiple comparison post-test. Arithmetic means of nP_s datasets are indicated in the figures (solid grey horizontal lines) for non-statistical visual purposes, and dashed grey lines mark the threshold for high-activity Ca^{2+} sparklet sites (n$P_s \geq 0.2$) (148-151). Statistically, nP_s values are presented as median values and their interquartile range. Active L-type Ca^{2+} channel sparklet site densities (Ca^{2+} sparklet sites per μm^2) were calculated by dividing the number of active sites by the area of cell membrane visible in the TIRF images. To maintain consistency and enhance reproducibility, image stacks of Ca^{2+} sparklet activity were analyzed after a minimum of 5 min and before a maximum of 10 min following each manipulation in all experiments. Normally distributed data are presented as means ± SEM. Two-sample comparisons of these data were performed using either a paired or unpaired (as appropriate) two-tailed Student's t-test and comparisons between more than two groups were performed using a one-way ANOVA with Tukey's multiple comparison post-test. P values < 0.05 were considered significant and asterisks (*) used in the figures indicate a significant difference between groups.

Mitochondrial ROS activity

Mitochondrial oxidation activity was measured using the cell permeant fluorescent indicator MitoSOX-Red (1 μM). αT3-1 cells were incubated in Ca^{2+}-free buffer containing the indicator for 30 min at 37ºC. MitoSOX-Red excitation was achieved with a 491-nm laser with excitation and emission light being separated with appropriate filters with the TIRF microscope. Cells were then exposed to treatments of GnRH (10 nM) or mitochondrial Complex III inhibitor antimycin A (500 nM) with or without pretreatment (10 min) with mitochondrial oxidative phosphorylation uncoupler carbonyl cyanide 3-chlorophenylhydrazone (CCCP, 1 μM) or NADPH oxidase inhibitor apocynin (25 μM). For analysis of the fluorescence intensity (indicative of

mitochondrial oxidation), raw images were background subtracted using the average background value per treatment group and mitochondrial region of interests (ROIs) were selected and compared. For an area of elevated MitoSOX-Red fluorescence to be considered indicative of subplasmalemmal mitochondria, a grid of 3 x 3 contiguous pixels must have a fluorescence amplitude equal to or larger than the mean basal fluorescence plus three times its standard deviation. Using this criterion, we identified normalized ROIs to compare mitochondrial oxidation before and after treatments. Background fluorescence within and between groups was not significantly different, therefore background subtracted intensity values were compared across different treatments.

Confocal microscopy

Laser scanning confocal microscopy was used to image the plasma membrane and mitochondria in αT3-1 cells. Mitochondria were labelled with MitoTracker Green (200 nM for 15 min) in Ca^{2+}-free buffer at 37˚C. The extracellular face of the plasma membrane was marked with a wheat germ agglutinin Alexa 633 conjugate (5 µg/mL, 5 min at room temperature (22 - 25°C)) and Alexa 633 was excited with a 633-nm laser and MitoTracker Green was excited with a 488-nm laser; excitation and emission light was separated with appropriate filters. Data were analyzed with Volocity 3D Image Analysis Software (PerkinElmer). Mitochondrial-associated fluorescence located ≤ 0.5 µm from the center of the Alexa 633-WGA signal was designated as peripheral as this value falls within the predicted functional distance of intracellular signaling H_2O_2.

Imaging of subplasmalemmal mitochondria with Ca^{2+}sparklets

TIRF microscopy was also used to image subplasmalemmal mitochondria in αT3-1 gonadotrope cells. Briefly, cells were incubated with MitoTracker Green (200 nM) for 15 min in Ca^{2+}-free buffer at 37˚C. Subplasmalemmal MitoTracker Green was excited with a 491-nm laser and excitation and emission light was separated with appropriate filters. For an area of elevated MitoTracker fluorescence to be considered indicative of subplasmalemmal mitochondria the

fluorescence amplitude had to be equal to or larger than the mean basal fluorescence plus three times its standard deviation. Using this criterion, we generated thresholded MitoTracker TIRF images to establish clear mitochondrial boundaries. The percentage of plasma membrane associated with subplasmalemmal mitochondria was calculated by dividing the area of membrane associated with mitochondria by the area of plasma membrane visible. We defined mitochondrial associated L-type Ca^{2+} channel sparklet sites as those sites with peaks (pixels of highest intensity) ≤ 0.5 μm from the edge of the nearest thresholded MitoTracker signal. Note that the subplasmalemmal MitoTracker fluorescence was obtained from the same cell in which Ca^{2+} influx was also recorded using the electrophysiology protocol and was done sequentially after MitoTracker Green incubation and imaging.

3.5 Results

To test the hypothesis that ROS are mediated by GnRH and induces local Ca^{2+} influx through L-type Ca^{2+} channels in pituitary gonadotropes we proposed the following experimental criteria: 1) GnRH must affect ROS formation on the subplasmalemmal surface; 2) H_2O_2 must stimulate localized Ca^{2+} influx through L-type Ca^{2+} channels in both immortalized gonadotropes and primary mouse gonadotropes; and 3) inhibition of endogenous ROS should decrease GnRH-mediated ROS formation and Ca^{2+} influx on the plasma membrane. Additionally, if ROS generated from mitochondria are important in GnRH-induced L-type Ca^{2+} channel activity in gonadotropes, then 1) mitochondrial ROS activity should increase with GnRH stimulation; 2) mitochondrial ROS must regulate L-type Ca^{2+} channel sparklets; and 3) active L-type Ca^{2+} channels should associate with subplasmalemmal mitochondria.

GnRH induces ROS formation on the plasmalemmal surface

If ROS are important for signaling to the L-type Ca^{2+} channel, we wanted to observe if ROS are spatially located on the plasma membrane. Therefore, our initial experiment used TIRF microscopy to image subplasmalemmal changes in intracellular oxidation in immortalized αT3-1 gonadotrope cells. αT3-1 cells were exposed to a physiologically relevant ROS, hydrogen

peroxide (H_2O_2; 100 μM), and oxidation was visualized with the cell-permeant fluorescent ROS indicator 2',7'-dichlorodihydrofluorescein diacetate (DCF; 1 μM). H_2O_2 is an important ROS signaling molecule and H_2O_2-dependent modulation of protein function is thought to occur by oxidation of key amino acids (e.g., cysteine) that operate as allosteric redox-dependent switches (7, 24, 42). H_2O_2 treatment produced a global increase in fluorescence (Figure 3.1A), indicating a homogenous increase in intracellular oxidation at the subplasmalemmal surface in gonadotropes as demonstrated by the two-fold increase in average background fluorescence

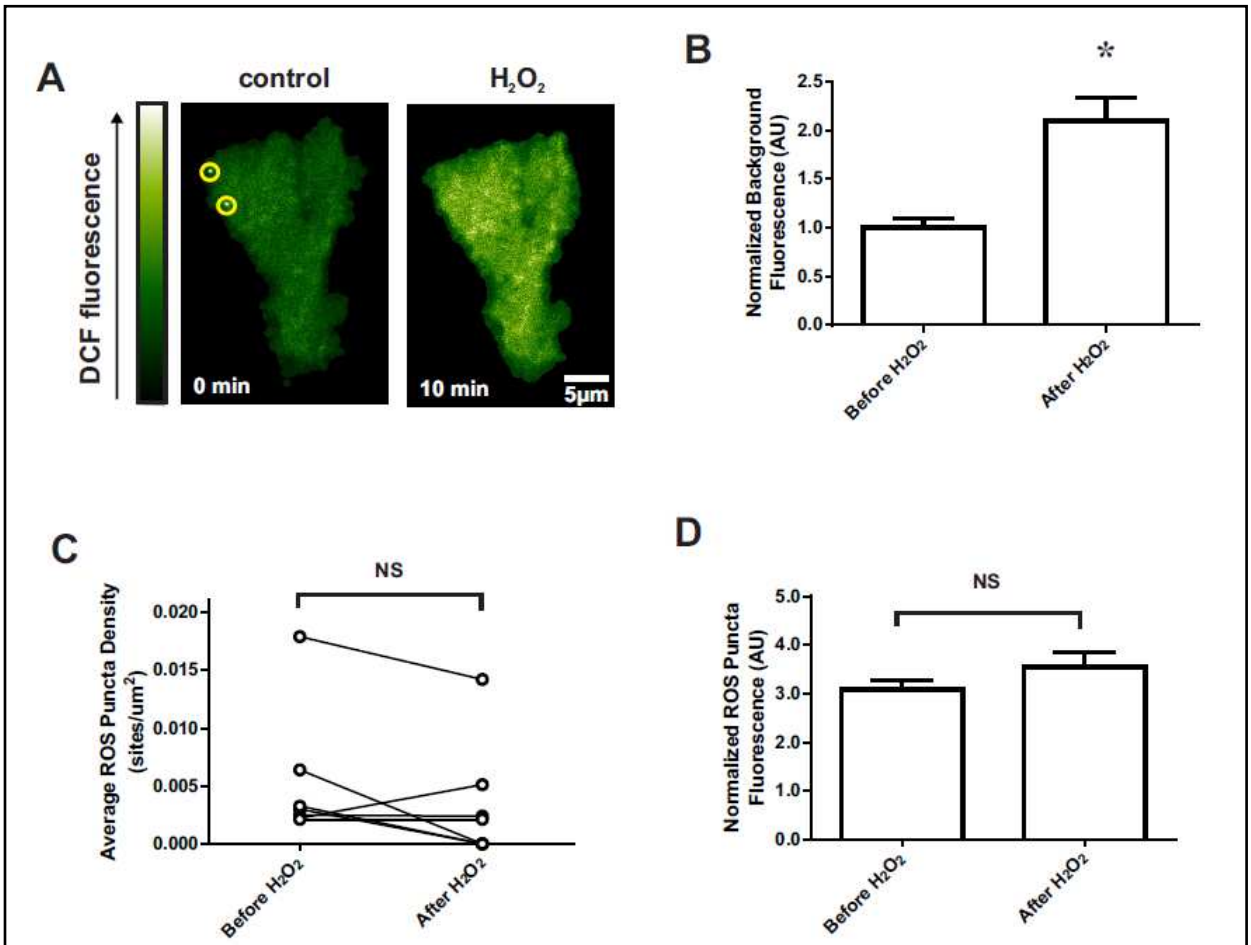

Figure 3.1. Hydrogen peroxide generates ROS on the plasmalemmal surface in αT3-1 cells. A, Representative TIRF images showing localized fluorescence (indicating ROS generation) in αT3-1 cells before and after H_2O_2 treatment (H_2O_2; 100 μM) using cell permeable ROS-indicator DCF (1μM). Note the yellow circles are sites of DCF fluorescence (ROS "puncta") that satisfied the criteria to be considered as a site of increased local ROS generation (see Materials and Methods). B, Plot of the normalized mean ± SEM cell background fluorescence (arbitrary units [AU]) before and after H_2O_2. C, Plot of the mean ± SEM ROS puncta density (ROS puncta sites/μm^2) before and after H_2O_2 (n = 7 cells). D, Plot of the normalized mean ± SEM ROS puncta fluorescence amplitude (arbitrary units [AU]) before and after H_2O_2. *$P < 0.05$

compared to control conditions (Figure 3.1B; $P < 0.05$; n = 7 cells). These observations demonstrate that the DCF indicator in our TIRF imaging experiments report changes at the level of the subplasmalemmal space without non-uniform intracellular compartmentalization of oxidation due to uneven loading of the fluorescent ROS indicator throughout the cell.

In addition to the increase in background fluorescence, the DCF indicator also demonstrated few, but very discreet, localized ROS "puncta" on the plasma membrane, seen under basal conditions in αT3-1 cells (yellow circles in Figure 3.1A). Despite H_2O_2 increasing DCF fluorescence globally across the cell membrane, the ROS puncta density, calculated by dividing the number of ROS puncta sites by the cell surface area did not significantly increase with H_2O_2 stimulation compared to control conditions (Figure 3.1C; $P > 0.05$; n = 7 cells). Additionally, the fluorescence amplitudes of the localized DCF generation also did not differ between groups (Figure 3.1D; $P > 0.05$). These data demonstrate that exogenous H_2O_2 stimulation globally changes the oxidation on the cell surface of gonadotropes, but does not change the local ROS puncta distribution in gonadotropes.

More importantly, however, we next investigated how ROS are regulated by GnRH receptor signaling. αT3-1 cells exposed to acute treatment with GnRH (10 nM) did not increase ROS globally like H_2O_2, but instead increased the number of distinct, localized areas of ROS on the subplasmalemmal surface as seen by elevated DCF fluorescence at discrete sites on the plasma membrane (Figure 3.2A). In the presence of GnRH, there is a four-fold increase in the ROS puncta density after 5 minutes of GnRH treatment (density before GnRH = 0.0021 ± 0.00047 ROS puncta sites/μm^2; density after GnRH = 0.0088 ± 0.0011 ROS puncta sites/μm^2; $P < 0.05$; n = 17 cells, Figure 3.2B). Therefore, GnRH receptor activation leads to an increase of very particular sites of ROS accumulation on the plasma membrane. This supports the concept of GnRH leading to very quick (within minutes), discreet microdomains on the cell surface for signaling, very similar to our previous data demonstrating GnRH receptor activation inducing

very distinct, localized L-type Ca^{2+} channel influx (Ca^{2+} sparklets) in gonadotropes for downstream ERK activation (206).

The increase in GnRH-induced ROS puncta density, however, only occurs when physiological levels of Ca^{2+} (2 mM) are present. In a Ca^{2+} free-buffer, there was a slight

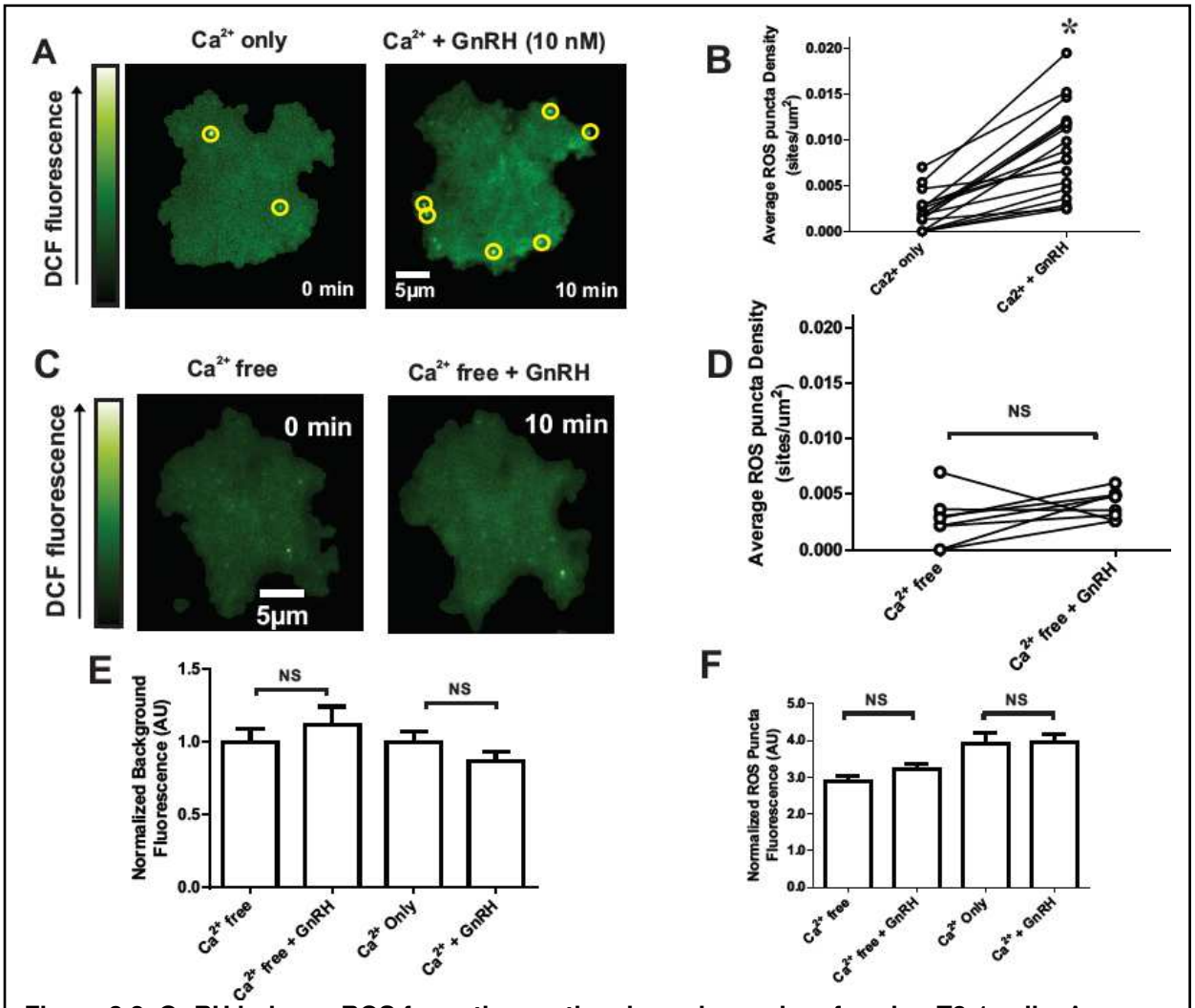

Figure 3.2. GnRH induces ROS formation on the plasmalemmal surface in αT3-1 cells. A, Representative TIRF images showing localized fluorescence (indicating ROS generation) in αT3-1 cells before and after GnRH (10 nM) in 2mM [Ca^{2+}] solution using cell permeable ROS-indicator DCF (1 µM). B and D, Plot of the mean ± SEM ROS puncta density (ROS puncta sites/µm^2) before and after GnRH in (B) 2 mM [Ca^{2+}] or (D) Ca^{2+}-free buffer (n = 17 cells in Ca^{2+} buffer, n = 8 cells in Ca^{2+} free buffer). C, Representative TIRF images showing localized fluorescence (indicating ROS generation) in αT3-1 cells before and after GnRH (10 nM) in Ca^{2+}-free buffer using DCF (1 µM). E, Plot of the normalized mean ± SEM cell background fluorescence (arbitrary units [AU]) before and after GnRH. F, Plot of the normalized mean ± SEM ROS puncta fluorescence amplitude (arbitrary units [AU]) before and after GnRH. Note that only sites of DCF fluorescence circled in yellow satisfied the criteria to be considered as a site of increased local ROS generation (see Materials and Methods). *$P < 0.05$

increase in ROS puncta density, but this was not significant (Figure 3.2, C & D; $P > 0.05$; n = 8 cells). This ROS puncta density increase under Ca^{2+} conditions is unique to gonadotropes and different than in other cells types, such as in smooth muscle cells in which ROS puncta stimulation with angiotensin was Ca^{2+}-independent (148,149). The average background fluorescence did not increase significantly with GnRH treatment in Ca^{2+} or Ca^{2+}-free buffer (average ΔDCF fluorescence over time does not increase) and the amplitude of the DCF puncta fluorescence before and after GnRH treatment was not different ($P > 0.05$, Figure 3.2, E &F). These data demonstrate that GnRH induces spatially regulated ROS generation in αT3-1 cells by increasing the number of ROS puncta sites on the plasma membrane in a Ca^{2+}-dependent manner.

Hydrogen peroxide stimulates localized Ca^{2+} influx through L-type Ca^{2+} channels in αT3-1 cells

Now that we have identified GnRH-induced localized ROS puncta on the plasma membrane, we next tested if ROS could modulate the activity of nearby L-type Ca^{2+} channels in gonadotropes. To do so, we used a combination of electrophysiology and TIRF microscopy to visualize local Ca^{2+} influx in αT3-1 cells in order to visualize small Ca^{2+} influx events in the plasma membrane with high temporal and spatial resolution (206). Exogenous H_2O_2 (100 μM) promoted discrete sites of repetitive Ca^{2+} influx (i.e. Ca^{2+} sparklets; Figure 3.3A). To quantify Ca^{2+} sparklet activity we determined the nP_s value for each site where n is the number of quantal levels observed and P_s is the probability that the Ca^{2+} sparklet site is active (1,148,150,184).

In αT3-1 cells, H_2O_2 increased Ca^{2+} sparklet site activity (nP_s) compared to vehicle control (Figure 3C; median control nP_s = 0.010, interquartile range (IQR) = 0.016, median H_2O_2 nP_s = 0.25 IQR = 0.41; $P < 0.05$; n = 9 cells). The density of detected Ca^{2+} sparklet sites (number of Ca^{2+} sparklet sites per μm^2) also increased following H_2O_2 exposure (Figure 3.3C; control density = 0.0024 ± 0.00083 sites/μm^2; H_2O_2 density = 0.011 ± 0.00088 sites/μm^2; $P <$

0.05). These data demonstrate that H_2O_2 induces localized Ca^{2+} influx in αT3-1 cells by increasing the number of active Ca^{2+} sparklet sites and by increasing the activity within each of those sites. The time frame of L-type Ca^{2+} channel activity (within 5 min) and the values for sparklet activity and density following H_2O_2 treatment was similar to that induced by GnRH (206), indicating that ROS can activate the Ca^{2+} channel in a similar fashion as GnRH receptor activation. These Ca^{2+} sparklets stimulated by H_2O_2 occurred specifically through L-type

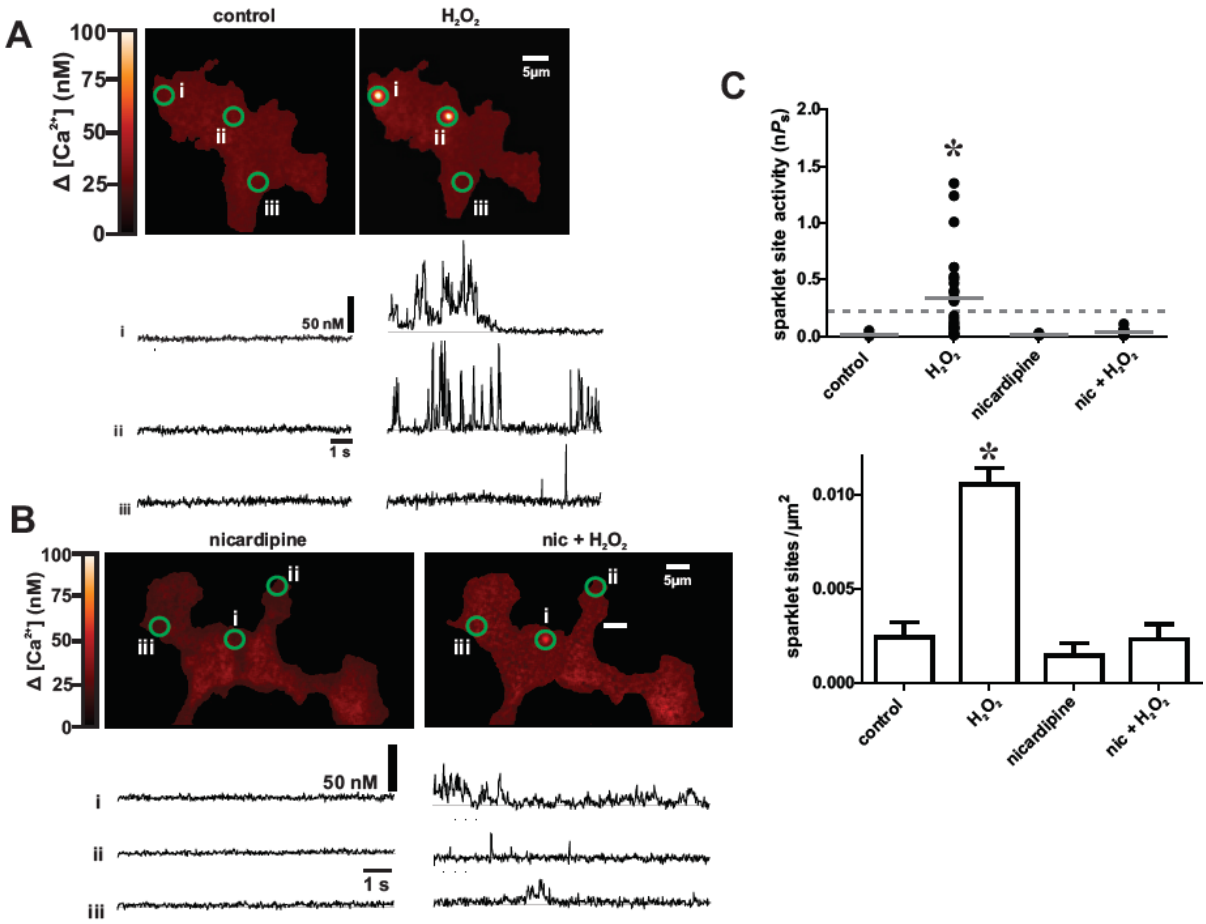

Figure 3.3. Hydrogen peroxide stimulates localized Ca^{2+} influx through L-type Ca^{2+} channels in αT3-1 cells. A, Representative TIRF images and traces showing time courses of localized Ca^{2+} influx in αT3-1 cells before and after (B) H_2O_2 (100 μM). The scale bar provides reference for changes in $[Ca^{2+}]_i$ during the traces (see Materials and Methods). B, Representative TIRF images and traces showing time courses of Ca^{2+} influx in an αT3-1 cell before and after application of H_2O_2 in the presence of the L-type Ca^{2+} channel antagonist nicardipine (10 min pretreatment). C, Plot of Ca^{2+} sparklet site activities (nP_s; see Materials and Methods) before and after H_2O_2 treatment with or without nicardipine (n = 9 H_2O_2, n=12 for H_2O_2 + nicardipine cells); solid grey lines are the arithmetic means of each group and dashed lines mark the threshold for high-activity Ca^{2+} sparklet sites ($nP_s \geq 0.2$; (1)). D, Plot of mean ± SEM Ca^{2+} sparklet site densities (Ca^{2+} sparklet sites/μm^2) during H_2O_2 treatment with or without nicardipine. *P < 0.05

Ca^{2+} channels, since H_2O_2 applied in the presence of the dihydropyridine L-type Ca^{2+} channel antagonist nicardipine (10 μM) did not significantly increase Ca^{2+} sparklet activity or density (Figure 3.3, B & C; $P > 0.05$; n = 12 cells). Taken together, these data support our hypothesis that ROS can stimulate localized L-type Ca^{2+} channel activity in gonadotrope cells.

Primary mouse gonadotropes also produce L-type Ca^{2+} channel sparklets induced by GnRH or hydrogen peroxide stimulation

Experiments thus far have been done using αT3-1 cells, which are immortalized gonadotropes. αT3-1 cells were carefully selected as this cell line recapitulates proximal GnRH receptor signaling mechanisms observed in native gonadotropes. Importantly, L-type Ca^{2+} channel-dependent ERK activation is observed in αT3-1 cells and in primary gonadotropes (86,128). In contrast, this mechanism appears to play a minor role in ERK activation in LβT2 cells (217). Consistent with this, our previous observations also indicate that L-type Ca^{2+} channel activity promotes ERK activation in αT3-1 cells (206). However, we cannot simply assume that our findings of L-type Ca^{2+} sparklets in αT3-1 cells reflect mechanisms occurring in native gonadotropes. To address this, we compared results from αT3-1 cell experiments with labelled primary mouse gonadotropes (23).

Our first key experiment in primary mouse gonadotropes demonstrated that GnRH does in fact induce localized Ca^{2+} channel activity as seen in αT3-1 cells (Figure 3.4A). GnRH increased Ca^{2+} sparklet site activity (Figure 3.4E; median before GnRH nP_s = 0.11, IQR = 0.25; median after GnRH nP_s = 0.32, IQR = 0.66) and density compared to vehicle controls (density before GnRH = 0.0033 ± 0.0015 sites/μm^2; after GnRH = 0.019 ± 0.0035 sites/μm^2; $P < 0.05$; n = 15 cells). The Ca^{2+} sparklet activity observed in mouse gonadotrope cells are qualitatively similar to αT3-1 cells (e.g., nP_s values, bimodal activity distribution, quantal amplitude of single channel Ca^{2+} influx events, and size of the Ca^{2+} sparklet itself) (206). Primary cells, however, had higher Ca^{2+} sparklet density values due to smaller total surface areas.

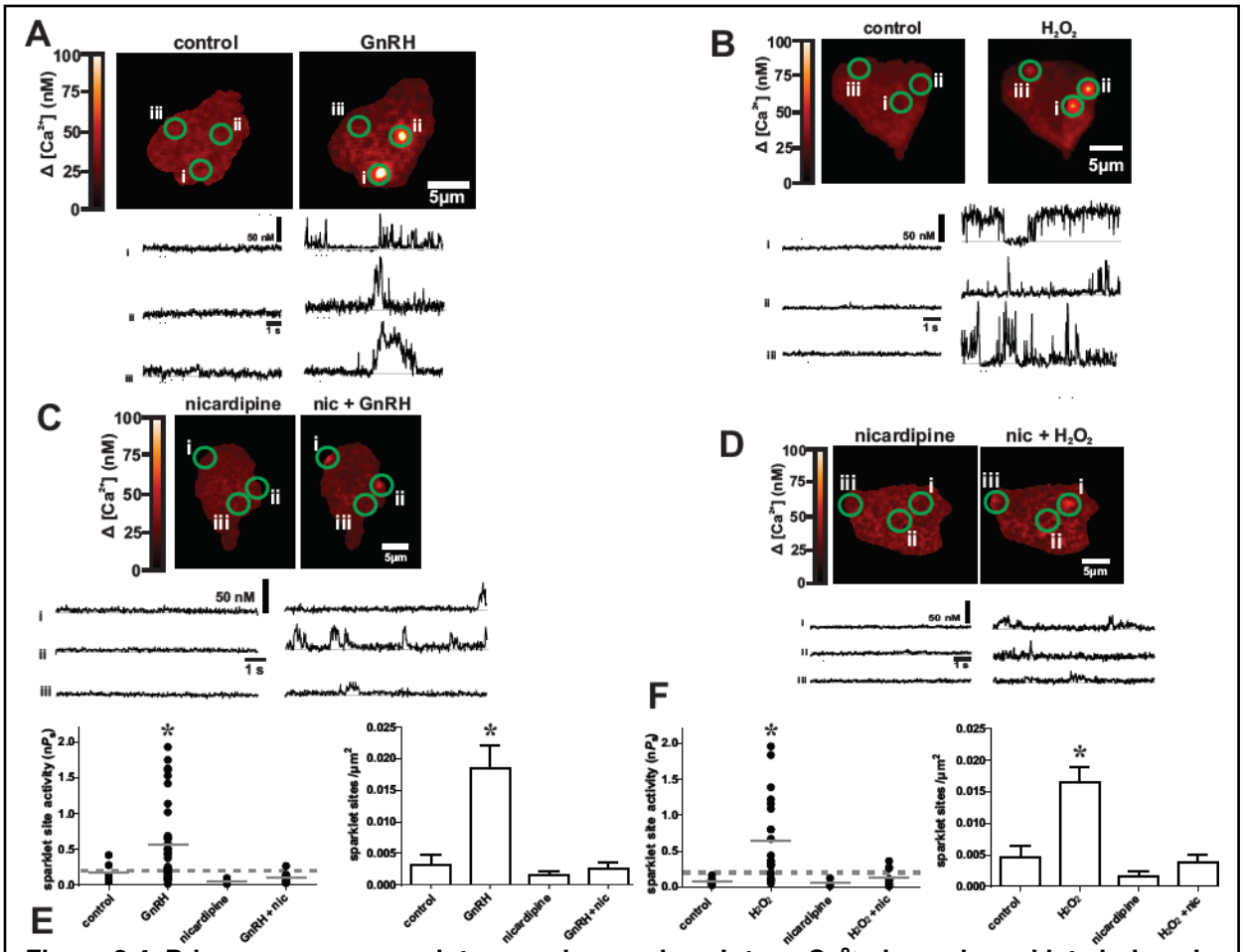

Figure 3.4. Primary mouse gonadotropes also produce L-type Ca^{2+} channel sparklets induced by GnRH or H_2O_2 stimulation. A and C, Representative TIRF images and traces showing time courses of localized Ca^{2+} influx in mouse gonadotrope cells exposed to (A) GnRH (10 nM, n = 15 cells) and (C) GnRH (10 nM) in the presence of L-type Ca^{2+} channel antagonist nicardipine (10 μM, n = 19 cells). B and D, Representative TIRF images and traces showing time courses of L-type Ca^{2+} channel influx in mouse gonadotrope cells exposed to (B) H_2O_2 (100 μM, n = 10 cells) and (D) H_2O_2 (100 μM) in the presence of L-type Ca^{2+} channel antagonist nicardipine (10 μM, n = 21 cells). E and F, Plots of Ca^{2+} sparklet site activities (nP_s) and mean ± SEM Ca^{2+} sparklet site densities (Ca^{2+} sparklet sites/μm^2) before and after (E) GnRH and (F) H_2O_2 in the presence of nicardipine. *P < 0.05

As expected, ROS are important for signaling in primary gonadotropes as well, regulating the L-type Ca^{2+} channel similarly to αT3-1 cells. H_2O_2 increased Ca^{2+} sparklet site activity (nP_s) in mouse gonadotrope cells (Figure 3.4, B & F; median control nP_s = 0.060, IQR = 0.06; median H_2O_2 nP_s = 0.36, IQR: 0.91; $P < 0.05$; n = 10 cells). Ca^{2+} sparklet density also increased following H_2O_2 exposure in primary gonadotrope cells (Figure 3.4F; control density = 0.0047 ± 0.0017 sites/μm^2; H_2O_2 density = 0.016 ± 0.0024 sites/μm^2; $P < 0.05$). Demonstrating the importance of the L-type Ca^{2+} channel for plasma membrane signaling, both GnRH-induced

(Figure 3.4, C & E; n = 19 cells) and H_2O_2-stimulated (Figure 3.4, D & F; n = 21 cells) Ca^{2+} sparklet activity and density were reduced in the presence of L-type Ca^{2+} channel inhibitor nicardipine (10 μM; $P > 0.05$).

We provide the first evidence of GnRH and H_2O_2-induced localized L-type Ca^{2+} channel microdomains in primary mouse gonadotropes to reveal a physiologically meaningful context. The fundamental concept that both GnRH and ROS modulate specific sites of Ca^{2+} influx seen in αT3-1 cells also translates to primary mouse gonadotropes and may suggest similar signaling pathways from GnRH receptor activation to L-type Ca^{2+} channel signaling necessary for ERK phosphorylation.

Inhibition of endogenous ROS decreases GnRH-mediated ROS formation on the plasma membrane

Our data thus far suggests GnRH increases ROS puncta density on the plasma membrane that can be important in activating downstream Ca^{2+} channel activity. In addition, H_2O_2 increased localized Ca^{2+} sparklets in a similar fashion to GnRH. Therefore, next we investigated if H_2O_2 production is mediated by GnRH physiologically. If this occurs, experiments blocking endogenous ROS during GnRH treatment may help identify the sources of ROS generation used for signaling. We examined GnRH-induced ROS puncta generation with TIRF microscopy in the presence of catalase, a physiologically relevant enzyme that converts H_2O_2 into water and oxygen. Pretreatment of αT3-1 cells with the membrane permeant PEGylated form of catalase (PEG-catalase; 500 Units/mL) before GnRH treatment reduced the observed number of subplasmalemmal ROS sites when decomposing H_2O_2 in the cell (Figure 3.5A). While PEG-catalase had no effect on baseline ROS production which was minimal to begin with, decomposing H_2O_2 attenuated the ROS puncta density in response to GnRH (Figure 3.5C; $P > 0.05$; n = 14 cells). GnRH in combination with PEG-catalase had no effect on puncta DCF fluorescence or the average background fluorescence (Figure 3.5D, $P > 0.05$). Therefore, these

data strengthen our hypothesis that H_2O_2 is important in GnRH-mediated ROS production at the cell surface in gonadotropes.

The plasmalemmal nicotinamide adenine dinucleotide phosphate (NADPH) oxidase protein complex is a common source of ROS generation in many cell types. Therefore, to examine the involvement of NADPH oxidase-derived ROS, which includes H_2O_2, we inhibited NADPH oxidase to investigate the effects on GnRH-dependent ROS puncta generation. Suggesting NADPH oxidase involvement, pretreatment of gonadotropes with NADPH oxidase inhibitor apocynin (25 µM) abolished the effect of GnRH on localized ROS generation, decreasing ROS puncta density in αT3-1 cells (Figure 3.5, B & C; n = 14 cells; $P > 0.05$). NADPH oxidase inhibition did not affect the average background DCF fluorescence or

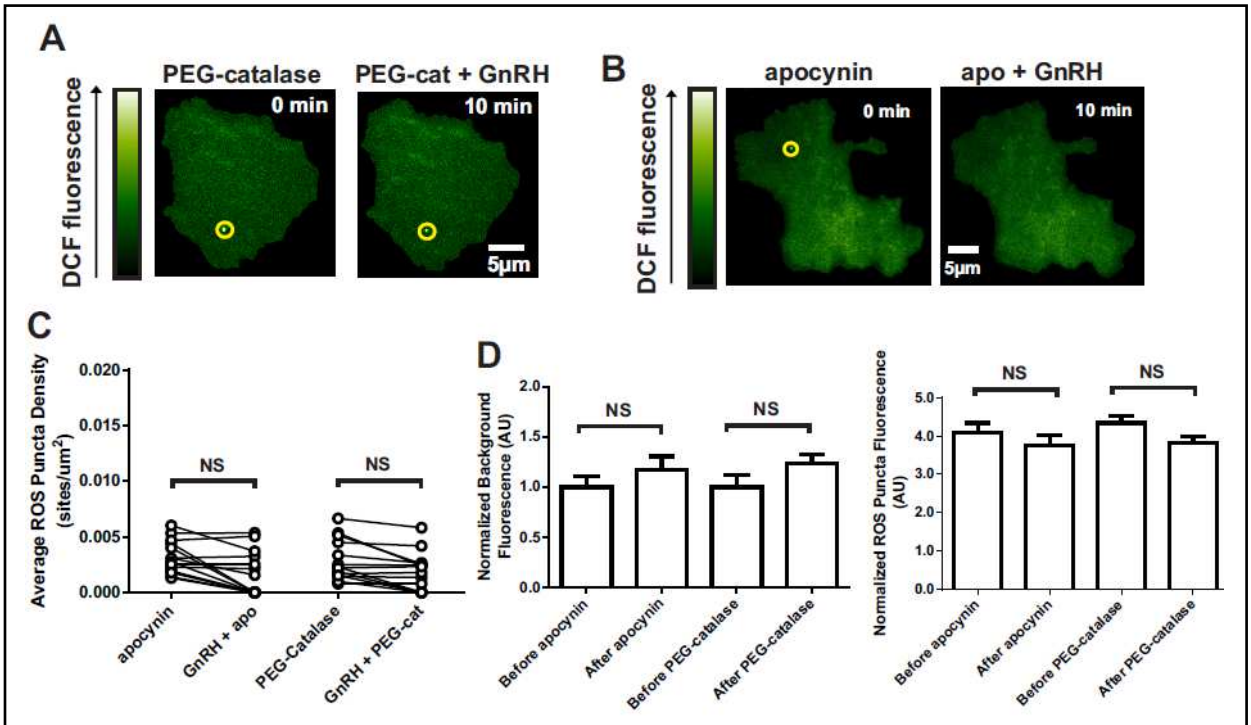

Figure 3.5. Inhibition of endogenous ROS decreases GnRH-mediated ROS formation on the plasma membrane. A and B, Representative TIRF images showing punctate DCF fluorescence in αT3-1 cells before and after GnRH in the presence of (A) NADPH oxidase inhibitor, apocynin (25 µM) or (B) cell permeant PEG-catalase (500 U/mL). C, Plot of the mean ± SEM ROS puncta density of gonadotrope cells exposed to apocynin (n = 14 cells) or PEG-catalase (n = 14 cells) before and after GnRH treatment. D, Plot of the normalized mean ± SEM background fluorescence and ROS puncta fluorescence amplitude before and after GnRH with apocynin or PEG-catalase pretreatment (10 min). Note that only sites of DCF fluorescence circled in yellow satisfied the criteria to be considered as a site of increased local ROS generation (see Materials and Methods). *$P < 0.05$

fluorescence intensity of the DCF ROS puncta themselves (Figure 3.5D; $P > 0.05$). From these experiments, endogenous ROS play a role in GnRH-induced ROS generation since catalase and NADPH oxidase inhibition prevented GnRH from increasing localized subplasmalemmal sites of increased oxidation in gonadotropes. These data suggesting NADPH oxidase regulation in gonadotropes supports previous findings that identified Nox isoforms in gonadotrope cells (180).

Inhibition of endogenous ROS generation decreases GnRH-induced Ca^{2+} influx

Next we examined the role of endogenous ROS in GnRH-dependent activation of L-type Ca^{2+} channels. Consistent with previous results (206), we found that GnRH (10 nM) increased L-type Ca^{2+} channel activity by increasing the number of active channel sites and by increasing the activity of the channels at those sites in αT3-1 cells (Figure 3.6, A & D; $P < 0.05$; n = 15 cells). However, pretreatment of cells with apocynin (25 μM) to inhibit NADPH oxidase activity reduced GnRH-dependent stimulation of L-type Ca^{2+} channels (Figure 3.6B). This suggests ROS generation involving NADPH oxidase mediates Ca^{2+} influx through L-type Ca^{2+} channels, since decreasing NADPH oxidase activity reduced Ca^{2+} sparklet activity and density in αT3-1 cells despite GnRH receptor stimulation (Figure 3.6D; $P > 0.05$; n = 19 cells). This finding is consistent with our previous observation that apocynin prevented GnRH-induced ROS generation on the subplasmalemmal surface of gonadotropes and suggests a role for the localized ROS in modulating L-type Ca^{2+} channel activity.

We have shown that although H_2O_2 stimulation produces global ROS across the plasma membrane, H_2O_2 can stimulate localized Ca^{2+} sparklet sites in a similar fashion to GnRH receptor activation. To examine the necessity of H_2O_2 for oxidant-dependent regulation of L-type Ca^{2+} channels in a more relevant, GnRH-dependent manner, we used catalase to decompose intracellular H_2O_2 during GnRH application. Intracellular application of catalase (by including 500 U/mL of the enzyme in the internal pipette solution of dialyzed cells) significantly decreased the

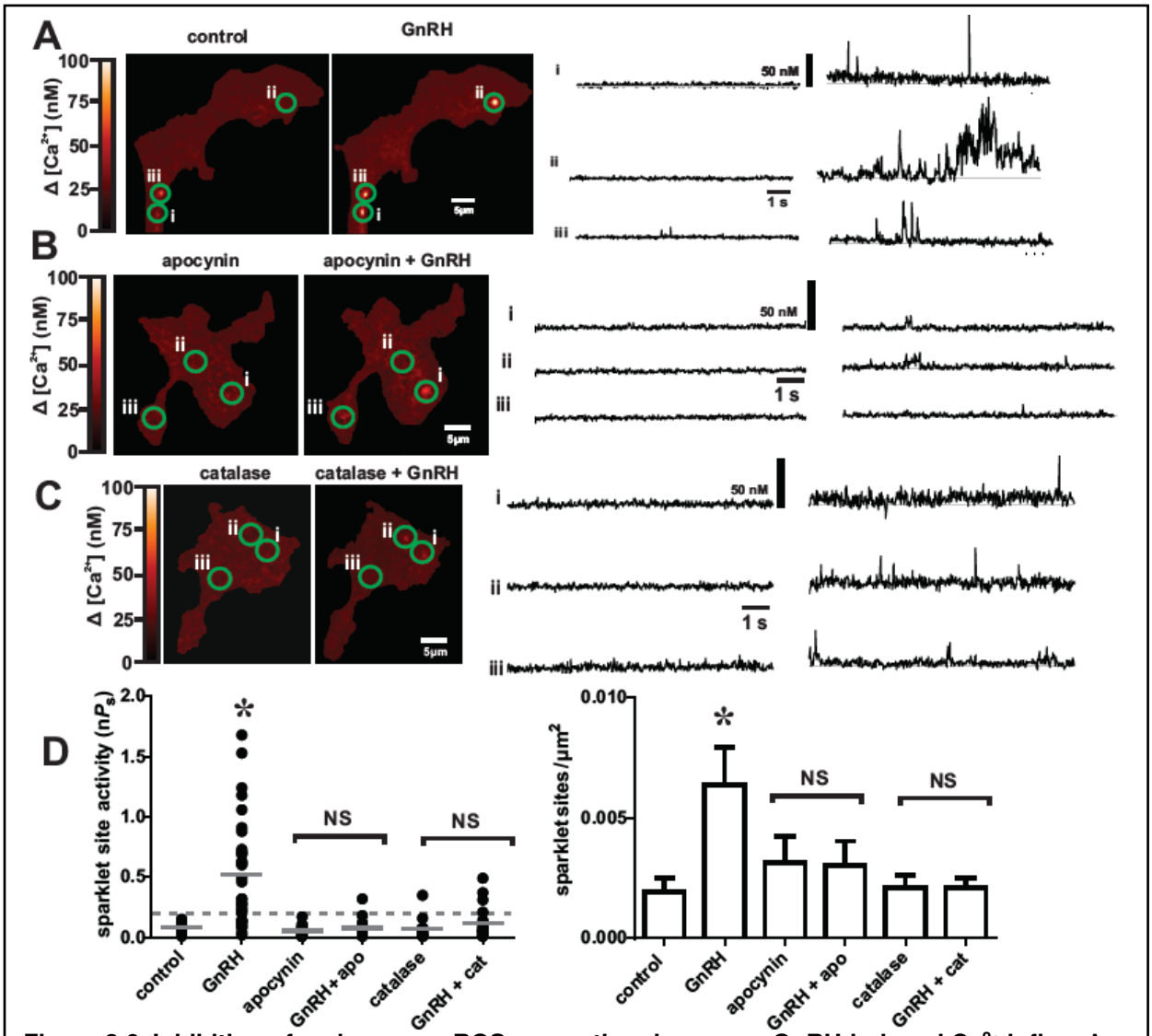

Figure 3.6. Inhibition of endogenous ROS generation decreases GnRH-induced Ca^{2+} influx. A, B, C, Representative TIRF images and time courses showing localized Ca^{2+} influx in αT3-1 cells treated with (A) GnRH (10 nM), or GnRH in the presence of (B) NADPH oxidase inhibitor apocynin (25 μM) or (C) catalase (500U/mL). D, Plots of Ca^{2+} sparklet site activities (nP_s) and mean ± SEM Ca^{2+} sparklet site densities (Ca^{2+} sparklet sites/μm^2) during GnRH treatment alone (n = 15 cells) or with apocynin (n = 19 cells) or catalase (n = 19 cells). *P < 0.05

stimulation of L-type Ca^{2+} channels by GnRH by reducing both Ca^{2+} sparklet activity and density compared to GnRH control (Figure 3.6, C & D; $P < 0.05$; n = 19 cells). Catalase dialysis had no effect on basal L-type Ca^{2+} channel activity ($P > 0.05$). From these data, we further emphasize the importance for H_2O_2 as the key oxidant second messenger in GnRH-dependent stimulation of L-type Ca^{2+} channels in gonadotropes. In context with our other experiments, these data support our hypothesis that localized generation of ROS stimulates Ca^{2+} sparklet activity in

gonadotrope cells since oxidative-dependent stimulation of L-type Ca^{2+} channels were prevented by blocking NADPH oxidase or through H_2O_2 removal.

Mitochondrial ROS activity increased with GnRH

Another common source of ROS originates from mitochondria during metabolism via the electron transport chain. During the physiological process of cellular respiration, ROS are generated as byproducts of shuttling electrons onto molecular oxygen. Given their prevalence and necessity in a cell, we were interested to see if mitochondrial ROS are sources that affect Ca^{2+} signaling. Therefore, we investigated whether mitochondrial ROS activity is regulated by GnRH or modulates L-type Ca^{2+} channel activity, in addition to identifying the distribution of mitochondria and L-type Ca^{2+} channels at the level of the plasma membrane.

In order to detect rates of oxidation specifically from mitochondria, we used a mitochondrial matrix-targeted fluorescent probe MitoSOX-Red (1 μM). Consistent with the previous data that demonstrated GnRH receptor activation increasing ROS puncta in gonadotropes, GnRH treatment (10 nM; n = 9 cells) increased the MitoSOX-Red fluorescence intensity of the mitochondria on the plasma membrane compared to Ca^{2+} only controls (n = 5 cells), indicating GnRH can specifically increase mitochondrial ROS in αT3-1 cells (Figure 3.7, A & F; $P < 0.05$). As a control to ensure measurement of specifically mitochondrial oxidation and not oxidation from other sources, we used antimycin A (500 nM), an electron transport chain complex III inhibitor that is known to increase oxidation in the matrix of mitochondria, and found similar increases in MitoSOX-Red fluorescence intensity compared to GnRH (Figure 3.7, B & F; n = 7 cells) (158,163). This increase in oxidation is specific to mitochondrial ROS since pretreatment with carbonyl cyanide 3-chlorophenylhydrazone (CCCP; 1 μM), a compound that uncouples oxidative phosphorylation in mitochondria, reduced the fluorescence of both GnRH (Figure 3.7, C & F; n = 6 cells) and antimycin A (Figure 3.7, D & F; n = 5 cells) treated gonadotropes ($P > 0.05$). The density of the mitochondria did not significantly change within or between treatment groups ($P > 0.05$), indicating that there was no recruitment or mobilization of

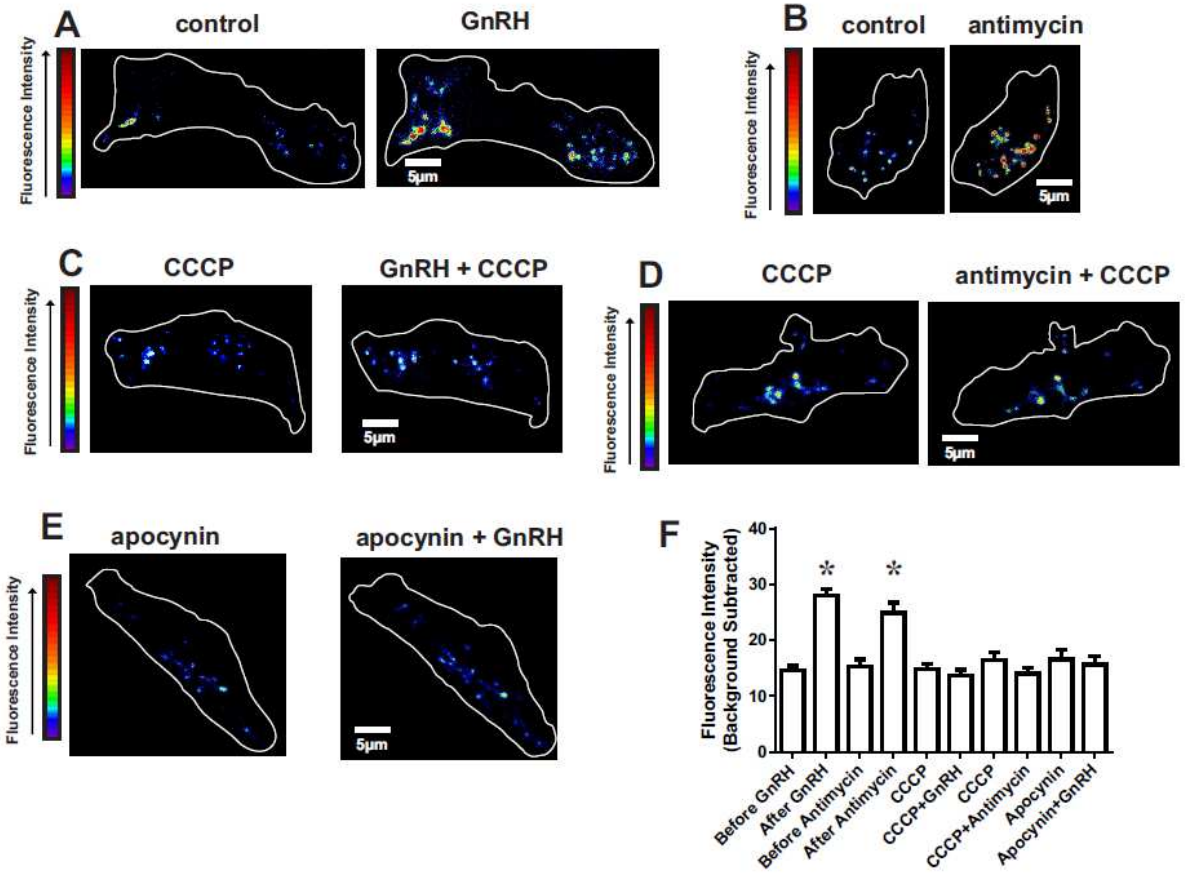

Figure 3.7. Mitochondrial ROS activity increased with GnRH. A and B, Representative TIRF images showing changes in fluorescence intensity in αT3-1 cells using cell permeable mitochondrial oxidation indicator MitoSOX-Red (1 µM) in GnRH (10 nM), mitochondrial Complex III inhibitor (increases mitochondrial oxidation) antimycin A (500 nM). C, D, and E, Representative TIRF images showing changes in fluorescence intensity in αT3-1 cells of MitoSOX-Red (1 µM) in cells pretreated (10 min) with (C and D) mitochondrial oxidative phosphorylation uncoupler carbonyl cyanide 3-chlorophenylhydrazone (CCCP, 1 µM), or (E) apocynin (25 µM) before GnRH (10 nM) or antimycin A (500 nM). F, Plot of the normalized mean ± SEM mitochondrial ROS puncta fluorescence amplitude (arbitrary units [AU]) using MitoSOX-Red (1 µM) in αT3-1 cells before and after GnRH (10 nM, n = 9 cells), antimycin A (500 nM, n = 7 cells), or pretreatment (10 min) with CCCP (1 µM; Antimycin + CCCP n = 5 cells, Antimycin + GnRH = 6 cells), or apocynin (25 µM, n = 5 cells) *P < 0.05

mitochondria on the cell surface, and that only oxidation of the existing mitochondria was altered. Distribution and shape of mitochondrial ROS on the cell surface of αT3-1 cells using TIRF microscopy were similar to the DCF puncta, in which there were discrete areas of mitochondrial oxidation on the plasma membrane without significant increases in background fluorescence across treatment groups. This is consistent with the notion that ROS signaling is localized and tightly regulated by GnRH, important for the modulation of Ca^{2+} channels nearby.

We next determined if ROS on the plasma membrane can influence ROS from another source such as mitochondria, known as ROS-induced-ROS release (RIRR) that occurs in different biological systems (162,163). Therefore, we looked at the role of NADPH oxidase in regulating mitochondrial oxidation. To test this hypothesis, GnRH was used to stimulate mitochondrial ROS, but to evaluate the role of NADPH oxidase activity, we treated gonadotropes with apocynin (25 μM) while measuring mitochondrial oxidation fluorescence. Inhibition of NADPH oxidase activity decreased mitochondrial ROS activity despite GnRH stimulation (Figure 3.7, E & F; $P > 0.05$; n = 5 cells). Therefore, these data suggest that ROS on the plasma membrane can regulate mitochondrial ROS activity in a reciprocating fashion and that mitochondrial RIRR may be an important mechanism in gonadotropes.

Mitochondrial ROS affects L-type Ca^{2+} channel sparklets

We have demonstrated that GnRH stimulates ROS puncta on the cell surface and can increase mitochondrial oxidation. In addition, H_2O_2 stimulated L-type Ca^{2+} channels in both αT3-1 cells and primary mouse gonadotropes. As mitochondria are important sources of ROS, we tested the hypothesis that localized ROS generated by subplasmalemmal mitochondria can stimulate nearby L-type Ca^{2+} channels. To promote mitochondrial ROS generation, we again exposed gonadotrope cells to the electron transport chain complex III inhibitor antimycin A (500 nM). As expected based on previous data showing antimycin A increasing mitochondrial oxidation, it also induced localized L-type Ca^{2+} channel sparklet activity and density (median before antimycin A nP_s = 0.020, IQR = 0.010; median after antimycin nP_s = 0.20, IQR = 0.54; density before antimycin A = 0.00078 ± 0.00042 sites/μm^2; after antimycin = 0.0048 ± 0.00079 sites/μm^2; Figure 3.8, A & C; $P < 0.05$; n = 14 cells). These data are consistent with the hypothesis that promotion of localized mitochondrial ROS generation as seen with the increased mitochondrial ROS oxidation is able to stimulate L-type Ca^{2+} channels.

Our previous results using the NADPH oxidase inhibitor apocynin (25 μM) indicate that NADPH oxidase activity is necessary for local regulation of L-type Ca^{2+} channels by GnRH–

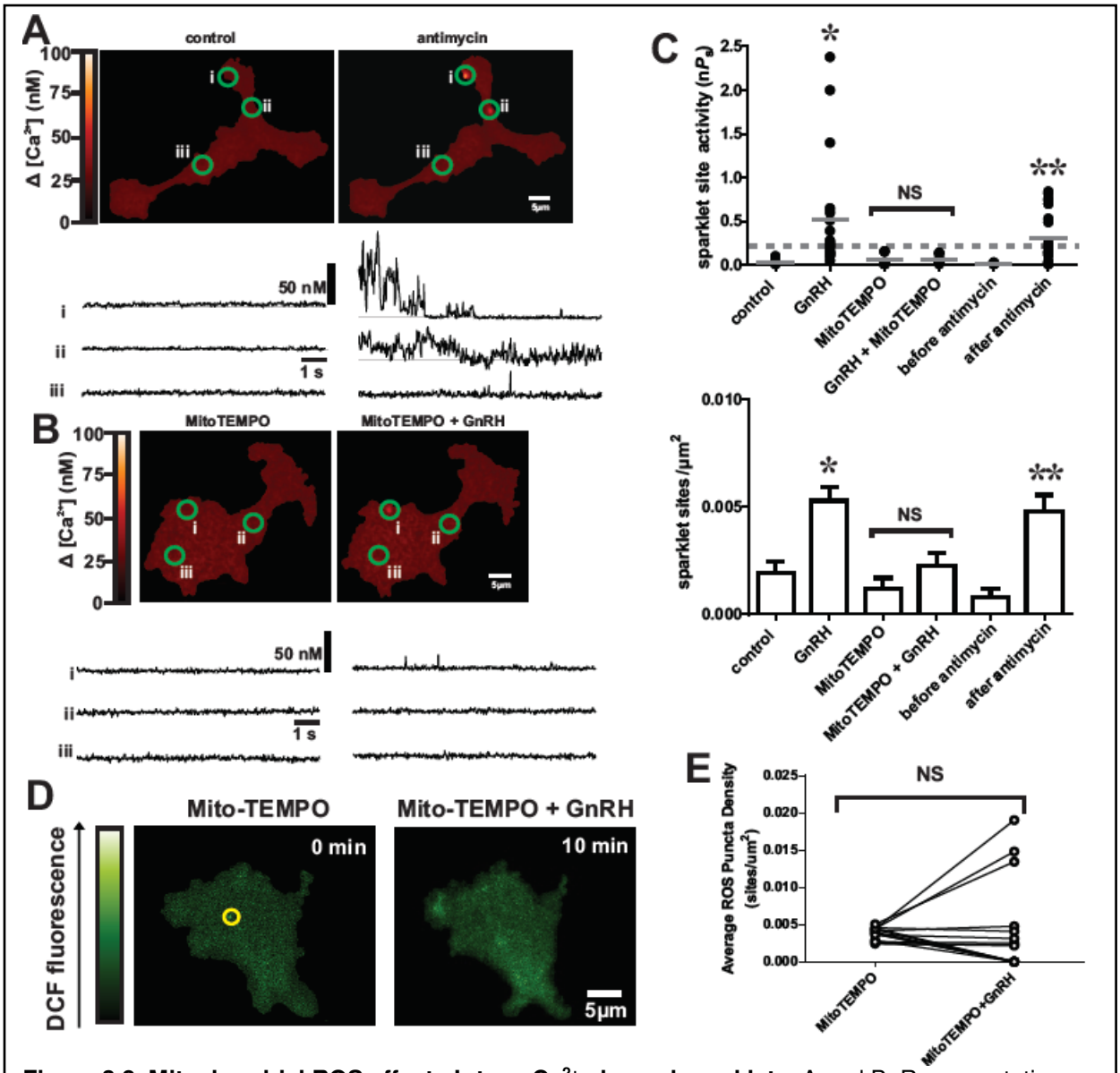

Figure 3.8. Mitochondrial ROS affects L-type Ca^{2+} channel sparklets. A and B, Representative TIRF images and traces showing the time course of localized Ca^{2+} influx in αT3-1 cells treated with (A) antimycin A (500 nM), (B) GnRH (10 nM) in the presence of mitochondrial ROS inhibitor/scavenger MitoTEMPO (25 nM). C, Plots of Ca^{2+} sparklet site activities (nP_s) and mean ± SEM Ca^{2+} sparklet site densities (Ca^{2+} sparklet sites/μm^2) during antimycin (n = 14 cells) or GnRH treatment with (n = 7 cells) or without (n = 14 cells) MitoTEMPO. Note the GnRH treated cells were done in parallel to αT3-1 cells pretreated with MitoTEMPO before GnRH treatment. *P < 0.05 D, Representative TIRF images showing localized fluorescence in αT3-1 cells using cell permeable ROS-indicator DCF (1 μM) before and after GnRH (10 nM) with mitoTEMPO (25 nM) pretreatment (10 min). E, Plot of the mean ± SEM ROS puncta density (ROS puncta sites/μm^2) before and after GnRH in the presence of mitoTEMPO (25 nM; n = 12 cells).

induced ROS microdomain signaling. GnRH also induced mitochondrial ROS generation.

Therefore, we tested the effect of inhibiting mitochondrial ROS generation on GnRH–dependent

stimulation of L-type Ca^{2+} channels. The mitochondrial-targeted antioxidant MitoTEMPO (25 nM; n = 7 cells) (218) attenuated the stimulatory effect of GnRH on L-type Ca^{2+} channel sparklet site activity and density compared to experiments done in parallel with GnRH treatment alone (Figure 3.8, B & C; $P > 0.05$; n = 14 cells). From these data, we can conclude a role for mitochondrial ROS-dependent regulation of Ca^{2+} influx in gonadotropes since the mitochondrial ROS production increased L-type Ca^{2+} channel activity and quenching mitochondrial ROS generation decreased GnRH-induced Ca^{2+} sparklet activity.

If mitochondrial ROS generation affects GnRH-induced ROS puncta on the cell surface, this would be additional evidence that would support the notion of RIRR. To test this concept, we pretreated gonadotropes with mitochondrial ROS inhibitor MitoTEMPO (25 nM) before GnRH (10 nM) application and used the ROS indicator DCF (1 μM) to identify ROS puncta changes on the plasma membrane. Interestingly, mitoTEMPO reduced the GnRH-induced ROS puncta density (Figure 3.8, D & E; $P > 0.05$; n = 12 cells). Although mitochondrial ROS inhibition did not completely abolish the ROS density following GnRH stimulation, the puncta density was less than GnRH treatment alone (compare to Figure 3.2B). This was an interesting observation since it may suggest a role for mitochondrial oxidation in modulating other ROS sources such as NADPH oxidase and demonstrates crosstalk between ROS and mitochondria in regulating important physiological events following GnRH receptor activation.

GnRH-induced L-type Ca^{2+} channel sparklets associate with subplasmalemmal mitochondria

Our results thus far have demonstrated that GnRH can increase mitochondrial oxidation and that mitochondrial ROS can affect L-type Ca^{2+} channel activity. Therefore, it would be plausible that mitochondria are positioned close enough to L-type Ca^{2+} channels at the level of the plasma membrane to permit local oxidative regulation. To directly assess the subcellular distribution of mitochondria in gonadotropes, we labeled mitochondria with fluorescent indicator MitoTracker Green (200 nM) and the plasma membrane of cells with a wheat germ agglutinin

conjugate (Alexa 633-wheat germ agglutinin (WGA); 5µg/mL), visualizing the fluorescence with confocal microscopy (Figure 3.9A, Panel 1 & 2). We found that 9.86 ± 0.88% of the total cell

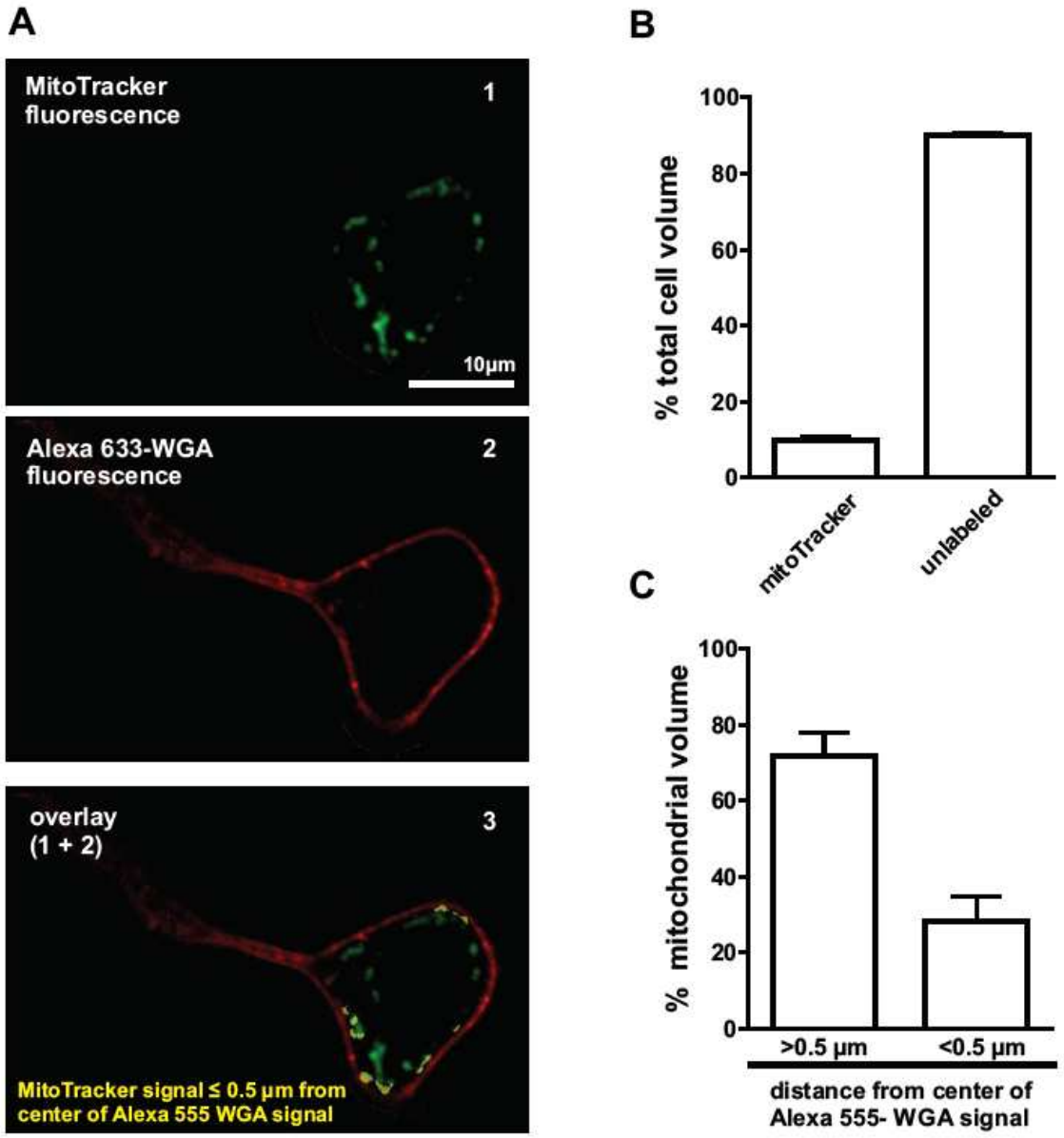

Figure 3.9. Plasma membrane associated mitochondria in gonadotropes. A, Representative confocal images showing mitochondria (MitoTracker fluorescence, green, Panels 1 and 3) and the plasma membrane (Alexa 633-wheat germ agglutinin [WGA] fluorescence, red, Panels 2 and 3) in an αT3-1 gonadotrope cell and. In panel 3, subplasmalemmal mitochondria (≤0.5 µm from the plasma membrane) are highlighted in yellow. B, Plot of the mean ± SEM mitochondrial and non-mitochondrial volumes (% of total cell volume; n=6 cells). C, Plot of the mean ± SEM non-peripheral (>0.5 µm from the plasma membrane) and subplasmalemmal (≤0.5 µm) mitochondrial volumes (% total mitochondrial volume; n = 6 cells).

volume was occupied by mitochondria (Figure 3.9B). Although the majority of the MitoTracker signal was located centrally (>0.5 μm from the center of the Alexa 633-WGA signal), 28.38 ± 6.36% of the mitochondrial volume was peripheral (≤0.5 μm; yellow signal in Figure 3.9A, Panel 3 & 3.9C).

Now that we have identified a subpopulation of mitochondria that associate with the plasma membrane in gonadotropes, the next crucial step is to examine whether specific mitochondrial populations on the plasma membrane associate or are located near active L-type Ca^{2+} channels. Therefore, to complement previous Ca^{2+} and ROS experiments, we imaged subplasmalemmal mitochondria and Ca^{2+} channel sparklets in the same cell to link L-type Ca^{2+} channel influx and ROS puncta to peripheral mitochondria. For these experiments, we used TIRF microscopy with fluorescent mitochondrial indicator MitoTracker Green (200 nM) in conjunction with voltage-clamp electrophysiology and Ca^{2+} indicator fluo-5F to identify Ca^{2+} channel sparklets in the same gonadotrope cell. MitoTracker fluorescence in αT3-1 cells with TIRF microscopy demonstrated the presence of subplasmalemmal mitochondria (Figure 3.10A, panel 1). Analysis of thresholded MitoTracker images revealed 13.34% ± 2.20% of the visible plasma membrane was associated with mitochondria (Figure 10A, Panel 2). L-type Ca^{2+} channel sparklets stimulated with GnRH (10 nM) in this experiment were not significantly different from the L-type Ca^{2+} channel sparklets observed previously with similar sparklet site activities and densities (Figure 3.10A, Panel 3).

To visualize the spatial relationship between subplasmalemmal mitochondria and Ca^{2+} sparklets, we overlaid both plasmalemmal Ca^{2+} fluorescence and thresholded MitoTracker images for analysis (Figure 3.10A, panel 4). We measured the distance from L-type Ca^{2+} channel sparklet site peaks (pixels of highest intensity) to the edge of the nearest thresholded MitoTracker signal (Figure 3.10A, Panel 2) and plotted the cumulative values (Figure 3.10B; n = 13 cells). Mitochondrial-associated L-type Ca^{2+} channel sparklet sites were defined a priori as those sites with peaks ≤ 0.5 μm from the edge of the nearest thresholded MitoTracker signal

(Figure 10B, vertical dashed gray line). From this analysis, we discovered that L-type Ca^{2+} sparklets were associated with subplasmalemmal mitochondria. The half distance of the observed L-type Ca^{2+} channel sparklet sites (n = 26 sites) to the nearest mitochondria was 0.64 (95% confidence interval, 0.54-0.74) µm, whereas the half distance of random points (n = 130 sites, 10 random sites per cell) within the visible plasma membrane to the nearest mitochondria was 2.78 (95% confidence interval, 2.69-2.87) µm.

Next, we compared the activity of mitochondrial-associated (distance ≤ 0.5 µm) and non-associated (> 0.5 µm) L-type Ca^{2+} channel sparklet sites. GnRH–induced L-type Ca^{2+} channel

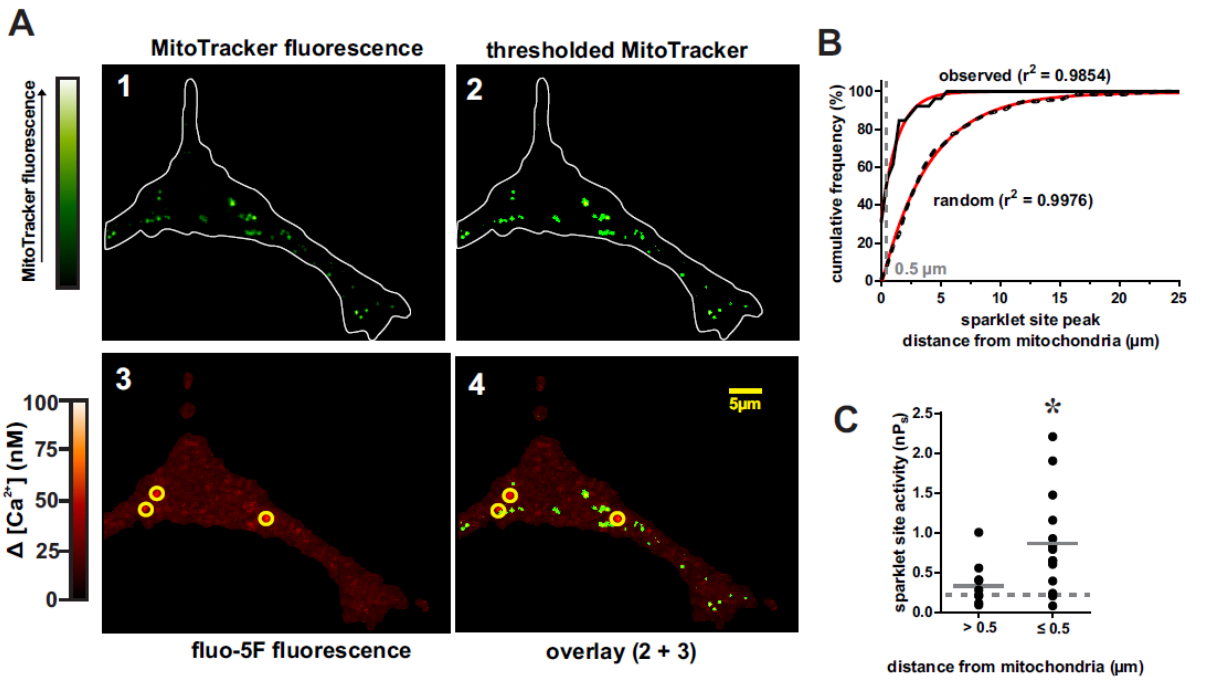

Figure 3.10. GnRH induced L-type Ca^{2+} channel sparklets associate with subplasmalemmal mitochondria. A, Representative total internal reflection fluorescence (TIRF) images showing subplasmalemmal mitochondria (MitoTracker fluorescence, panel 1; thresholded MitoTracker fluorescence, panel 2), L-type Ca^{2+} channel-mediated Ca^{2+} influx (fluo-5F fluorescence; panel 3), and an overlay of panels 2 and 3 (panel 4). Yellow circles in panels 3 and 4 indicate sites of L-type Ca^{2+} channel sparklet activity. B, Euclidean distance mapping showing cumulative distribution functions representing the distance of observed Ca^{2+} sparklet site peaks from mitochondria (solid black line; n = 13 cells) and from randomly distributed points (130 points, 10 points per cell) within the visible TIRF footprint (dashed black line). Solid red lines are best fits of the cumulative distributions with a single exponential function (see Methods). The vertical dashed gray line marks the distance separating mitochondrial associated (≤ 0.5 µm) and non-associated (> 0.5 µm) Ca^{2+} sparklet sites. C, Plot of Ca^{2+} sparklet site activities (nP_s) at sites > 0.5 and ≤ 0.5 µm from the nearest thresholded MitoTracker signal (n = 13 cells). The horizontal dashed gray line marks the threshold for high-activity Ca^{2+} sparklet sites ($nP_s \geq 0.2$). *P < 0.05.

sparklet sites associated with mitochondria were more active than those not associated with mitochondria (Figure 3.10C; $P < 0.05$). Although most of the Ca^{2+} sparklets were high activity ($nP_s > 0.2$), sparklets with higher nP_s values were closer to mitochondria (median $nP_s = 0.72$, IQR = 0.88) than Ca^{2+} sparklets with lower nP_s values (median $nP_s = 0.24$ IQR = 0.20). From these data, we conclude that the spatial distribution of L-type Ca^{2+} channel activity is highly correlated with subplasmalemmal mitochondria and supports the notion that mitochondrial ROS oxidation is able stimulate neighboring L-type Ca^{2+} channels in gonadotropes.

3.6 Discussion

In this study, we combined TIRF imaging with electrophysiological techniques to test the hypothesis that ROS are regulated by GnRH and affects L-type Ca^{2+} channel activity in gonadotropes. The major findings that support this hypothesis include: 1) GnRH induces subplasmalemmal ROS puncta; 2) ROS influence localized L-type Ca^{2+} channel activity in both αT3-1 cells and primary mouse gonadotrope cells; 3) mitochondrial ROS are regulated by GnRH receptor activation and affects L-type Ca^{2+} channel sparklets; and 4) active L-type Ca^{2+} channels associate with subplasmalemmal mitochondria.

Herein we investigated the role of ROS as a physiological signaling molecule, and identified these diffuse molecules to act locally in gonadotropes. Although ROS generation occurred throughout the entire cell using exogenous H_2O_2 treatment, GnRH only stimulated very particular discreet microdomains of ROS “puncta”. This localized response can be important in rapid downstream signaling, and is consistent with other sources that demonstrate high compartmentalization of H_2O_2 production (219-221). If there is dysfunction or disruption of normal signaling, such as an excess or imbalance of ROS availability, this can lead to different disease states due to altered bioavailability of NADPH or increased oxidative stress. Our results suggest that NADPH oxidase is involved in ROS-dependent stimulation of L-type Ca^{2+} channels in gonadotropes since inhibition of NADPH oxidase with apocynin prevented GnRH-dependent stimulation of both localized ROS generation (Fig. 3.5) and L-type Ca^{2+} channel function (Fig.

3.6). However, apocynin is reported to have intrinsic antioxidant properties that are independent of NADPH oxidase inhibition (222). Although these effects were shown at concentrations greater than that used in our study (25 μM), and despite our data being consistent with studies demonstrating an inhibitory effect specifically on NADPH oxidase activity that used alternative NADPH oxidase inhibitors (149,177,186), it is possible that a portion of the observed inhibitory effect of apocynin on ROS puncta generation and L-type Ca^{2+} channel function could result from antioxidant activity rather than NADPH oxidase inhibition. This implies that alternative sources of H_2O_2 (e.g., mitochondria) could participate in oxidant-dependent regulation of L-type Ca^{2+} channels in gonadotropes. Future studies should address this hypothesis to better understand physiological oxidative mechanisms to provide insight into understanding normal or disrupted cell function.

Since the spatial distribution of ROS generation mirrors that of local Ca^{2+} influx through L-type Ca^{2+} channels, we predicted ROS to be strong candidates for linking GnRH signaling and Ca^{2+} regulation in gonadotropes. Indeed, we provided evidence that ROS signaling are involved in GnRH-dependent stimulation of L-type Ca^{2+} channels. In addition, we also found that GnRH-mediated ROS generation required Ca^{2+}. These data strengthen the notion that Ca^{2+} and ROS microdomains are spatially localized and functionally coupled. Consistent with previous studies that identified the functional coupling of ROS and Ca^{2+} in other biological systems (148,149) and data indicating Ca^{2+} to be important in enhancing NADPH oxidase and mitochondrial-dependent ROS generation (207,223,224), we suggest that these colocalized microdomains produce a self-amplifying unit via a reciprocal coupling mechanism with two outputs (i.e., Ca^{2+} and ROS). This functional coupling may result at least in part from oxidation-dependent activation of PKC (225), which induces local Ca^{2+} influx through L-type Ca^{2+} channels. A recent study identifying PKC isoforms in specific compartmentalized subcellular regions supports this notion of locally regulated PKC (75). Exploring oxidative regulation of PKC for downstream L-type Ca^{2+} channel signaling will be a future area of investigation.

Recently, researchers have demonstrated the role of ROS regulating ERK activation and early response genes in gonadotropes (180). Our data complement these findings by establishing a mechanistic link between ROS and ERK phosphorylation, in which localized ROS generation modulated local influx through L-type Ca^{2+} channels necessary for downstream ERK activity. We have also identified these single channel Ca^{2+} influx events in primary mouse gonadotropes as well, demonstrating that these localized L-type Ca^{2+} channel events seen in αT3-1 cells to be physiologically pertinent, especially since localized Ca^{2+} sparklets were modulated by both GnRH and H_2O_2 in mouse gonadotrope cells. This exquisite specificity for subcellular compartmentalization on the plasma membrane may suggest that Ca^{2+} and ROS play crucial roles for signaling cascades necessary for physiological homeostasis. Therefore, identification of Ca^{2+} and ROS signaling components are important for potential therapeutic targets that manipulate GnRH receptor function for fertility, obesity-related endocrine dysfunction (226), polycystic ovarian syndrome (227,228), and GnRH-sensitive carcinomas (213,215,229).

In addition to NADPH oxidase regulation of Ca^{2+} activity, we also identified an important role for mitochondrial ROS in gonadotropes. GnRH receptor activation modulated mitochondrial oxidation in gonadotropes, suggesting that mitochondria may be important for downstream signaling. This supports recent findings in which mitochondrial components were associated with the GnRH receptor (230). Furthermore, we identified a subset of mitochondria associated with the plasma membrane, strengthening our hypothesis of localized microdomains at the subplasmalemmal surface that could regulate nearby L-type Ca^{2+} channels. Indeed, we show for the first-time mitochondrial ROS as an important source to regulate Ca^{2+} channel activity and provided evidence that areas of higher Ca^{2+} influx through L-type Ca^{2+} channels associated with nearby mitochondria in αT3-1 cells. Additionally, our findings demonstrating NADPH oxidase to influence mitochondrial oxidation, and inhibition of mitochondrial ROS decreasing ROS puncta on the cell surface may suggest an interdependence between different ROS sources in

gonadotropes. This method for RIRR would be an interesting mechanism for cells to amplify appropriate signals in spatially confined areas, however further exploration to clarify this possible interaction are needed. Nonetheless, these data provide exciting new insight into Ca^{2+}- and ROS-dependent modulation of mitochondrial function in gonadotropes. Although mitochondria have gained popularity as potential therapeutic targets in different disease states (218,231), little is known about the mechanistic properties of mitochondria for reproduction. Genetic mutations in mitochondrial DNA that disrupt electron transport complexes have been shown to produce faulty mitochondrial production in infants (Leigh syndrome) (232-234), but specific mitochondrial oxidation perturbations within the HPG axis have been unexplored despite its possible role in impacting reproduction.

GnRH signaling is highly regulated by actin cytoskeleton dynamics (57,58,125,126) and an intact cellular structural framework is necessary for Ca^{2+} channel signaling (206). With these additional findings of GnRH-regulated ROS and oxidative modulation of L-type Ca^{2+}channels, we suggest a functional mechanistic link between the cytoskeletal reorganization and these ROS components may be possible. A dynamic cytoarchitecture creating localized signaling microdomains is necessary for cells to be positioned appropriately for physiological purposes, such as cell-to-cell communication and ultimately hormone release. Interestingly, we empirically observed that some cells had ROS puncta and mitochondria distributed near processes and extensions of the gonadotrope, which may be important for cell migration and mobilization. However, these observations of ROS-mediated actin cytoskeletal dynamics need to be further investigated. Indeed, there has been evidence that actin dynamics can be oxidatively regulated (235-239), so future directions would include whether cytoskeletal components (e.g. cofilin, Rac1) are important for GnRH receptor signaling and their effects on Ca^{2+} and ROS microdomains.

In conclusion, these data provide evidence that ROS generation from NADPH oxidase and mitochondria are involved in GnRH-dependent stimulation of L-type Ca^{2+} channels. This

supports the concept that there is crosstalk between Ca^{2+} and ROS with the notion of spatially colocalized Ca^{2+} and ROS compartmentalization. We propose that these coupled signaling microdomains underlie macro-physiological processes such as gonadotrope activation and subsequent ovulation and reproductive behavior. Moreover, our functionally coupled Ca^{2+} and ROS microdomain hypothesis implies that reciprocal modulation of L-type Ca^{2+} channels and ROS generated from NADPH-oxidase and mitochondria extends beyond that of simple colocalization of ROS generation and Ca^{2+} influx. For example, this model suggests potential regulation of cellular function in conditions such as metabolic dysfunction (e.g., obesity and diabetes) by influencing the availability of the reducing equivalent NADPH or bioenergetic activity in adjacent subplasmalemmal mitochondria.

Chapter 4. Conclusion

Very early works in gonadotropes identified various voltage-gated channels in gonadotropes, including classification of Ca^{2+} channels on the plasma membrane using classical electrophysiology techniques (87,135). Additionally, many studies focused on the role of this extracellular Ca^{2+} for GnRH-stimulated gonadotropin secretion (131,132,240). However, later research and emphasis shifted to the role of intracellular Ca^{2+} and various Ca^{2+} oscillation patterns since this robust rapid rise in Ca^{2+} from internal stores was also important for gonadotropin release. However, the discovery of divergent Ca^{2+} signals for separate MAPK cascades has provided a unique pathway with compartmentalized signaling cascades for downstream gonadotropin gene expression (86,128). This demonstrated the ability of a cell to separate and distinguish different Ca^{2+} sources for various intracellular functions that provide specific physiological responses (e.g. FSH vs. LH production) during different stages of the ovulatory cycle. These findings suggest that microdomains of Ca^{2+} would be plausible in order to parse out the differences in gonadotropin synthesis, but technical limitations hindered the identification of these localized signals and further characterization for the role of L-type Ca^{2+} channels in GnRH signaling were limited.

However, the use of combined TIRF microscopy and electrophysiology techniques has provided greater insight into understanding L-type Ca^{2+} channel signaling in gonadotropes. We have been able visualize with high spatial and temporal resolution L-type Ca^{2+} channel sparklets in localized microdomains on the plasma membrane, separate from Ca^{2+} from internal stores. Using this method, we were also able to identify various mechanisms in the GnRH signaling cascade that regulate these Ca^{2+} sparklets. Given past evidence for the importance of an organized cellular architecture for signaling, we identified the need for dynamic actin cytoskeletal components for GnRH-induced L-type Ca^{2+} influx. In addition, by observing the functional coupling of Ca^{2+} and ROS in other cell types, we have identified NADPH oxidase and

mitochondria to be important in modulating Ca^{2+} sparklets as well. This section concludes the dissertation by providing a summary of the major findings of this dissertation and future directions to build upon these discoveries.

4.1 GnRH Signaling

The central dogma of reproduction and appropriate fertility relies on precise asynchronous and unparalleled phased secretion of LH and FSH in response to GnRH during the ovulatory cycle. Our experiments identifying localized L-type Ca^{2+} channel activity following GnRH receptor activation provided a compelling mechanism for fast acting, specific signaling downstream for ERK activation and LH transcription, contrary to JNK activation for FSH secretion. Acute and lower concentrations of GnRH treatment (using 10nM for 5-10 minutes) to identify rapid and immediate events following GnRH receptor activation gives greater insight into proximal events after GnRH stimulation than other experiments that use longer and greater GnRH treatments (e.g. 100nM for 30 minutes or more). Consistent with the notion of rapid and precise signaling, previous studies have shown that genes were also rapidly regulated by GnRH in LβT2 cells (108). The biosynthetic rate of the induced genes was dependent on GnRH concentration, and regulated genes were all activated by 1 hour and actually returned to basal levels at 3 hours (241). Therefore, narrowing down the timeframe and understanding the role for rapid and sensitive plasmalemmal signaling for downstream nuclear gene expression is essential.

Additionally, identifying acute GnRH stimulation is important since previous studies found prolonged GnRH exposure to reduce gonadotropin secretion. This was possibly due to either desensitization of the GnRHR, decreased GnRHR availability at the cell surface, or changes in $G\alpha_{q/11}$ levels in αT3-1 cells (42,242,243). Therefore, it is likely GnRH release from GnRH neurons trigger rapid dynamic changes through quick and localized L-type Ca^{2+} channel responses following GnRH receptor activation, allowing for quick recovery for downstream signaling and increased sensitivity for each incoming pulse during various stages of the

ovulatory cycle. Given the inherent pulsatile nature of GnRH secretion, future experiments to recapitulate appropriate GnRH pulse frequencies and subsequent L-type Ca^{2+} sparklet responses would provide a more physiologically relevant paradigm beyond acute GnRH treatment.

In addition to GnRH pulsatility, further knowledge of GnRH receptor mobilization is important to understand how GnRH activates localized Ca^{2+} domains. The unique slower kinetics of GnRHR desensitization and the prolonged availability for signaling at the plasma membrane supports an interaction with the L-type Ca^{2+} channel. Previous studies demonstrated a decrease in lateral mobilization of GnRHRs following GnRH stimulation (45-47). Given our findings that L-type Ca^{2+} sparklets only make up less than 3% of the cell surface, exploring the possibility that GnRHRs mobilize to discrete L-type Ca^{2+} channel clusters on the plasma membrane to elicit a localized response is enticing.

Using methods that provide real time localization and funcion would progress the study of GnRH pathways dramatically compared to traditional methods of protein–protein and enzyme–substrate interactions that lose kinetic information of cell signaling. New advancements in technology such as single particle tracking of labeled proteins and receptors allow for real time tracking of individual GnRHRs in living cells and provide insightful information on organized receptor signaling. In addition, this technique with simultaneous labeling of L-type Ca^{2+} channels or Ca^{2+} sparklets can provide evidence of spatial and temporal organization and possible microdomains in gonadotropes.

As seen previously, appropriate architecture with extensive cytoskeletal regulation is necessary for rapid, plasmalemmal signaling in gonadotropes. Lack of these signaling complexes can lead to interrupted and aberrant signaling. Given that the GnRHR is not internalized rapidly, an organized platform at the plasma membrane is likely to be important for downstream events. We have identified actin dynamics to be important for GnRH-mediated L-type Ca^{2+} channel sparklets (Fig 2.4). Recently, researchers have identified a role for dynamin, a

GTPase that possesses mechanochemical properties important in cellular membrane remodeling events, in GnRH-mediated actin reorganization in gonadotropes (244). Specifically, dynamin was found at plasma membrane protrusions and co-localized with actin and cortactin at the leading edges of the membrane following GnRH stimulation. Importantly, disruption of dynamin also affected L-type Ca^{2+} channel influx as well, decreasing both GnRH-induced Ca^{2+} sparklet activity and density in αT3-1 cells. Given these findings, experiments to see if disruption of actin cytoskeletal elements change the distribution of GnRH receptor mobilization on the cell surface relative to the areas of localized Ca^{2+} should be further investigated in the future.

Previously, PKC was shown to be required for ERK activation, but the mechanisms were unknown. Some provided studies demonstrating an interdependence between PKC and Ca^{2+} in regulating gonadotropin mRNA expression and secretion (76-78). Our findings provide a mechanistic connection among previous findings with evidence that PKC mediates an increase in L-type Ca^{2+} channel sparklets (Fig 2.3) necessary for downstream ERK phosphorylation. However, further details about which specific isoforms of PKC regulate Ca^{2+} sparklets and how PKC activates the L-type Ca^{2+} channel are still unknown. In other cell types, different isoforms of PKC have been shown to phosphorylate serine residues on L-type Ca^{2+} channel subunits (245,246). However, it is unknown whether direct phosphorylation by PKC or intermediates between PKC and the L-type Ca^{2+} channel is necessary for L-type Ca^{2+} channel sparklets in gonadotropes.

4.2 L-type Ca^{2+} Channel Activity in Gonadotropes

Identification of Ca^{2+} sparklets in gonadotropes has been useful in further understanding L-type Ca^{2+} channel responses to GnRH. Specifically, our studies suggest L-type Ca^{2+} channels spatially cluster together, often with multiple channels grouped at one site to produce high activity Ca^{2+} sparklets. However, alternative methods to address this organization of L-type Ca^{2+} channels using super resolution microscopy (e.g. STORM or PALM) can provide additional evidence to support this notion. In addition, further investigation of the mechanisms that allow

for channels to cluster together would be useful. AKAP, an anchoring protein was found to be important in L-type Ca^{2+} channel clustering in specific cell types (194,247), but the role for AKAP in gonadotropes has yet to be addressed. Also, pharmacological inhibitors lack specificity for distinguishing specific isoforms of L-type Ca^{2+} channels, and alternative methods to identify the role of Cav1.2 compared to Cav1.3 in gonadotropes and whether different isoforms can cluster together would be insightful.

4.3 Ca^{2+}-mediated ERK Activation

In recognizing the importance of ERK activation for downstream LH synthesis and secretion, attempts to explore signaling mechanisms required for ERK phosphorylation have been heavily explored. Our findings add to this body of knowledge by identifying a role for localized Ca^{2+} sparklets within a rapid timeframe (~5-10 minutes) that is consistent with maximal phosphorylation of ERK (Fig 2.2). However, exact mechanisms for how localized Ca^{2+} influx leads to ERK activation and whether an appropriate Ca^{2+} influx threshold at these particular sites is necessary for phosphorylating ERK is unknown. Given previous findings of ERK in lipid raft compartments, ERK may be activated within the membrane bound signaling platforms (123,124). This supports our hypothesis of a localized signaling microdomain and very localized Ca^{2+} at the plasma membrane able to activate nearby ERK. Future experiments to identify exact compartmentalization and localization of ERK, using methods such as ERK reporters (248,249) that can show ERK activation in discrete compartments of the cell are necessary to investigate where ERK activation occurs relative to the L-type Ca^{2+} channel sparklets.

The transduction mechanisms between plasma membrane signaling events and ERK have been elusive in gonadotropes. Canonical MAPK cascade activation suggests the GTP-ase Ras leading to Raf activation ultimately phosphorylates ERK. It has been suggested that discretely localized Ca^{2+} domains are necessary for Ras signaling at the plasma membrane (250), but direct experiments to address this interaction in gonadotropes to demonstrate if L-type Ca^{2+} channel sparklet activity can interact with Ras need to be conducted. Furthermore,

Raf is widely believed to be the key upstream activator of ERK signaling in gonadotropes. PKC has been suggested to directly activate Raf, but little evidence exists of this interaction. Additionally, Raf in GnRH-induced ERK activation has also not been identified. Therefore, our findings of the localized L-type Ca^{2+} channel activity may be one component of this mechanistic link for plasma membrane signaling and the initiation of the MAPK cascade, but studies to conclusively identify this relationship need to be conducted.

4.4 ROS Signaling and Ca^{2+} Coupling

ROS have been previously shown to play a role in gonadotrope signaling and ERK activation (180), but we have provided a mechanistic link in which ROS from NADPH oxidase and mitochondrial modulate localized L-type Ca^{2+} channel activity in gonadotropes. Additionally, we have identified that GnRH generated confined ROS puncta at the level of the plasma membrane, consistent with the concept of an organized platform for localized and rapid signaling (Fig 3.2). We provided some evidence that H_2O_2 plays a role as the key oxidant second messenger, although the role of other ROS such as O_2^- would clarify if more than one form of ROS is necessary. Additionally, although we have been able to demonstrate spatially localized areas of ROS on the plasma membrane, temporal information has not been addressed. Therefore, future experiments utilizing ratiometric ROS sensors would be a valuable tool to understand the kinetics of ROS signaling in gonadotropes and its relationship to L-type Ca^{2+} channel activity.

Although we have demonstrated that H_2O_2 stimulation increased Ca^{2+} sparklet activity and inhibition of NADPH oxidase decreased GnRH-induced L-type Ca^{2+}channel influx in gonadotropes (Fig 3.6), these mechanisms have yet to be established. As mentioned previously, we found PKC to be important for GnRH-induced increases in Ca^{2+} influx through L-type Ca^{2+} channels. Therefore, it would be possible that ROS and PKC are interdependent for activating L-type Ca^{2+} channels. Indeed, there is evidence that cysteine residues found in the C1

domain of conventional PKCs are preferentially oxidized under lower levels of oxidant exposure (225), but further identification of this mechanism in gonadotropes is needed.

ROS generation from mitochondria also play a role in stimulating L-type Ca^{2+} sparklets in gonadotropes. We have identified a high number of mitochondria associated near the plasma membrane, and even showed higher activity Ca^{2+} sparklets spatially associated with mitochondria (mean distance <0.5µm; Figure 3.10). Mitochondria located near Ca^{2+} sources in cellular compartments such as ER-mitochondria contact sites have been studied in other cell types (251,252). However, understanding how mitochondria are contained to the plasma membrane near these L-type Ca^{2+} channels in gonadotropes is unknown. Whether mitochondria mobilization is GnRH-dependent, a dynamic and mobile process, or if cytoskeletal components help traffic mitochondria to the specific compartments of the plasma membrane or areas of highly localized Ca^{2+} from L-type Ca^{2+} channels are intriguing questions to answer. Mobilization of mitochondria utilizing motor proteins across microtubules and Ca^{2+} sensitive Miro GTP-ases have been investigated in other biological systems (253,254), and whether parallel mechanisms occur in gonadotropes is worth exploring.

Experiments demonstrating NADPH oxidase inhibition decreasing GnRH-induced mitochondrial oxidation and L-type Ca^{2+} channel influx suggests a relationship among localized Ca^{2+}, NADPH oxidase and mitochondria. Localization of ROS and Ca^{2+} into compartmentalized domains, and tight regulation of ROS signal amplification via RIRR allows for specific areas of Ca^{2+} and ROS interaction within a cell. In contrast, global elevation of ROS can lead to non-specific activation of various cascades associated with oxidative stress. Additional experiments are needed to investigate the mechanisms of RIRR in gonadotropes. Given the importance of cytoskeletal dynamics for appropriate GnRH signaling and L-type Ca^{2+} channel activity, investigating the oxidative regulation of cytoskeletal components can provide valuable insight on the how these components cooperatively modulate L-type Ca^{2+} channel influx. In other systems, NOX subunits were directed to specific platforms and oxidants were found to concentrate within

membrane ruffles, indicative of oxidant-dependent cytoskeletal function (255). Additionally, NADPH oxidase subunits were found to bind to proteins on the leading edge of lamellipodia (256,257). In addition, whether oxidative regulation of actin cytoskeletal proteins (e.g. cofilin and rac1) seen in other biological systems (235-239) occurs in gonadotropes would also support our hypothesis that integrates the role of ROS in conjunction with an organized signaling domain for localized L-type Ca^{2+} channel activity.

4.5 Final Remarks

In this study, we provided the first evidence for localized L-type Ca^{2+} influx important for GnRH signaling and downstream ERK activation. Additionally, we identified different mechanisms that regulate L-type Ca^{2+} channel influx, recognizing that Ca^{2+} sparklet activity is PKC-dependent and requires an active cytoskeletal organization for appropriate GnRH signaling. We also identified GnRH-mediated ROS generation in spatially confined areas at the plasma membrane from both NADPH oxidase and mitochondria, and find this to be important for L-type Ca^{2+} sparklet influx in gonadotropes. These findings highlight elegant cell signaling mechanisms, in which signaling cascades occur in tightly regulated domains to provide specificity. This is important for physiological purposes since gonadotropes are sensitive to GnRH pulsatility and need to quickly adapt to various GnRH pulse frequencies during different stages of the ovulatory cycle for appropriate gonadotropin gene expression and secretion. Therefore, understanding the cell machinery and regulation of L-type Ca^{2+} channels can provide insight into therapeutic solutions when normal processes become disrupted leading to reproductive dysfunction or disease states.

References

1. Navedo MF, Amberg GC, Votaw VS, Santana LF. Constitutively active L-type Ca2+ channels. Proceedings of the National Academy of Sciences of the United States of America 2005; 102:11112-11117

2. Bliss SP, Navratil AM, Xie J, Roberson MS. GnRH signaling, the gonadotrope and endocrine control of fertility. Frontiers in neuroendocrinology 2010; 31:322-340

3. Chowdhury I, Sridaran R. GnRH-GnRH-Receptor System in the Mammalian Female Reproductive Tract. In: Chedrese PJ, ed. Reproductive Endocrinology: A Molecular Approach. Boston, MA: Springer US; 2009:131-143.

4. Knobil E. The neuroendocrine control of the menstrual cycle. Recent progress in hormone research 1980; 36:53-88

5. Thompson IR, Kaiser UB. GnRH Pulse Frequency-dependent Differential Regulation of LH and FSH Gene Expression. Molecular and cellular endocrinology 2014; 385:28-35

6. Krsmanovic LZ, Hu L, Leung P-K, Feng H, Catt KJ. The Hypothalamic GnRH Pulse Generator: Multiple Regulatory Mechanisms. Trends in endocrinology and metabolism: TEM 2009; 20:402-408

7. Naor Z. Signaling by G-protein-coupled receptor (GPCR): studies on the GnRH receptor. Frontiers in neuroendocrinology 2009; 30:10-29

8. Belchetz PE, Plant TM, Nakai Y, Keogh EJ, Knobil E. Hypophysial responses to continuous and intermittent delivery of hypopthalamic gonadotropin-releasing hormone. Science 1978; 202:631-633

9. Marshall JC, Kelch RP. Gonadotropin-releasing hormone: role of pulsatile secretion in the regulation of reproduction. The New England journal of medicine 1986; 315:1459-1468

10. Tsutsumi R, Webster NJ. GnRH pulsatility, the pituitary response and reproductive dysfunction. Endocrine journal 2009; 56:729-737

11. Haisenleder DJ, Dalkin AC, Ortolano GA, Marshall JC, Shupnik MA. A pulsatile gonadotropin-releasing hormone stimulus is required to increase transcription of the gonadotropin subunit genes: evidence for differential regulation of transcription by pulse frequency in vivo. Endocrinology 1991; 128:509-517

12. Hall JE, Taylor AE, Hayes FJ, Crowley WF, Jr. Insights into hypothalamic-pituitary dysfunction in polycystic ovary syndrome. Journal of endocrinological investigation 1998; 21:602-611

13. Reame NE, Sauder SE, Case GD, Kelch RP, Marshall JC. Pulsatile gonadotropin secretion in women with hypothalamic amenorrhea: evidence that reduced frequency of gonadotropin-releasing hormone secretion is the mechanism of persistent anovulation. The Journal of clinical endocrinology and metabolism 1985; 61:851-858

14. Dodé C, Levilliers J, Dupont J-M, De Paepe A, Le Dû N, Soussi-Yanicostas N, Coimbra RS, Delmaghani S, Compain-Nouaille S, Baverel F. Loss-of-function mutations in FGFR1 cause autosomal dominant Kallmann syndrome. Nature genetics 2003; 33:463-465

15. Tilbrook AJ, Clarke IJ. Negative Feedback Regulation of the Secretion and Actions of Gonadotropin-Releasing Hormone in Males. Biology of reproduction 2001; 64:735-742

16. Glidewell-Kenney C, Hurley LA, Pfaff L, Weiss J, Levine JE, Jameson JL. Nonclassical estrogen receptor alpha signaling mediates negative feedback in the female mouse reproductive axis. Proceedings of the National Academy of Sciences of the United States of America 2007; 104:8173-8177

17. Naftolin F, Garcia-Segura LM, Horvath TL, Zsarnovszky A, Demir N, Fadiel A, Leranth C, Vondracek-Klepper S, Lewis C, Chang A, Parducz A. Estrogen-induced hypothalamic

synaptic plasticity and pituitary sensitization in the control of the estrogen-induced gonadotrophin surge. Reproductive sciences (Thousand Oaks, Calif) 2007; 14:101-116

18. Petersen SL, Ottem EN, Carpenter CD. Direct and indirect regulation of gonadotropin-releasing hormone neurons by estradiol. Biology of reproduction 2003; 69:1771-1778

19. Le Tissier PR, Hodson DJ, Lafont C, Fontanaud P, Schaeffer M, Mollard P. Anterior pituitary cell networks. Frontiers in neuroendocrinology 2012; 33:252-266

20. Lloyd JM, Childs GV. Differential storage and release of luteinizing hormone and follicle-releasing hormone from individual gonadotropes separated by centrifugal elutriation. Endocrinology 1988; 122:1282-1290

21. Turgeon JL, Kimura Y, Waring DW, Mellon PL. Steroid and pulsatile gonadotropin-releasing hormone (GnRH) regulation of luteinizing hormone and GnRH receptor in a novel gonadotrope cell line. Molecular endocrinology (Baltimore, Md) 1996; 10:439-450

22. Windle JJ, Weiner RI, Mellon PL. Cell lines of the pituitary gonadotrope lineage derived by targeted oncogenesis in transgenic mice. Molecular endocrinology (Baltimore, Md) 1990; 4:597-603

23. Wen S, Schwarz JR, Niculescu D, Dinu C, Bauer CK, Hirdes W, Boehm U. Functional characterization of genetically labeled gonadotropes. Endocrinology 2008; 149:2701-2711

24. Kraus S, Naor Z, Seger R. Intracellular signaling pathways mediated by the gonadotropin-releasing hormone (GnRH) receptor. Archives of medical research 2001; 32:499-509

25. Eidne KA, Flanagan CA, Harris NS, Millar RP. Gonadotropin-Releasing Hormone (GnRH)-Binding Sites in Human Breast Cancer Cell Lines and Inhibitory Effects of GnRH Antagonists*. The Journal of Clinical Endocrinology & Metabolism 1987; 64:425-432

26. Smith MR, Finkelstein JS, McGovern FJ, Zietman AL, Fallon MA, Schoenfeld DA, Kantoff PW. Changes in Body Composition during Androgen Deprivation Therapy for Prostate Cancer. The Journal of Clinical Endocrinology & Metabolism 2002; 87:599-603

27. Tsutsumi M, Zhou W, Millar RP, Mellon PL, Roberts JL, Flanagan CA, Dong K, Gillo B, Sealfon SC. Cloning and functional expression of a mouse gonadotropin-releasing hormone receptor. Molecular endocrinology (Baltimore, Md) 1992; 6:1163-1169

28. Luttrell LM, Lefkowitz RJ. The role of beta-arrestins in the termination and transduction of G-protein-coupled receptor signals. Journal of cell science 2002; 115:455-465

29. Vrecl M, Heding A, Hanyaloglu A, Taylor PL, Eidne KA. Internalization kinetics of the gonadotropin-releasing hormone (GnRH) receptor. Pflugers Archiv : European journal of physiology 2000; 439:r019-r020

30. Willars GB, Heding A, Vrecl M, Sellar R, Blomenrohr M, Nahorski SR, Eidne KA. Lack of a C-terminal tail in the mammalian gonadotropin-releasing hormone receptor confers resistance to agonist-dependent phosphorylation and rapid desensitization. The Journal of biological chemistry 1999; 274:30146-30153

31. Willars GB, Royall JE, Nahorski SR, El-Gehani F, Everest H, McArdle CA. Rapid down-regulation of the type I inositol 1,4,5-trisphosphate receptor and desensitization of gonadotropin-releasing hormone-mediated Ca2+ responses in alpha T3-1 gonadotropes. The Journal of biological chemistry 2001; 276:3123-3129

32. Castro-Fernandez C, Conn PM. Regulation of the gonadotropin-releasing hormone receptor (GnRHR) by RGS proteins: role of the GnRHR carboxyl-terminus. Molecular and cellular endocrinology 2002; 191:149-156

33. Finch AR, Caunt CJ, Armstrong SP, McArdle CA. Agonist-induced internalization and downregulation of gonadotropin-releasing hormone receptors. American journal of physiology Cell physiology 2009; 297:C591-600

34. Hanyaloglu AC, Vrecl M, Kroeger KM, Miles LE, Qian H, Thomas WG, Eidne KA. Casein kinase II sites in the intracellular C-terminal domain of the thyrotropin-releasing hormone receptor and chimeric gonadotropin-releasing hormone receptors contribute to beta-arrestin-dependent internalization. The Journal of biological chemistry 2001; 276:18066-18074

35. Heding A, Vrecl M, Bogerd J, McGregor A, Sellar R, Taylor PL, Eidne KA. Gonadotropin-releasing hormone receptors with intracellular carboxyl-terminal tails undergo acute desensitization of total inositol phosphate production and exhibit accelerated internalization kinetics. The Journal of biological chemistry 1998; 273:11472-11477

36. Heding A, Vrecl M, Hanyaloglu AC, Sellar R, Taylor PL, Eidne KA. The rat gonadotropin-releasing hormone receptor internalizes via a beta-arrestin-independent, but dynamin-dependent, pathway: addition of a carboxyl-terminal tail confers beta-arrestin dependency. Endocrinology 2000; 141:299-306

37. Hislop JN, Caunt CJ, Sedgley KR, Kelly E, Mundell S, Green LD, McArdle CA. Internalization of gonadotropin-releasing hormone receptors (GnRHRs): does arrestin binding to the C-terminal tail target GnRHRs for dynamin-dependent internalization? Journal of molecular endocrinology 2005; 35:177-189

38. Pawson AJ, Faccenda E, Maudsley S, Lu ZL, Naor Z, Millar RP. Mammalian type I gonadotropin-releasing hormone receptors undergo slow, constitutive, agonist-independent internalization. Endocrinology 2008; 149:1415-1422

39. Hislop JN, Everest HM, Flynn A, Harding T, Uney JB, Troskie BE, Millar RP, McArdle CA. Differential internalization of mammalian and non-mammalian gonadotropin-releasing hormone receptors. Uncoupling of dynamin-dependent internalization from mitogen-activated protein kinase signaling. The Journal of biological chemistry 2001; 276:39685-39694

40. Vrecl M, Anderson L, Hanyaloglu A, McGregor AM, Groarke AD, Milligan G, Taylor PL, Eidne KA. Agonist-induced endocytosis and recycling of the gonadotropin-releasing hormone receptor: effect of beta-arrestin on internalization kinetics. Molecular endocrinology (Baltimore, Md) 1998; 12:1818-1829

41. Perrett RM, McArdle CA. Molecular Mechanisms of Gonadotropin-Releasing Hormone Signaling: Integrating Cyclic Nucleotides into the Network. Frontiers in Endocrinology 2013; 4:180

42. McArdle CA, Franklin J, Green L, Hislop JN. Signalling, cycling and desensitisation of gonadotrophin-releasing hormone receptors. The Journal of endocrinology 2002; 173:1-11

43. Themmen APN, Huhtaniemi IT. Mutations of gonadotropins and gonadotropin receptors: elucidating the physiology and pathophysiology of pituitary-gonadal function. Endocrine reviews 2000; 21:551-583

44. Leanos-Miranda A, Janovick JA, Conn PM. Receptor-misrouting: an unexpectedly prevalent and rescuable etiology in gonadotropin-releasing hormone receptor-mediated hypogonadotropic hypogonadism. The Journal of clinical endocrinology and metabolism 2002; 87:4825-4828

45. Cornea A, Conn PM. Measurement of changes in fluorescence resonance energy transfer between gonadotropin-releasing hormone receptors in response to agonists. Methods 2002; 27:333-339

46. Horvat RD, Roess DA, Nelson SE, Barisas BG, Clay CM. Binding of agonist but not antagonist leads to fluorescence resonance energy transfer between intrinsically fluorescent gonadotropin-releasing hormone receptors. Molecular endocrinology (Baltimore, Md) 2001; 15:695-703

47. Nelson S, Horvat RD, Malvey J, Roess DA, Barisas BG, Clay CM. Characterization of an intrinsically fluorescent gonadotropin-releasing hormone receptor and effects of ligand binding on receptor lateral diffusion. Endocrinology 1999; 140:950-957

48. Cornea A, Janovick JA, Maya-Núñez G, Conn PM. Gonadotropin-releasing hormone receptor microaggregation. Rate monitored by fluorescence resonance energy transfer. The Journal of biological chemistry 2001; 276:2153-2158

49. Brown DA, London E. Structure and origin of ordered lipid domains in biological membranes. The Journal of membrane biology 1998; 164:103-114

50. Edidin M. The state of lipid rafts: from model membranes to cells. Annu Rev Biophys Biomol Struct 2003; 32:257-283

51. Simons K, Vaz WL. Model systems, lipid rafts, and cell membranes. Annu Rev Biophys Biomol Struct 2004; 33:269-295

52. Navratil AM, Bliss SP, Berghorn KA, Haughian JM, Farmerie TA, Graham JK, Clay CM, Roberson MS. Constitutive localization of the gonadotropin-releasing hormone (GnRH) receptor to low density membrane microdomains is necessary for GnRH signaling to ERK. The Journal of biological chemistry 2003; 278:31593-31602

53. Navratil AM, Bliss SP, Roberson MS. Membrane rafts and GnRH receptor signaling. Brain research 2010; 1364:53-61

54. Bliss SP, Navratil AM, Breed M, Skinner DC, Clay CM, Roberson MS. Signaling complexes associated with the type I gonadotropin-releasing hormone (GnRH) receptor: colocalization of extracellularly regulated kinase 2 and GnRH receptor within membrane rafts. Molecular endocrinology (Baltimore, Md) 2007; 21:538-549

55. Porat-Shliom N, Milberg O, Masedunskas A, Weigert R. Multiple roles for the actin cytoskeleton during regulated exocytosis. Cellular and molecular life sciences : CMLS 2013; 70:2099-2121

56. Ridley AJ, Schwartz MA, Burridge K, Firtel RA, Ginsberg MH, Borisy G, Parsons JT, Horwitz AR. Cell Migration: Integrating Signals from Front to Back. Science 2003; 302:1704-1709

57. Navratil AM, Dozier MG, Whitesell JD, Clay CM, Roberson MS. Role of cortactin in dynamic actin remodeling events in gonadotrope cells. Endocrinology 2014; 155:548-557

58. Navratil AM, Knoll JG, Whitesell JD, Tobet SA, Clay CM. Neuroendocrine plasticity in the anterior pituitary: gonadotropin-releasing hormone-mediated movement in vitro and in vivo. Endocrinology 2007; 148:1736-1744

59. Alim Z, Hartshorn C, Mai O, Stitt I, Clay C, Tobet S, Boehm U. Gonadotrope plasticity at cellular and population levels. Endocrinology 2012; 153:4729-4739

60. Stanislaus D, Janovick JA, Brothers S, Conn PM. Regulation of G(q/11)alpha by the gonadotropin-releasing hormone receptor. Molecular endocrinology (Baltimore, Md) 1997; 11:738-746

61. Shah BH, MacEwan DJ, Milligan G. Gonadotrophin-releasing hormone receptor agonist-mediated down-regulation of Gq alpha/G11 alpha (pertussis toxin-insensitive) G proteins in alpha T3-1 gonadotroph cells reflects increased G protein turnover but not alterations in mRNA levels. Proceedings of the National Academy of Sciences of the United States of America 1995; 92:1886-1890

62. Shah BH, Milligan G. The gonadotrophin-releasing hormone receptor of alpha T3-1 pituitary cells regulates cellular levels of both of the phosphoinositidase C-linked G proteins, Gq alpha and G11 alpha, equally. Molecular pharmacology 1994; 46:1-7

63. Grosse R, Schmid A, Schoneberg T, Herrlich A, Muhn P, Schultz G, Gudermann T. Gonadotropin-releasing hormone receptor initiates multiple signaling pathways by exclusively coupling to G(q/11) proteins. The Journal of biological chemistry 2000; 275:9193-9200

64. Naor Z, Azrad A, Limor R, Zakut H, Lotan M. Gonadotropin-releasing hormone activates a rapid Ca2+-independent phosphodiester hydrolysis of polyphosphoinositides in pituitary gonadotrophs. The Journal of biological chemistry 1986; 261:12506-12512

65. Drin G, Scarlata S. Stimulation of phospholipase Cbeta by membrane interactions, interdomain movement, and G protein binding--how many ways can you activate an enzyme? Cellular signalling 2007; 19:1383-1392

66. Chidiac P, Ross EM. Phospholipase C-beta1 directly accelerates GTP hydrolysis by Galphaq and acceleration is inhibited by Gbeta gamma subunits. The Journal of biological chemistry 1999; 274:19639-19643

67. Montell C. PLC fills a GAP in G-protein-coupled signalling. Nature cell biology 2000; 2:E82-E83

68. Kikkawa U, Ogita K, Shearman MS, Ase K, Sekiguchi K, Naor Z, Kishimoto A, Nishizuka Y, Saito N, Tanaka C, et al. The family of protein kinase C: its molecular heterogeneity and differential expression. Cold Spring Harbor symposia on quantitative biology 1988; 53 Pt 1:97-102

69. Newton AC. Protein kinase C: structure, function, and regulation. The Journal of biological chemistry 1995; 270:28495-28498

70. Dorn GW, 2nd, Mochly-Rosen D. Intracellular transport mechanisms of signal transducers. Annual review of physiology 2002; 64:407-429

71. Naor Z. Signaling by G-protein-coupled receptor (GPCR): Studies on the GnRH receptor. Frontiers in neuroendocrinology 2009; 30:10-29

72. Kratzmeier M, Poch A, Mukhopadhyay AK, McArdle CA. Selective translocation of non-conventional protein kinase C isoenzymes by gonadotropin-releasing hormone (GnRH) in the gonadotrope-derived alpha T3-1 cell line. Molecular and cellular endocrinology 1996; 118:103-111

73. Shraga-Levine Z, Ben-Menahem D, Naor Z. Activation of protein kinase C beta gene expression by gonadotropin-releasing hormone in alpha T3-1 cell line. Role of Ca2+ and autoregulation by protein kinase C. The Journal of biological chemistry 1994; 269:31028-31033

74. Harris D, Reiss N, Naor Z. Differential activation of protein kinase C delta and epsilon gene expression by gonadotropin-releasing hormone in alphaT3-1 cells. Autoregulation by protein kinase C. The Journal of biological chemistry 1997; 272:13534-13540

75. Mugami S, Dobkin-Bekman M, Rahamim–Ben Navi L, Naor Z. Differential roles of PKC isoforms (PKCs) in GnRH stimulation of MAPK phosphorylation in gonadotrope derived cells. Molecular and cellular endocrinology

76. Naor Z. Signal transduction mechanisms of Ca2+ mobilizing hormones: the case of gonadotropin-releasing hormone. Endocrine reviews 1990; 11:326-353

77. Stojilkovic SS, Catt KJ. Expression and signal transduction pathways of gonadotropin-releasing hormone receptors. Recent progress in hormone research 1995; 50:161-205

78. Ando H, Hew CL, Urano A. Signal transduction pathways and transcription factors involved in the gonadotropin-releasing hormone-stimulated gonadotropin subunit gene expression. Comparative biochemistry and physiology Part B, Biochemistry & molecular biology 2001; 129:525-532

79. Berridge MJ, Lipp P, Bootman MD. The versatility and universality of calcium signalling. Nature reviews Molecular cell biology 2000; 1:11-21

80. Burger LL, Haisenleder DJ, Aylor KW, Marshall JC. Regulation of intracellular signaling cascades by GNRH pulse frequency in the rat pituitary: roles for CaMK II, ERK, and JNK activation. Biology of reproduction 2008; 79:947-953

81. Haisenleder DJ, Workman LJ, Burger LL, Aylor KW, Dalkin AC, Marshall JC. Gonadotropin subunit transcriptional responses to calcium signals in the rat: evidence for regulation by pulse frequency. Biology of reproduction 2001; 65:1789-1793

82. Stojilkovic SS, Iida T, Merelli F, Torsello A, Krsmanovic LZ, Catt KJ. Interactions between calcium and protein kinase C in the control of signaling and secretion in pituitary gonadotrophs. The Journal of biological chemistry 1991; 266:10377-10384

83. Leong DA, Thorner MO. A potential code of luteinizing hormone-releasing hormone-induced calcium ion responses in the regulation of luteinizing hormone secretion among individual gonadotropes. The Journal of biological chemistry 1991; 266:9016-9022

84. Li YX, Rinzel J, Vergara L, Stojilkovic SS. Spontaneous electrical and calcium oscillations in unstimulated pituitary gonadotrophs. Biophysical journal 1995; 69:785-795

85. Tasaka K, Stojilkovic SS, Izumi S, Catt KJ. Biphasic activation of cytosolic free calcium and LH responses by gonadotropin-releasing hormone. Biochemical and biophysical research communications 1988; 154:398-403

86. Mulvaney JM, Zhang T, Fewtrell C, Roberson MS. Calcium influx through L-type channels is required for selective activation of extracellular signal-regulated kinase by gonadotropin-releasing hormone. The Journal of biological chemistry 1999; 274:29796-29804

87. Tse FW, Tse A, Hille B, Horstmann H, Almers W. Local Ca2+ release from internal stores controls exocytosis in pituitary gonadotrophs. Neuron 1997; 18:121-132

88. Haisenleder DJ, Yasin M, Marshall JC. Gonadotropin Subunit and Gonadotropin-Releasing Hormone Receptor Gene Expression Are Regulated by Alterations in the Frequency of Calcium Pulsatile Signals*. Endocrinology 1997; 138:5227-5230

89. Cargnello M, Roux PP. Activation and function of the MAPKs and their substrates, the MAPK-activated protein kinases. Microbiology and molecular biology reviews : MMBR 2011; 75:50-83

90. Pearson G, Robinson F, Beers Gibson T, Xu BE, Karandikar M, Berman K, Cobb MH. Mitogen-activated protein (MAP) kinase pathways: regulation and physiological functions. Endocrine reviews 2001; 22:153-183

91. Yoon S, Seger R. The extracellular signal-regulated kinase: multiple substrates regulate diverse cellular functions. Growth factors (Chur, Switzerland) 2006; 24:21-44

92. Naor Z, Benard O, Seger R. Activation of MAPK cascades by G-protein-coupled receptors: the case of gonadotropin-releasing hormone receptor. Trends in endocrinology and metabolism: TEM 2000; 11:91-99

93. Harris D, Bonfil D, Chuderland D, Kraus S, Seger R, Naor Z. Activation of MAPK cascades by GnRH: ERK and Jun N-terminal kinase are involved in basal and GnRH-stimulated activity of the glycoprotein hormone LHbeta-subunit promoter. Endocrinology 2002; 143:1018-1025

94. Levi NL, Hanoch T, Benard O, Rozenblat M, Harris D, Reiss N, Naor Z, Seger R. Stimulation of Jun N-terminal kinase (JNK) by gonadotropin-releasing hormone in pituitary alpha T3-1 cell line is mediated by protein kinase C, c-Src, and CDC42. Molecular endocrinology (Baltimore, Md) 1998; 12:815-824

95. Lim S, Pnueli L, Tan JH, Naor Z, Rajagopal G, Melamed P. Negative feedback governs gonadotrope frequency-decoding of gonadotropin releasing hormone pulse-frequency. PloS one 2009; 4:e7244

96. Roberson MS, Zhang T, Li HL, Mulvaney JM. Activation of the p38 mitogen-activated protein kinase pathway by gonadotropin-releasing hormone. Endocrinology 1999; 140:1310-1318

97. Sim P, Mitchell R, Thorfinn L. Activation of MAP kinase in alpha T3-1 cells by luteinising hormone-releasing hormone. Biochemical Society transactions 1993; 21:357s

98. Dobkin-Bekman M, Naidich M, Pawson AJ, Millar RP, Seger R, Naor Z. Activation of mitogen-activated protein kinase (MAPK) by GnRH is cell-context dependent. Molecular and cellular endocrinology 2006; 252:184-190

99. Liu F, Austin DA, Mellon PL, Olefsky JM, Webster NJ. GnRH activates ERK1/2 leading to the induction of c-fos and LHbeta protein expression in LbetaT2 cells. Molecular endocrinology (Baltimore, Md) 2002; 16:419-434

100. Sundaresan S, Colin IM, Pestell RG, Jameson JL. Stimulation of mitogen-activated protein kinase by gonadotropin-releasing hormone: evidence for the involvement of protein kinase C. Endocrinology 1996; 137:304-311

101. Reiss N, Llevi LN, Shacham S, Harris D, Seger R, Naor Z. Mechanism of mitogen-activated protein kinase activation by gonadotropin-releasing hormone in the pituitary of alphaT3-1 cell line: differential roles of calcium and protein kinase C. Endocrinology 1997; 138:1673-1682

102. Benard O, Naor Z, Seger R. Role of dynamin, Src, and Ras in the protein kinase C-mediated activation of ERK by gonadotropin-releasing hormone. The Journal of biological chemistry 2001; 276:4554-4563

103. Yokoi T, Ohmichi M, Tasaka K, Kimura A, Kanda Y, Hayakawa J, Tahara M, Hisamoto K, Kurachi H, Murata Y. Activation of the luteinizing hormone beta promoter by gonadotropin-releasing hormone requires c-Jun NH2-terminal protein kinase. The Journal of biological chemistry 2000; 275:21639-21647

104. Bonfil D, Chuderland D, Kraus S, Shahbazian D, Friedberg I, Seger R, Naor Z. Extracellular signal-regulated kinase, Jun N-terminal kinase, p38, and c-Src are involved in gonadotropin-releasing hormone-stimulated activity of the glycoprotein hormone follicle-stimulating hormone beta-subunit promoter. Endocrinology 2004; 145:2228-2244

105. Caunt CJ, Finch AR, Sedgley KR, Oakley L, Luttrell LM, McArdle CA. Arrestin-mediated ERK Activation by Gonadotropin-releasing Hormone Receptors RECEPTOR-SPECIFIC ACTIVATION MECHANISMS AND COMPARTMENTALIZATION. Journal of Biological Chemistry 2006; 281:2701-2710

106. Fowkes RC, King P, Burrin JM. Regulation of human glycoprotein hormone alpha-subunit gene transcription in LbetaT2 gonadotropes by protein kinase C and extracellular signal-regulated kinase 1/2. Biology of reproduction 2002; 67:725-734

107. Roberson MS, Bliss SP, Xie J, Navratil AM, Farmerie TA, Wolfe MW, Clay CM. Gonadotropin-releasing hormone induction of extracellular-signal regulated kinase is blocked by inhibition of calmodulin. Molecular endocrinology (Baltimore, Md) 2005; 19:2412-2423

108. Wurmbach E, Yuen T, Ebersole BJ, Sealfon SC. Gonadotropin-releasing hormone receptor-coupled gene network organization. The Journal of biological chemistry 2001; 276:47195-47201

109. Duan WR, Ito M, Park Y, Maizels ET, Hunzicker-Dunn M, Jameson JL. GnRH regulates early growth response protein 1 transcription through multiple promoter elements. Molecular endocrinology (Baltimore, Md) 2002; 16:221-233

110. Dorn C, Ou Q, Svaren J, Crawford PA, Sadovsky Y. Activation of luteinizing hormone beta gene by gonadotropin-releasing hormone requires the synergy of early growth response-1 and steroidogenic factor-1. The Journal of biological chemistry 1999; 274:13870-13876

111. Fortin J, Lamba P, Wang Y, Bernard DJ. Conservation of mechanisms mediating gonadotrophin-releasing hormone 1 stimulation of human luteinizing hormone beta subunit transcription. Molecular human reproduction 2009; 15:77-87

112. Maudsley S, Naor Z, Bonfil D, Davidson L, Karali D, Pawson AJ, Larder R, Pope C, Nelson N, Millar RP, Brown P. Proline-rich tyrosine kinase 2 mediates gonadotropin-releasing hormone signaling to a specific extracellularly regulated kinase-sensitive transcriptional locus in the luteinizing hormone beta-subunit gene. Molecular endocrinology (Baltimore, Md) 2007; 21:1216-1233

113. Bliss SP, Miller A, Navratil AM, Xie J, McDonough SP, Fisher PJ, Landreth GE, Roberson MS. ERK signaling in the pituitary is required for female but not male fertility. Molecular endocrinology (Baltimore, Md) 2009; 23:1092-1101

114. Caunt CJ, Keyse SM. Dual-specificity MAP kinase phosphatases (MKPs): shaping the outcome of MAP kinase signalling. The FEBS journal 2013; 280:489-504

115. Zhang T, Mulvaney JM, Roberson MS. Activation of mitogen-activated protein kinase phosphatase 2 by gonadotropin-releasing hormone. Molecular and cellular endocrinology 2001; 172:79-89

116. Nguyen KA, Intriago RE, Upadhyay HC, Santos SJ, Webster NJ, Lawson MA. Modulation of gonadotropin-releasing hormone-induced extracellular signal-regulated kinase activation by dual-specificity protein phosphatase 1 in LbetaT2 gonadotropes. Endocrinology 2010; 151:4882-4893

117. Zhang T, Roberson MS. Role of MAP kinase phosphatases in GnRH-dependent activation of MAP kinases. Journal of molecular endocrinology 2006; 36:41-50

118. Zhang T, Wolfe MW, Roberson MS. An early growth response protein (Egr) 1 cis-element is required for gonadotropin-releasing hormone-induced mitogen-activated protein kinase phosphatase 2 gene expression. The Journal of biological chemistry 2001; 276:45604-45613

119. Armstrong SP, Caunt CJ, McArdle CA. Gonadotropin-releasing hormone and protein kinase C signaling to ERK: spatiotemporal regulation of ERK by docking domains and dual-specificity phosphatases. Molecular endocrinology (Baltimore, Md) 2009; 23:510-519

120. Burger LL, Haisenleder DJ, Aylor KW, Marshall JC. Regulation of Lhb and Egr1 gene expression by GNRH pulses in rat pituitaries is both c-Jun N-terminal kinase (JNK)- and extracellular signal-regulated kinase (ERK)-dependent. Biology of reproduction 2009; 81:1206-1215

121. Kanasaki H, Bedecarrats GY, Kam KY, Xu S, Kaiser UB. Gonadotropin-releasing hormone pulse frequency-dependent activation of extracellular signal-regulated kinase pathways in perifused LbetaT2 cells. Endocrinology 2005; 146:5503-5513

122. Harris D, Chuderland D, Bonfil D, Kraus S, Seger R, Naor Z. Extracellular signal-regulated kinase and c-Src, but not Jun N-terminal kinase, are involved in basal and gonadotropin-releasing hormone-stimulated activity of the glycoprotein hormone alpha-subunit promoter. Endocrinology 2003; 144:612-622

123. Tohgo A, Choy EW, Gesty-Palmer D, Pierce KL, Laporte S, Oakley RH, Caron MG, Lefkowitz RJ, Luttrell LM. The stability of the G protein-coupled receptor-beta-arrestin interaction determines the mechanism and functional consequence of ERK activation. The Journal of biological chemistry 2003; 278:6258-6267

124. Torii S, Kusakabe M, Yamamoto T, Maekawa M, Nishida E. Sef is a spatial regulator for Ras/MAP kinase signaling. Developmental cell 2004; 7:33-44

125. Davidson L, Pawson AJ, Millar RP, Maudsley S. Cytoskeletal reorganization dependence of signaling by the gonadotropin-releasing hormone receptor. The Journal of biological chemistry 2004; 279:1980-1993

126. Edwards BS, Isom WJ, Navratil AM. Gonadotropin releasing hormone activation of the mTORC2/Rictor complex regulates actin remodeling and ERK activity in LβT2 cells. Molecular and cellular endocrinology 2017; 439:346-353

127. Dobkin-Bekman M, Naidich M, Rahamim L, Przedecki F, Almog T, Lim S, Melamed P, Liu P, Wohland T, Yao Z, Seger R, Naor Z. A preformed signaling complex mediates GnRH-activated ERK phosphorylation of paxillin and FAK at focal adhesions in LbT2 gonadotrope cells. Molecular endocrinology (Baltimore, Md) 2009; 23:1850-1864

128. Mulvaney JM, Roberson MS. Divergent signaling pathways requiring discrete calcium signals mediate concurrent activation of two mitogen-activated protein kinases by

gonadotropin-releasing hormone. The Journal of biological chemistry 2000; 275:14182-14189

129. Catterall WA. Ion channel voltage sensors: structure, function, and pathophysiology. Neuron 2010; 67:915-928

130. Catterall WA. Voltage-gated calcium channels. Cold Spring Harbor perspectives in biology 2011; 3:a003947

131. Marian J, Conn PM. Gonadotropin releasing hormone stimulation of cultured pituitary cells requires calcium. Molecular pharmacology 1979; 16:196-201

132. Wakabayashi K, Kamberi IA, McCann SM. In vitro response of the rat pituitary to gonadotrophin-releasing factors and to ions. Endocrinology 1969; 85:1046-1056

133. Naor Z, Capponi AM, Rossier MF, Ayalon D, Limor R. Gonadotropin-releasing hormone-induced rise in cytosolic free Ca2+ levels: mobilization of cellular and extracellular Ca2+ pools and relationship to gonadotropin secretion. Molecular endocrinology (Baltimore, Md) 1988; 2:512-520

134. Bosma MM, Hille B. Electrophysiological properties of a cell line of the gonadotrope lineage. Endocrinology 1992; 130:3411-3420

135. Tse A, Hille B. Role of voltage-gated Na+ and Ca2+ channels in gonadotropin-releasing hormone-induced membrane potential changes in identified rat gonadotropes. Endocrinology 1993; 132:1475-1481

136. Heyward PM, Chen C, Clarke IJ. Inward Membrane Currents and Electrophysiological Responses to GnRH in Ovine Gonadotropes. Neuroendocrinology 1995; 61:609-621

137. Mason WT, Sikdar SK. Characterization of voltage-gated sodium channels in ovine gonadotrophs: relationship to hormone secretion. J Physiol 1988; 399:493-517

138. Van Goor F, Zivadinovic D, Stojilkovic SS. Differential expression of ionic channels in rat anterior pituitary cells. Molecular endocrinology (Baltimore, Md) 2001; 15:1222-1236

139. Stojilkovic SS, Tabak J, Bertram R. Ion channels and signaling in the pituitary gland. Endocrine reviews 2010; 31:845-915

140. Berridge MJ. Calcium microdomains: organization and function. Cell calcium 2006; 40:405-412

141. Cheng H, Lederer WJ, Cannell MB. Calcium sparks: elementary events underlying excitation-contraction coupling in heart muscle. Science 1993; 262:740-744

142. Parker I, Yao Y. Regenerative release of calcium from functionally discrete subcellular stores by inositol trisphosphate. Proceedings Biological sciences 1991; 246:269-274

143. Yao Y, Choi J, Parker I. Quantal puffs of intracellular Ca2+ evoked by inositol trisphosphate in Xenopus oocytes. J Physiol 1995; 482 (Pt 3):533-553

144. Wang SQ, Song LS, Lakatta EG, Cheng H. Ca2+ signalling between single L-type Ca2+ channels and ryanodine receptors in heart cells. Nature 2001; 410:592-596

145. Kim JM, Lee M, Kim N, Heo WD. Optogenetic toolkit reveals the role of Ca2+ sparklets in coordinated cell migration. Proceedings of the National Academy of Sciences of the United States of America 2016; 113:5952-5957

146. Moreno CM, Dixon RE, Tajada S, Yuan C, Opitz-Araya X, Binder MD, Santana LF. Ca(2+) entry into neurons is facilitated by cooperative gating of clustered CaV1.3 channels. 2016; 5

147. Demuro A, Parker I. Imaging the activity and localization of single voltage-gated Ca(2+) channels by total internal reflection fluorescence microscopy. Biophysical journal 2004; 86:3250-3259

148. Amberg GC, Earley S, Glapa SA. Local regulation of arterial L-type calcium channels by reactive oxygen species. Circulation research 2010; 107:1002-1010

149. Chaplin NL, Amberg GC. Hydrogen peroxide mediates oxidant-dependent stimulation of arterial smooth muscle L-type calcium channels. American journal of physiology Cell physiology 2012; 302:C1382-1393

150. Navedo MF, Amberg GC, Nieves M, Molkentin JD, Santana LF. Mechanisms underlying heterogeneous Ca2+ sparklet activity in arterial smooth muscle. The Journal of general physiology 2006; 127:611-622

151. Navedo MF, Cheng EP, Yuan C, Votaw S, Molkentin JD, Scott JD, Santana LF. Increased coupled gating of L-type Ca^{2+} channels during hypertension and Timothy syndrome. Circulation research 2010; 106:748-756

152. Nieves-Cintron M, Amberg GC, Navedo MF, Molkentin JD, Santana LF. The control of Ca2+ influx and NFATc3 signaling in arterial smooth muscle during hypertension. Proceedings of the National Academy of Sciences of the United States of America 2008; 105:15623-15628

153. Nieves-Cintron M, Amberg GC, Nichols CB, Molkentin JD, Santana LF. Activation of NFATc3 down-regulates the beta1 subunit of large conductance, calcium-activated K+ channels in arterial smooth muscle and contributes to hypertension. The Journal of biological chemistry 2007; 282:3231-3240

154. Hancock JT, Desikan R, Neill SJ. Role of reactive oxygen species in cell signalling pathways. Biochemical Society transactions 2001; 29:345-350

155. Rhee SG. Cell signaling. H2O2, a necessary evil for cell signaling. Science 2006; 312:1882-1883

156. Bayir H. Reactive oxygen species. Critical care medicine 2005; 33:S498-501

157. Vignais PV. The superoxide-generating NADPH oxidase: structural aspects and activation mechanism. Cellular and molecular life sciences : CMLS 2002; 59:1428-1459

158. Murphy MP. How mitochondria produce reactive oxygen species. The Biochemical journal 2009; 417:1-13

159. Boveris A, Oshino N, Chance B. The cellular production of hydrogen peroxide. The Biochemical journal 1972; 128:617-630

160. Herrero A, Barja G. Localization of the site of oxygen radical generation inside the complex I of heart and nonsynaptic brain mammalian mitochondria. Journal of bioenergetics and biomembranes 2000; 32:609-615

161. Kudin AP, Bimpong-Buta NY, Vielhaber S, Elger CE, Kunz WS. Characterization of superoxide-producing sites in isolated brain mitochondria. The Journal of biological chemistry 2004; 279:4127-4135

162. Zorov DB, Juhaszova M, Sollott SJ. Mitochondrial ROS-induced ROS release: An update and review. Biochimica et Biophysica Acta (BBA) - Bioenergetics 2006; 1757:509-517

163. Zorov DB, Juhaszova M, Sollott SJ. Mitochondrial reactive oxygen species (ROS) and ROS-induced ROS release. Physiological reviews 2014; 94:909-950

164. Terada LS. Specificity in reactive oxidant signaling: think globally, act locally. The Journal of cell biology 2006; 174:615-623

165. Berthier S, Paclet MH, Lerouge S, Roux F, Vergnaud S, Coleman AW, Morel F. Changing the conformation state of cytochrome b558 initiates NADPH oxidase activation: MRP8/MRP14 regulation. The Journal of biological chemistry 2003; 278:25499-25508

166. Hu Q, Zheng G, Zweier JL, Deshpande S, Irani K, Ziegelstein RC. NADPH oxidase activation increases the sensitivity of intracellular Ca2+ stores to inositol 1,4,5-trisphosphate in human endothelial cells. The Journal of biological chemistry 2000; 275:15749-15757

167. Rizzuto R, Pinton P, Carrington W, Fay FS, Fogarty KE, Lifshitz LM, Tuft RA, Pozzan T. Close contacts with the endoplasmic reticulum as determinants of mitochondrial Ca2+ responses. Science 1998; 280:1763-1766

168. Csordas G, Thomas AP, Hajnoczky G. Quasi-synaptic calcium signal transmission between endoplasmic reticulum and mitochondria. The EMBO journal 1999; 18:96-108

169. Kaftan EJ, Xu T, Abercrombie RF, Hille B. Mitochondria shape hormonally induced cytoplasmic calcium oscillations and modulate exocytosis. The Journal of biological chemistry 2000; 275:25465-25470

170. Camello-Almaraz MC, Pozo MJ, Murphy MP, Camello PJ. Mitochondrial production of oxidants is necessary for physiological calcium oscillations. Journal of cellular physiology 2006; 206:487-494

171. Isaeva EV, Shkryl VM, Shirokova N. Mitochondrial redox state and Ca2+ sparks in permeabilized mammalian skeletal muscle. J Physiol 2005; 565:855-872

172. Xi Q, Cheranov SY, Jaggar JH. Mitochondria-derived reactive oxygen species dilate cerebral arteries by activating Ca2+ sparks. Circulation research 2005; 97:354-362

173. Davidson SM, Duchen MR. Calcium microdomains and oxidative stress. Cell calcium 2006; 40:561-574

174. Song YH, Choi E, Park SH, Lee SH, Cho H, Ho WK, Ryu SY. Sustained CaMKII activity mediates transient oxidative stress-induced long-term facilitation of L-type Ca(2+) current in cardiomyocytes. Free radical biology & medicine 2011; 51:1708-1716

175. Tang H, Viola HM, Filipovska A, Hool LC. Ca(v)1.2 calcium channel is glutathionylated during oxidative stress in guinea pig and ischemic human heart. Free radical biology & medicine 2011; 51:1501-1511

176. Santiago E, Contreras C, Garcia-Sacristan A, Sanchez A, Rivera L, Climent B, Prieto D. Signaling pathways involved in the H2O2-induced vasoconstriction of rat coronary arteries. Free radical biology & medicine 2013; 60:136-146

177. Chaplin NL, Nieves-Cintrón M, Fresquez AM, Navedo MF, Amberg GC. Arterial Smooth Muscle Mitochondria Amplify Hydrogen Peroxide Microdomains Functionally Coupled to L-Type Calcium Channels. Circulation research 2015; 117:1013-1023

178. Gu Y, Xu YC, Wu RF, Souza RF, Nwariaku FE, Terada LS. TNFalpha activates c-Jun amino terminal kinase through p47(phox). Experimental cell research 2002; 272:62-74

179. Agarwal A, Gupta S, Sharma RK. Role of oxidative stress in female reproduction. Reproductive biology and endocrinology : RB&E 2005; 3:28

180. Kim T, Lawson MA. GnRH Regulates Gonadotropin Gene Expression Through NADPH/Dual Oxidase-Derived Reactive Oxygen Species. Endocrinology 2015; 156:2185-2199

181. Roberson MS, Misra-Press A, Laurance ME, Stork PJ, Maurer RA. A role for mitogen-activated protein kinase in mediating activation of the glycoprotein hormone alpha-subunit promoter by gonadotropin-releasing hormone. Molecular and cellular biology 1995; 15:3531-3539

182. White BR, Duval DL, Mulvaney JM, Roberson MS, Clay CM. Homologous regulation of the gonadotropin-releasing hormone receptor gene is partially mediated by protein kinase C activation of an activator protein-1 element. Molecular endocrinology (Baltimore, Md) 1999; 13:566-577

183. Counis R, Laverrière JN, Garrel G, Bleux C, Cohen-Tannoudji J, Lerrant Y, Kottler ML, Magre S. Gonadotropin-releasing hormone and the control of gonadotrope function. Reproduction, nutrition, development 2005; 45:243-254

184. Amberg GC, Navedo MF, Nieves-Cintrón M, Molkentin JD, Santana LF. Calcium sparklets regulate local and global calcium in murine arterial smooth muscle. J Physiol 2007; 579:187-201

185. Maravall M, Mainen ZF, Sabatini BL, Svoboda K. Estimating intracellular calcium concentrations and buffering without wavelength ratioing. Biophysical journal 2000; 78:2655-2667

186. Navedo MF, Amberg GC. Local regulation of L-type Ca^{2+} channel sparklets in arterial smooth muscle. Microcirculation 2013; 20:290-298

187. Zheng W, Rampe D, Triggle DJ. Pharmacological, radioligand binding, and electrophysiological characteristics of FPL 64176, a novel nondihydropyridine Ca^{2+}

channel activator, in cardiac and vascular preparations. Molecular pharmacology 1991; 40:734-741

188. Toullec D, Pianetti P, Coste H, Bellevergue P, Grand-Perret T, Ajakane M, Baudet V, Boissin P, Boursier E, Loriolle F, et al. The bisindolylmaleimide GF 109203X is a potent and selective inhibitor of protein kinase C. The Journal of biological chemistry 1991; 266:15771-15781

189. Gekeler V, Boer R, Überall F, Ise W, Schubert C, Utz I, Hofmann J, Sanders KH, Schächtele C, Klemm K, Grunicke H. Effects of the selective bisindolylmaleimide protein kinase C inhibitor GF 109203X on P-glycoprotein-mediated multidrug resistance. British journal of cancer 1996; 74:897-905

190. Dobkin-Bekman M, Rahamin-Ben Navi L, Shterntal B, Sviridonov L, Przedecki F, Naidich-Exler M, Brodie C, Seger R, Naor Z. Differential role of PKC isoforms in GnRH and phorbol 12-myristate 13-acetate activation of extracellular signal-regulated kinase and Jun N-terminal kinase. Endocrinology 2010; 151:4894-4907

191. Gschwendt M, Dieterich S, Rennecke J, Kittstein W, Mueller HJ, Johannes FJ. Inhibition of protein kinase C m by various inhibitors. Differentiation from protein kinase c isoenzymes. FEBS letters 1996; 392:77-80

192. Hille B. Ion channels of excitable membranes, 3rd Edition. Suderland, Massachusetts: Sinauer Associates, Inc; 2001.

193. Dixon RE, Yuan C, Cheng EP, Navedo MF, Santana LF. Ca^{2+} signaling amplification by oligomerization of L-type Cav1.2 channels. Proceedings of the National Academy of Sciences of the United States of America 2012; 109:1749-1754

194. Navedo MF, Nieves-Cintrón M, Amberg GC, Yuan C, Votaw VS, Lederer WJ, McKnight GS, Santana LF. AKAP150 is required for stuttering persistent Ca^{2+} sparklets and angiotensin II-induced hypertension. Circulation research 2008; 102:e1-e11

195. Santana LF, Navedo MF, Amberg GC, Nieves-Cintrón M, Votaw VS, Ufret-Vincenty CA. Calcium sparklets in arterial smooth muscle. Clin Exp Pharmacol Physiol 2008; 35:1121-1126

196. Nieves-Cintrón M, Amberg GC, Navedo MF, Molkentin JD, Santana LF. The control of Ca^{2+} influx and NFATc3 signaling in arterial smooth muscle during hypertension. Proc Natl Acad Sci U S A 2008; 105:15623-15628

197. Touyz RM, Schiffrin EL. Signal transduction mechanisms mediating the physiological and pathophysiological actions of angiotensin II in vascular smooth muscle cells. Pharmacol Rev 2000; 52:639-672

198. Chaplin NL, Amberg GC. Stimulation of arterial smooth muscle L-type calcium channels by hydrogen peroxide requires protein kinase C. Channels 2012; 6

199. Naor Z, Benard O, Seger R. Activation of MAPK Cascades by G-protein-coupled Receptors: The Case of Gonadotropin-releasing Hormone Receptor. Trends in Endocrinology & Metabolism 2000; 11:91-99

200. Selway J, Rigatti R, Storey N, Lu J, Willars GB, Herbert TP. Evidence that Ca2+ within the microdomain of the L-type voltage gated Ca2+ channel activates ERK in MIN6 cells in response to glucagon-like peptide-1. PloS one 2012; 7:e33004

201. Kousta E, White DM, Franks S. Modern use of clomiphene citrate in induction of ovulation. Human reproduction update 1997; 3:359-365

202. Hughes E, Collins J, Vandekerckhove P. Clomiphene citrate for ovulation induction in women with oligo-amenorrhoea. The Cochrane database of systematic reviews 2000:CD000056

203. Use of clomiphene citrate in infertile women: a committee opinion. Fertil Steril 2013; 100:341-348

204. Tomao F, Lo Russo G, Spinelli GP, Stati V, Prete AA, Prinzi N, Sinjari M, Vici P, Papa A, Chiotti MS, Benedetti Panici P, Tomao S. Fertility drugs, reproductive strategies and ovarian cancer risk. Journal of ovarian research 2014; 7:51

205. Grosse R, Schmid A, Schöneberg T, Herrlich A, Muhn P, Schultz G, Gudermann T. Gonadotropin-releasing hormone receptor initiates multiple signaling pathways by exclusively coupling to $G_{q/11}$ proteins. The Journal of biological chemistry 2000; 275:9193-9200

206. Dang AK, Murtazina DA, Magee C, Navratil AM, Clay CM, Amberg GC. GnRH evokes localized subplasmalemmal calcium signaling in gonadotropes. Molecular endocrinology (Baltimore, Md) 2014; 28:2049-2059

207. Feissner RF, Skalska J, Gaum WE, Sheu SS. Crosstalk signaling between mitochondrial Ca^{2+} and ROS. Front Biosci 2009; 14:1197-1218

208. Hidalgo C, Donoso P. Crosstalk between calcium and redox signaling: from molecular mechanisms to health implications. Antioxidants & redox signaling 2008; 10:1275-1312

209. Ermak G, Davies KJ. Calcium and oxidative stress: from cell signaling to cell death. Molecular immunology 2002; 38:713-721

210. Gorlach A, Bertram K, Hudecova S, Krizanova O. Calcium and ROS: A mutual interplay. Redox biology 2015; 6:260-271

211. Mattson MP. Excitotoxic and excitoprotective mechanisms: abundant targets for the prevention and treatment of neurodegenerative disorders. Neuromolecular medicine 2003; 3:65-94

212. Uttara B, Singh AV, Zamboni P, Mahajan RT. Oxidative stress and neurodegenerative diseases: a review of upstream and downstream antioxidant therapeutic options. Current neuropharmacology 2009; 7:65-74

213. Chatzaki E, Bax CM, Eidne KA, Anderson L, Grudzinskas JG, Gallagher CJ. The expression of gonadotropin-releasing hormone and its receptor in endometrial cancer, and its relevance as an autocrine growth factor. Cancer research 1996; 56:2059-2065

214. Locker GY. Hormonal therapy of breast cancer. Cancer treatment reviews 1998; 24:221-240

215. von Minckwitz G, Kaufmann M. New endocrine approaches in the treatment of breast cancer. Biomedicine & pharmacotherapy = Biomedecine & pharmacotherapie 1998; 52:122-132

216. Amberg GC, Navedo MF, Nieves-Cintron M, Molkentin JD, Santana LF. Calcium sparklets regulate local and global calcium in murine arterial smooth muscle. J Physiol 2007; 579:187-201

217. Liu F, Austin DA, Mellon PL, Olefsky JM, Webster NJ. GnRH activates ERK1/2 leading to the induction of *c-fos* and LHb protein expression in LbT2 cells. Molecular endocrinology (Baltimore, Md) 2002; 16:419-434

218. Dikalova AE, Bikineyeva AT, Budzyn K, Nazarewicz RR, McCann L, Lewis W, Harrison DG, Dikalov SI. Therapeutic targeting of mitochondrial superoxide in hypertension. Circulation research 2010; 107:106-116

219. Li Q, Harraz MM, Zhou W, Zhang LN, Ding W, Zhang Y, Eggleston T, Yeaman C, Banfi B, Engelhardt JF. Nox2 and Rac1 regulate H2O2-dependent recruitment of TRAF6 to endosomal interleukin-1 receptor complexes. Molecular and cellular biology 2006; 26:140-154

220. Ushio-Fukai M. Localizing NADPH oxidase-derived ROS. Science's STKE : signal transduction knowledge environment 2006; 2006:re8

221. Vilhardt F, van Deurs B. The phagocyte NADPH oxidase depends on cholesterol-enriched membrane microdomains for assembly. The EMBO journal 2004; 23:739-748

222. Heumuller S, Wind S, Barbosa-Sicard E, Schmidt HH, Busse R, Schroder K, Brandes RP. Apocynin is not an inhibitor of vascular NADPH oxidases but an antioxidant. Hypertension 2008; 51:211-217

223. Seshiah PN, Weber DS, Rocic P, Valppu L, Taniyama Y, Griendling KK. Angiotensin II stimulation of NAD(P)H oxidase activity: upstream mediators. Circulation research 2002; 91:406-413

224. Wang G, Anrather J, Glass MJ, Tarsitano MJ, Zhou P, Frys KA, Pickel VM, Iadecola C. Nox2, Ca2+, and protein kinase C play a role in angiotensin II-induced free radical production in nucleus tractus solitarius. Hypertension 2006; 48:482-489

225. Knapp LT, Klann E. Superoxide-induced stimulation of protein kinase C via thiol modification and modulation of zinc content. The Journal of biological chemistry 2000; 275:24136-24145

226. Roelfsema F, Kok P, Veldhuis JD, Pijl H. Altered multihormone synchrony in obese patients with polycystic ovary syndrome. Metabolism 2011; 60:1227-1233

227. Roland AV, Moenter SM. Reproductive neuroendocrine dysfunction in polycystic ovary syndrome: insight from animal models. Frontiers in neuroendocrinology 2014; 35:494-511

228. Burt Solorzano CM, Beller JP, Abshire MY, Collins JS, McCartney CR, Marshall JC. Neuroendocrine dysfunction in polycystic ovary syndrome. Steroids 2012; 77:332-337

229. Imai A, Takagi A, Horibe S, Takagi H, Tamaya T. Evidence for tight coupling of gonadotropin-releasing hormone receptor to stimulated Fas ligand expression in reproductive tract tumors: possible mechanism for hormonal control of apoptotic cell death. The Journal of clinical endocrinology and metabolism 1998; 83:427-431

230. Allen-Worthington K, Xie J, Brown JL, Edmunson AM, Dowling A, Navratil AM, Scavelli K, Yoon H, Kim DG, Bynoe MS, Clarke I, Roberson MS. The F0F1 ATP Synthase

Complex Localizes to Membrane Rafts in Gonadotrope Cells. Molecular endocrinology (Baltimore, Md) 2016; 30:996-1011

231. Rao VK, Carlson EA, Yan SS. Mitochondrial permeability transition pore is a potential drug target for neurodegeneration. Biochim Biophys Acta 2014; 1842:1267-1272

232. Loeffen J, Smeitink J, Triepels R, Smeets R, Schuelke M, Sengers R, Trijbels F, Hamel B, Mullaart R, van den Heuvel L. The first nuclear-encoded complex I mutation in a patient with Leigh syndrome. American journal of human genetics 1998; 63:1598-1608

233. Rahman S, Blok RB, Dahl HH, Danks DM, Kirby DM, Chow CW, Christodoulou J, Thorburn DR. Leigh syndrome: clinical features and biochemical and DNA abnormalities. Annals of neurology 1996; 39:343-351

234. Zhu Z, Yao J, Johns T, Fu K, De Bie I, Macmillan C, Cuthbert AP, Newbold RF, Wang J, Chevrette M, Brown GK, Brown RM, Shoubridge EA. SURF1, encoding a factor involved in the biogenesis of cytochrome c oxidase, is mutated in Leigh syndrome. Nature genetics 1998; 20:337-343

235. Bernstein BW, Shaw AE, Minamide LS, Pak CW, Bamburg JR. Incorporation of cofilin into rods depends on disulfide intermolecular bonds: implications for actin regulation and neurodegenerative disease. The Journal of neuroscience : the official journal of the Society for Neuroscience 2012; 32:6670-6681

236. Kim JS, Huang TY, Bokoch GM. Reactive oxygen species regulate a slingshot-cofilin activation pathway. Molecular biology of the cell 2009; 20:2650-2660

237. Klamt F, Zdanov S, Levine RL, Pariser A, Zhang Y, Zhang B, Yu LR, Veenstra TD, Shacter E. Oxidant-induced apoptosis is mediated by oxidation of the actin-regulatory protein cofilin. Nature cell biology 2009; 11:1241-1246

238. Klemke M, Wabnitz GH, Funke F, Funk B, Kirchgessner H, Samstag Y. Oxidation of cofilin mediates T cell hyporesponsiveness under oxidative stress conditions. Immunity 2008; 29:404-413

239. Schulte B, John I, Simon B, Brockmann C, Oelmeier SA, Jahraus B, Kirchgessner H, Riplinger S, Carlomagno T, Wabnitz GH, Samstag Y. A reducing milieu renders cofilin insensitive to phosphatidylinositol 4,5-bisphosphate (PIP_2) inhibition. The Journal of biological chemistry 2013; 288:29430-29439

240. Wakabayashi K, Date Y, Tamaoki B-I. On the Mechanism of Action of Luteinizing Hormone-Releasing Factor and Prolactin Release Inhibiting Factor 1. Endocrinology 1973; 92:698-704

241. Yuen T, Wurmbach E, Ebersole BJ, Ruf F, Pfeffer RL, Sealfon SC. Coupling of GnRH Concentration and the GnRH Receptor-Activated Gene Program. Molecular Endocrinology 2002; 16:1145-1153

242. Poulin B, Rich N, Mas JL, Kordon C, Enjalbert A, Drouva SV. GnRH signalling pathways and GnRH-induced homologous desensitization in a gonadotrope cell line (alphaT3-1). Molecular and cellular endocrinology 1998; 142:99-117

243. Liu F, Usui I, Evans LG, Austin DA, Mellon PL, Olefsky JM, Webster NJG. Involvement of Both G(q/11) and G(s) Proteins in Gonadotropin-releasing Hormone Receptor-mediated Signaling in LβT2 Cells. The Journal of biological chemistry 2002; 277:32099-32108

244. Edwards BS, Dang AK, Murtazina DA, Dozier MG, Whitesell JD, Khan SA, Cherrington BD, Amberg GC, Clay CM, Navratil AM. Dynamin is required for GnRH signaling to L-type calcium channels and activation of ERK. Endocrinology 2015:en20151575-en20151575

245. Yang L, Doshi D, Morrow J, Katchman A, Chen X, Marx SO. Protein kinase C isoforms differentially phosphorylate Ca(v)1.2 alpha(1c). Biochemistry 2009; 48:6674-6683

246. Yang L, Liu G, Zakharov SI, Morrow JP, Rybin VO, Steinberg SF, Marx SO. Ser1928 is a common site for Cav1.2 phosphorylation by protein kinase C isoforms. The Journal of biological chemistry 2005; 280:207-214

247. Zhang J, Carver Chase M, Choveau Frank S, Shapiro Mark S. Clustering and Functional Coupling of Diverse Ion Channels and Signaling Proteins Revealed by Super-resolution STORM Microscopy in Neurons. Neuron 92:461-478

248. Tang S, Yasuda R. Imaging ERK and PKA Activation in Single Dendritic Spines during Structural Plasticity. Neuron 2017; 93:1315-1324.e1313

249. Harvey CD, Ehrhardt AG, Cellurale C, Zhong H, Yasuda R, Davis RJ, Svoboda K. A genetically encoded fluorescent sensor of ERK activity. Proceedings of the National Academy of Sciences of the United States of America 2008; 105:19264-19269

250. Cullen PJ, Lockyer PJ. Integration of calcium and Ras signalling. Nature reviews Molecular cell biology 2002; 3:339-348

251. Rowland AA, Voeltz GK. Endoplasmic reticulum-mitochondria contacts: function of the junction. Nature reviews Molecular cell biology 2012; 13:607-625

252. Giorgi C, De Stefani D, Bononi A, Rizzuto R, Pinton P. Structural and functional link between the mitochondrial network and the endoplasmic reticulum. The international journal of biochemistry & cell biology 2009; 41:1817-1827

253. Welte MA. Bidirectional transport along microtubules. Current Biology 2004; 14:R525-R537

254. Morlino G, Barreiro O, Baixauli F, Robles-Valero J, Gonzalez-Granado JM, Villa-Bellosta R, Cuenca J, Sanchez-Sorzano CO, Veiga E, Martin-Cofreces NB, Sanchez-Madrid F. Miro-1 links mitochondria and microtubule Dynein motors to control lymphocyte migration and polarity. Molecular and cellular biology 2014; 34:1412-1426

255. Heyworth PG, Robinson JM, Ding J, Ellis BA, Badwey JA. Cofilin undergoes rapid dephosphorylation in stimulated neutrophils and translocates to ruffled membranes enriched in products of the NADPH oxidase complex. Evidence for a novel cycle of phosphorylation and dephosphorylation. Histochemistry and cell biology 1997; 108:221-233

256. Wientjes FB, Reeves EP, Soskic V, Furthmayr H, Segal AW. The NADPH oxidase components p47(phox) and p40(phox) bind to moesin through their PX domain. Biochemical and biophysical research communications 2001; 289:382-388

257. Wu RF, Gu Y, Xu YC, Nwariaku FE, Terada LS. Vascular endothelial growth factor causes translocation of p47phox to membrane ruffles through WAVE1. The Journal of biological chemistry 2003; 278:36830-36840

Appendix. Permission to Reproduce Copyright Protected Works

Chapter 2: Molecular Endocrinology

Permissions information for authors:

Requests to reproduce your own work:

Bioscientifica grants to authors the right to reproduce their work free of charge in any publication of which they are the author or editor, subject only to giving proper credit in the work to the original publication by Bioscientifica. **Therefore, authors do not need to contact Bioscientifica to request permission to reproduce their work**.

Should you require formal confirmation that permission is not required to reproduce your own work, please use the Rightslink system as described in the below section. You will not be charged for this.

http://jme.endocrinology-journals.org/site/misc/permissions_commercial_reprints.xhtml

OXFORD UNIVERSITY PRESS LICENSE
TERMS AND CONDITIONS

May 30, 2017

This Agreement between Colorado State University -- An Dang ("You") and Oxford University Press ("Oxford University Press") consists of your license details and the terms and conditions provided by Oxford University Press and Copyright Clearance Center.

License Number	4118921461296
License date	May 30, 2017
Licensed content publisher	Oxford University Press
Licensed content publication	Molecular Endocrinology
Licensed content title	GnRH Evokes Localized Subplasmalemmal Calcium Signaling in Gonadotropes
Licensed content author	Dang, An K.; Murtazina, Dilyara A.
Licensed content date	Dec 1, 2014
Type of Use	Thesis/Dissertation
Institution name	
Title of your work	Regulation of local l-type calcium channel signaling in anterior pituitary gonadotropes
Publisher of your work	n/a
Expected publication date	Dec 2017
Permissions cost	0.00 USD
Value added tax	0.00 USD
Total	0.00 USD
Requestor Location	Colorado State University 1617 Campus Delivery FORT COLLINS, CO 80523 United States Attn: An Dang
Publisher Tax ID	GB125506730
Billing Type	Invoice
Billing Address	Colorado State University 1617 Campus Delivery FORT COLLINS, CO 80523 United States Attn: An Dang
Total	0.00 USD
Terms and Conditions	

STANDARD TERMS AND CONDITIONS FOR REPRODUCTION OF MATERIAL FROM AN OXFORD UNIVERSITY PRESS JOURNAL

1. Use of the material is restricted to the type of use specified in your order details.
2. This permission covers the use of the material in the English language in the following territory: world. If you have requested additional permission to translate this material, the terms and conditions of this reuse will be set out in clause 12.
3. This permission is limited to the particular use authorized in (1) above and does not allow you to sanction its use elsewhere in any other format other than specified above, nor does it apply to quotations, images, artistic works etc that have been reproduced from other sources which may be part of the material to be used.
4. No alteration, omission or addition is made to the material without our written consent. Permission must be re-cleared with Oxford University Press if/when you decide to reprint.
5. The following credit line appears wherever the material is used: author, title, journal, year, volume, issue number, pagination, by permission of Oxford University Press or the sponsoring society if the journal is a society journal. Where a journal is being published on behalf of a learned society, the details of that society must be included in the credit line.
6. For the reproduction of a full article from an Oxford University Press journal for whatever purpose, the corresponding author of the material concerned should be informed of the proposed use. Contact details for the corresponding authors of all Oxford University Press journal contact can be found alongside either the abstract or full text of the article concerned, accessible from www.oxfordjournals.org Should there be a problem clearing these rights, please contact journals.permissions@oup.com
7. If the credit line or acknowledgement in our publication indicates that any of the figures, images or photos was reproduced, drawn or modified from an earlier source it will be necessary for you to clear this permission with the original publisher as well. If this permission has not been obtained, please note that this material cannot be included in your publication/photocopies.
8. While you may exercise the rights licensed immediately upon issuance of the license at the end of the licensing process for the transaction, provided that you have disclosed complete and accurate details of your proposed use, no license is finally effective unless and until full payment is received from you (either by Oxford University Press or by Copyright Clearance Center (CCC)) as provided in CCC's Billing and Payment terms and conditions. If full payment is not received on a timely basis, then any license preliminarily granted shall be deemed automatically revoked and shall be void as if never granted. Further, in the event that you breach any of these terms and conditions or any of CCC's Billing and Payment terms and conditions, the license is automatically revoked and shall be void as if never granted. Use of materials as described in a revoked license, as well as any use of the materials beyond the scope of an unrevoked license, may constitute copyright infringement and Oxford University Press reserves the right to take any and all action to protect its copyright in the materials.
9. This license is personal to you and may not be sublicensed, assigned or transferred by you to any other person without Oxford University Press's written permission.
10. Oxford University Press reserves all rights not specifically granted in the combination of (i) the license details provided by you and accepted in the course of this licensing transaction, (ii) these terms and conditions and (iii) CCC's Billing and Payment terms and conditions.
11. You hereby indemnify and agree to hold harmless Oxford University Press and CCC, and their respective officers, directors, employs and agents, from and against any and all claims arising out of your use of the licensed material other than as specifically authorized pursuant to this license.